UNIVERSIDAD AUTÓNOMA DE MADRID

FACULTAD DE CIENCIAS

DEPARTAMENTO DE BIOLOGÍA MOLECULAR

Regulation of PTS systems and their interplay with central carbon metabolism in *Pseudomonas putida*

TESIS DOCTORAL

Memoria presentada para optar al grado de Doctor en Ciencias

Max Chavarría Vargas

DIRECTOR

Víctor de Lorenzo Prieto

CONSEJO SUPERIOR DE INVESTIGACIONES CIENTÍFICAS

CENTRO NACIONAL DE BIOTECNOLOGÍA

Madrid, 2011

To God, my wife Adriana and my daughter Angélica

ACKNOWLEDGMENTS

This work would not have been possible without the support and collaboration of many people. I would like to thank:

-To Víctor de Lorenzo, for accepting me in his Lab, support and encourage me at all the times. Thanks for his understanding, good advice and his daily efforts to teach me to be a good scientist.

-To Juan Ayala for accepting to be my tutor.

-To Uwe Sauer for giving me the opportunity to learn about fluxomics and metabolomics in his lab at Institute of Molecular Systems Biology (IMSB), ETH Zürich.

-To Roelco J. Kleijn and Tobias Fuhrer at IMSB (ETH, Zürich) for their guidance and contribution in this work.

-To Tino Krell at EEZ, Granada for his contribution in ITC measurements.

-To Cesar Santiago and Jose María Casasnovas at CNB for their contribution in structural analysis by X-ray crystallography.

-To University of Costa Rica for doctoral scholarship. Especially to OAICE staff for their support and high efficiency in their work.

To Chemistry School at University of Costa Rica for their support, trust and giving me the opportunity to be part of their professional staff.

-Especially to Katharina Pflüger for her guidance and teach me the first steps of this work.

-To Esteban and Danilo at VdL lab for their imput, critical discussions and sharing their ideas.

To Sofía Fraile for her invaluable technical support and friendship.

-To everybody at the Victor de Lorenzo lab: Aitor, Carlos, David, Jose Ignacio, Rafa, Aleyo, Belén, Pablo, Javier, Raúl, Gonzalo, Ilaria, Chu, Inés for their friendship and make the lab a great place to work.

GENERAL INDEX

INDEX OF FIGURES

INDEX OF TABLES

ABBREVIATIONS

2K3D6P	2-keto-3-deoxy-6-phosphogluconate
2OG	2-oxoglutarate
6PG	6-phosphogluconate
16S ARNr	16S RNA ribosomal gen
AcCoA	Acetyl Coenzyme A
Ap	Ampicillin
ATP	Adenosine triphosphate
BSA	Bovine seroalbumine
CDW	Cellular Dry weight
Cit	Citrate
CTAB	Cetyl trimethyl ammonium bromide
Da	Dalton
DHAP	Dihydroxyacetone phosphate
DMSO	Dimethyl sulfoxide
DNA	Deoxyribonucleic acid
dNTPs	Deoxynucleotide triphosphate
DTT	Dithiothreitol
ED	Entner-Doudoroff
EDTA	Ethylenediaminetetraacetic acid
EMP	Embden-Meyerhof-Parnas
EMSA	Non-radioactive electrophoretic mobility shift assays
F1P	Fructose-1-Phosphate
F6P	Fructose-6-Phosphate
FBP	Fructose-1,6-bisphosphate
Fum	Fumarate
GA3P	Glyceraldehyde-3-phosphate
G6P	Glucose-6-phosphate
g	Gram
HPLC	High-performance liquid chromatography
IPTG	Isopropyl-1-thio-β-galactopyranoside
ITC	Isothermal microcalorimetry
Km	Kanamycin
kb	1000 base pairs

LB	Luria-Bertani medium
LC-MS	Liquid chromatography with mass spectrometry
Mal	Malate
mg	Miligram
min	Minute
ml	Milliliter
mM	Millimolar
MS	Mass spectrometry
NAD	Nicotinamide adenine dinucleotide
NADH	Nicotinamide adenine dinucleotide reduced form
NADP	Nicotinamide adenine dinucleotide phosphate reduced form
NCBI	National Center for Biotechnology Information
nl	Nanoliter
nm	Nanometers
OAA	Oxaloacetate
OD	Optical density
ORF	Open reading frame
PAGE	Polyacrylamide gel electrophoresis
PBS	Phosphate Buffered Saline
PCR	Polymerase chain reaction
PDB	Protein Data Bank
PEP	Phosphoenolpyruvate
PHAs	Polyhydroxyalkanoates
PP	Pentose phosphate
PTS	Phosphoenolpyruvate (PEP):carbohydrate phosphotransferase system
Pyr	Pyruvate
Rif	Rifampicin
RNA	Ribonucleic acid
SDS	Sodium dodecyl sulfate
sec	Seconds
Suc	Succinate
TCA	Citric acid cycle
Tc	Tetracycline
Tel	Tellurite
X-gal	5-bromo-4-chloro-3-indolyl-β-D-galactopyranoside

µbar	Microbars
µl	Microliter
µM	Micromolar
µm	Micrometers
σ	Sigma factor of RNA polymerase

ABSTRACT

The environmental bacterium *Pseudomonas putida* is known for its metabolic versatility and endurance to various types of stresses. This requires various layers of control to coordinate the expression of specific genes to the overall physiology of the cell in diverse conditions. One prevalent physiological sensor to this end is the phosphoenolpyruvate-carbohydrate phosphotransferase transport system (PTS), which carries out both uptake of carbohydrates to central metabolism as well as regulatory functions such as carbon catabolite repression. Apart from the classical PTS system many prokaryotes harbour also a PTS branch that is not involved in carbohydrate traffic, but participates in regulation of some metabolic processes. In *P. putida*, one sugar-specific PTS for fructose transport (FruA/EIIBC and FruB/EI-HPr-EIIA) coexists with the PTS^{Ntr} ($PtsP/EI^{Ntr}$, PtsO/NPr, and $PtsN/EIIA^{Ntr}$).

This work analyzes: [i] the carbon flow in the central metabolism in *P. putida* as well its interplay with the PTS^{Ntr} system, and [ii] the control exerted by the catabolite repressor activator (Cra) protein on PTS systems in this bacterium. Specifically, in **Chapter 1** we analyzed the carbon utilization of PTS and no-PTS substrates through metabolic flux analysis and metabolomic approaches. The results showed that the Entner-Doudoroff (ED) pathway is the most prevalent pathway for sugar degradation *in P. putida* and that this pathway operates in an unusual cyclical mode. Moreover, flux analysis and enzymatic assays revealed that the $EIIA^{Ntr}$ protein controls the connection of pyruvate to the TCA cycle by downregulating the pyruvate shunt, that bypasses malate dehydrogenase in the TCA cycle. **Chapter 2** describes the link between PTS^{Fru}, the transcriptional regulator Cra and its effector Fructose 1-phosphate (F1P) through *in vitro* approaches. Electrophoretic mobility shift assays (EMSA) and Isothermal Titration Microcalorimetry (ITC) experiments showed that Cra recognized the palindromic sequence TTAAACGTTTCA in the regulatory region of *fruBKA* operon. In addition, Cra crystal structure, EMSA and ITC experiments point to F1P as the only metabolic effector of this bacterial regulator. Finally, in **Chapter 3**, we showed with *in vivo* experiments that Cra is a repressor of the PTS^{Fru} in *P. putida*. Moreover in this chapter, we demonstrated that Cra is a fine-tuning regulator of PTS^{Ntr} since the repression exerted by Cra on *fruB* expression affects the phosphorylated/non-phosphorylated PtsN ratio *via* PTS cross-talk. In summary, we have contributed to the understanding of carbon central metabolism and PTS systems in the soil bacterium *P. putida*, which according to our findings in some aspects differ importantly to model species such as *E. coli* or *B. subtilis*.

RESUMEN

La bacteria del suelo *Pseudomonas putida* es conocida por su versatilidad metabólica y resistencia a diversos tipos de estrés. Esto requiere diversos niveles de control para coordinar la expresión génica y así mantener la fisiología general de la célula en diversas condiciones. Un importante sensor fisiológico es el sistema de transporte fosfoenolpiruvato fosfotransferasa de azúcares (PTS), que lleva a cabo la asimilación de hidratos de carbono hacia el metabolismo central, así como funciones reguladoras (*p.e.* en el fenómeno de represión catabólica). Aparte de los sistemas PTS clásicos, muchos procariotas tienen un tipo de sistema PTS que no está involucrado en el tráfico de hidratos de carbono, el cual participa en la regulación de algunos procesos metabólicos. En *P. putida*, el sistema PTS de azúcar específico para el transporte de fructosa (FruA / EIIBC y FruB / EI-HPR-EIIA) coexiste con el llamado sistema PTS de nitrógeno PTS^{Ntr} (PtsP / EI^{NTR}, PtsO / Npr, y PtsN / $EIIA^{Ntr}$).

En este trabajo se analiza: [i] el flujo del carbono en el metabolismo central de *P. putida*, así como su interacción con el sistema PTS^{Ntr} y [ii] el control ejercido por el regulador transcripcional Cra sobre los sistemas PTS de esta bacteria. En concreto, en el **Capítulo 1** se analizó a través de herramientas de fluxómica y metabolómica la utilización de varias fuentes de carbono (PTS y no PTS). Los resultados mostraron que el Entner-Doudoroff (ED) es la vía más común para la degradación de azúcares en *P. putida*. Además, se demostró que la vía del ED en *P. putida* opera en un inusual modo cíclico. Además, en el **Capítulo 1** a través de análisis de flujos y ensayos enzimáticos se demostró que la proteína $EIIA^{Ntr}$ controla *el desvío del piruvato (pyruvate shunt)* que controla la conexión entre el piruvato y el ciclo de Krebs. El **Capítulo 2** describe a través de estudios *in vitro* la relación entre el sistema PTS^{Fru}, el regulador transcripcional Cra y su efector (fructosa 1-fosfato; F1P). Ensayos de movilidad electroforética (EMSA) y de microcalorimetría de titulación isotérmica (ITC), mostraron que Cra reconoce la secuencia palindrómica TTAAACGTTTCA en la región reguladora del operón *fruBKA*. Además, la estructura cristalina del regulador se obtuvo en ausencia y presencia de la F1P. Por tanto, todos nuestros resultados apuntan a la F1P como el único efector de este regulador transcripcional bacteriano. Por último, en el **Capítulo 3**, se mostró con experimentos *in vivo* que Cra es un represor del sistema PTS^{Fru} en *P. putida*. Por otra parte, se observó que Cra controla bajo ciertas condiciones metabólicas el estado de fosforilación de PtsN a través de FruB.

En este trabajo hemos contribuido a la comprensión del metabolismo central y los sistemas PTS en la bacteria del suelo *P. putida* los cuales, de acuerdo a nuestros resultados, pueden diferir en importantes aspectos a otras bacterias modelo como *E. coli* o *B. subtilis*.

I. INTRODUCTION

1. Overview of *Pseudomonas putida*

1.1. The genus *Pseudomonas* and its metabolic diversity

Pseudomonas genus was defined by W. Migula in 1894 such as a genus of Gram-negative, rod-shaped and polar-flagella cells. This very general definition was accepted for many years, until the 60's, when the definition was made more precise thanks to the inclusion of morphological and physiological characteristics as a method of bacterial classification (Stanier *et al*, 1966). Thus, in the 60-70's according to the Bergey´s manual of systematic bacteriology, *Pseudomonas* was defined such as cells with diameter usually less than 1 μm, length from 1.5 to 5 μm; rod-shaped, curved or straight but no helical; they have not appendices and are not surrounded by sheaths. Then, with the development of new methodologies and the inclusion of approaches based on the studies of conservative macromolecules many strains were reclassified. In this regard, DNA/DNA and RNAr/DNA hybridization techniques (Doi and Igarashi, 1965; Johnson and Ordal, 1968; Palleroni *et al*, 1972; Palleroni *et al*, 1973) allowed a division of *Pseudomonas* species, which were grouped into five taxonomic groups (RNA-I to RNA-V). Later, with the use of 16S rRNA gene sequences (Palleroni *et al*, 1973) to study bacterial phylogeny and taxonomy, the diversity of RNA-I and RNA-V groups was evident which led to the clustering of *Pseudomonas* into the RNA-I group within the subclass of γ-Proteobacteria, that is until today the most widely accepted classification (Palleroni, 2003). The current affiliation of *Pseudomonas* genus is:

Kingdom:	Bacteria
Phylum:	Proteobacteria
Class:	Gamma proteobacteria
Order:	Pseudomonodales
Family:	Pseudomonodaceae
Genus:	Pseudomonas

After its discovery, *Pseudomonas* were isolated from many natural niches and around 148 species have been reported (Palleroni and Moore, 2004). Of these, just *P. aeruginosa* (Govan and Deretic, 1996), is a opportunistic pathogen to humans (*P. mallei* and *P. pseudomallei* have been moved to the genus *Burkolderia*), therefore in general terms most *Pseudomonas* species are innocuous to humans. Moreover, there are phytopathogenic

species such as *P. syringae* (Buell *et al*, 2003) and plant growth-promoting rhizobacterium such as *P. fluorescens* (Paulsen *et al*, 2005). The strains are aerobic, with a strictly respiratory type of metabolism with oxygen as terminal electron acceptor, although in some cases, nitrate can be used as alternative electron aceptor under anaerobic conditions (Jensen *et al*, 2004; Moore *et al*, 2006).

Pseudomonas are able to colonize various environments, including soil, water, marshes, coastal marine habitats, plant rhizosphere and plant and animal tissues (Jensen *et al*, 2004). Maybe the most prominent characteristic of *Pseudomonas* species is its metabolic versatility (Clarke, 1982; Stanier *et al*, 1966). This allows them to use a large amount of organic compounds such as carbohydrates, lineal hydrocarbons, aliphatic acids, amines, amides, amino acids, alcohols and aromatic compounds. At the beginning of this century the sequencing of the entire genome of 6 members of the genus *Pseudomonas*: *P. aeruginosa* PAO1 (Stover *et al*, 2000), *P. putida* KT2440 (Frank *et al*, 2011; Nelson *et al*, 2002), *P. syringae* pv tomato DC3000 (Buell *et al*, 2003), *P. syringae* pv syringae B728a (Feil *et al*, 2005), *P. fluorescens* Pf-5 (Paulsen *et al*, 2005) and *P. entomophila* (Vodovar *et al*, 2006), has allowed understanding of the unique and versatile adaptive capacity of this genus. It was possible possible to see in these sequenced genomes an extensive collection of enzymes and metabolic pathways that can degrade a large number of organic compounds including xenobiotics. Today, the genome of 38 strains of the genus *Pseudomonas* have been sequenced (nine of them correspond to different species: *P. aeruginosa, P. putida, P. fluorescens, P. mendocina, P. syringae, P. savastanoi, P. resinovorans, P. stutzeri* and *P. entomophila*) so that knowledge about the genus *Pseudomonas* has increased markedly in the last years, being more evident its metabolic versatility. Therefore, due to their strong skills for degradation of a great variety of chemical compounds, Pseudomonads have great potential for different biotechnological applications, particularly in the areas of bioremediation and biocatalysis (Loh and Cao, 2008).

1.2. Description of *Pseudomonas putida*

The bacterium *P. putida* belongs to the group of fluorescent *Pseudomonas* well known for producing fluorescent pigments (Meyer, 2000). Strains of *P. putida* display a wide range of metabolic activities, which is indicative of their adaptation to various niches (Jensen *et al*, 2004). *P. putida* KT2440 (Nelson *et al*, 2002) is probably the best-characterized saprophytic laboratory Pseudomonad, that has retained its ability to survive and

function in the environment (Frank *et al*, 2011; Jimenez *et al*, 2002). The bacterium is a plasmid-free derivative of a toluene-degrading bacterium isolated in Japan by Hosahawa in 1963 (Nelson *et al*, 2002), which was originally designated as *Pseudomonas arvilla* strain mt-2 and then reclassified as *P. putida* mt-2 (Williams and Murray, 1974).

P. putida KT2440 was the first host vector biosafety system for gene cloning in Gram-negative soil bacteria (Duque *et al*, 2007; Stjepandic *et al*, 2002). This strain has been extensively used as a host for cloning and gene expression, and its most prominent characteristic is its capability to degrade aromatic compounds such as toluene or *m*-xylene so it is considered as a model organism for biodegradation studies (Jimenez *et al*, 2002; Loh *et al*, 2008). *P. putida* KT2440 is thus considered as the workhorse for Pseudomonas research (Martins dos Santos *et al*, 2004; Timmis, 2002; Wu *et al*, 2011).

The genome of strain KT2440 consists of a single circular chromosome of 6,181,863 bas pairs (bp) whose G+C content varies between 43% and 69%, and has a mean value of 61.6% (Duque *et al*, 2007). A total of 5420 open reading frames (ORFs) with an average length of 998 bp were identified. A putative role assignments could be made for 3571 ORFs, with another 600 (11.1%) being unique to *P. putida* (Martins dos Santos *et al*, 2004). A total of 1037 (19.1%) of the ORFs encode conserved hypothetical proteins. Comparative genome analysis with the currently completed microbial genomes revealed that 4610 ORFs (85%) of the KT2440 genome have homologues in the *P. aeruginosa* PAO1 genome (Stover *et al*, 2000).

1.3. Carbohydrate metabolism in *P. putida*

The central pathways of metabolism are responsible for the generation of stored biological energy and formation of the metabolic precursors that serve as the starting point for biosynthesis of the building blocks that are in turn polymerized to form the essential cellular constituents of all living cells (Downs, 2006; Romano and Conway, 1996). This set of reactions, occurs in all three domains of the live; hence it must have been established before divergence of the domains (Romano *et al*, 1996). In the literature we can find the expression *carbon central metabolism*, refers to the classic metabolic pathways such as those found in yeast or *Escherichia coli* (Romano *et al*, 1996), and includes the Embden-Meyerhof-Parnas (EMP) pathway, the pentose phosphate (PP) pathway, Entner-Doudoroff (ED) pathway and the tricarboxylic acid (TCA) cycle.

Interestingly, each of these pathways can be replaced by alternative pathways or can operate in abbreviated schemes. In fact, all possible combination of these classic, alternative and abbreviated metabolic pathways can be found together in microorganisms (Conway, 1992).

Specifically, the genome of *P. putida* KT2440 contains all the genes encoding enzymes that make the three prominent metabolic pathways in bacteria: the ED pathway, the EMP pathway and the PP pathway (Fig. 1) with the intriguing exception of the glycolytic enzyme 6-phosphofructokinase, Pfk (Velazquez *et al*, 2004). The key glycolytic enzyme Pfk catalyzes the transformation of fructose-6-phosphate (F6P) to fructose 1,6-bisphosphate (FBP) by transferring a phosphate group from ATP or pyrophosphate, to the C1-position (Ronimus and Morgan, 2001). In bacteria, Pfk enzymes are usually absent in aerobic organisms but they are very common in anaerobic organisms in which is not possible the formation of ATP by oxidative phosphorylation and therefore the formation of ATP by EMP pathway is essential. The absence of this enzyme in *P. putida* can explain why this bacterium uses only the ED pathway for degrading glucose and it is unable to use the EMP pathway, which has been previously demonstrated through experiments of radioactivity with ^{14}C (Vicente and Canovas, 1973) and metabolic flux analysis (Fuhrer, 2005). On the other hand, catabolism of fructose could be slightly different to hexoses metabolism since this sugar directly enters into EMP pathway *via* FruBKA (Velazquez *et al*, 2004; Velazquez *et al*, 2007; Vicente, 1975). In principle, fructose could be degraded through the ED pathway and/or EMP pathway (Velazquez *et al*, 2004), however, previous studies showed that this pentose is catabolized primarily through the ED pathway (Sawyer *et al*, 1977). Therefore, it seems that ED route is the most important pathway for sugar degradation in upper central metabolism in *P. putida*. The ED pathway was first discovered in 1952 in *Pseudomonas saccharophila* (Entner and Doudoroff, 1952) and several years later was shown to be present in *E. coli* (Eisenberg and Dobrogosz, 1967). We currently know that the ED pathway is present in all three phylogenetic domains, including the most deeply rooted Archaea (Peekhaus and Conway, 1998). The wide distribution of the ED pathway suggests that it is of much greater importance in Nature than was previously assigned. In fact, an analysis of the evolution of the central metabolism suggested that ED pathway is earlier than EMP pathway (Romano *et al*, 1996). The main difference between the ED and EMP pathways comes in the characteristics of the metabolites that serve as substrates for aldol cleavage (Conway, 1992). For the ED pathway, the 6-phosphogluconate dehydratase

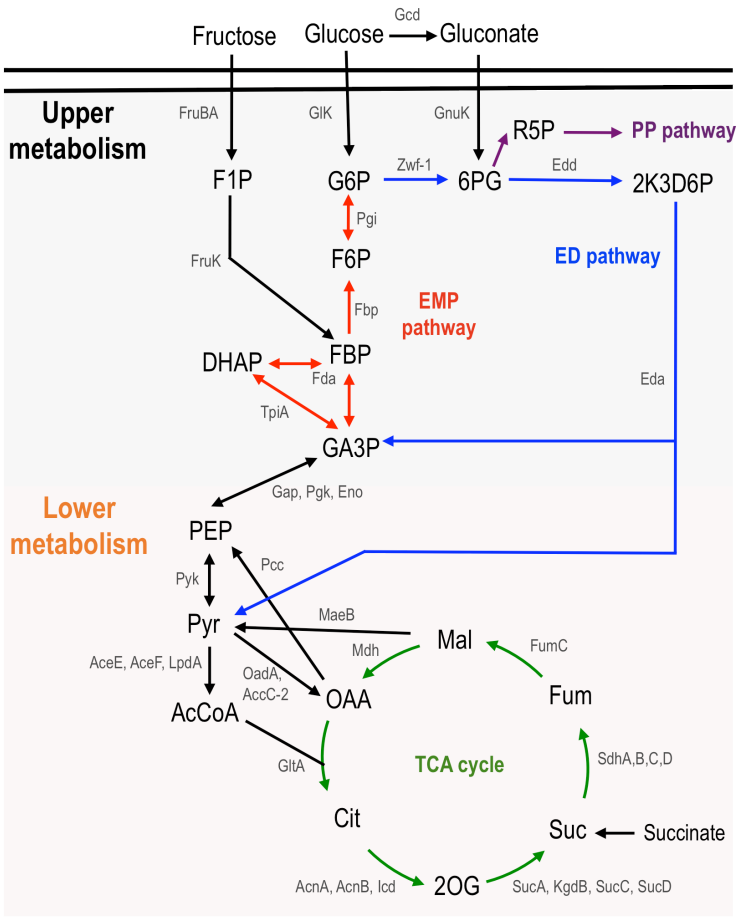

Figure 1. Carbon central metabolism in *P. putida* KT2440. Representation of glucose, fructose, gluconate and succinate metabolism in *P. putida* KT2440. The EMP pathway (red), ED pathway (blue) and TCA cycle (green) are highlighted with different colors. Note the absence of any Pfk enzyme in the upper central metabolism. **Abbreviations**: F1P Fructose-1-Phosphate; FBP Fructose-1,6-bisphosphate; F6P Fructose-6-Phosphate; G6P Glucose-6-phosphate; 6PG 6-phosphogluconate; 2K3D6P 2-keto-3-deoxy-6-phosphogluconate; Pyr Pyruvate; GA3P Glyceraldehyde-3-phosphate; DHAP Dihydroxyacetone phosphate; PEP Phosphoenolpyruvate; AcCoA Acetyl Coenzyme A; Mal Malate; OAA Oxaloacetate; Cit Citrate; 2OG 2-oxoglutarate; Suc Succinate; Fum Fumarate; FruBA PTS^{Fru} system; FruK 1-Phosphofructokinase; GlK Glucokinase; GnuK Glucokinase; Gcd glucose dehydrogenase; Fbp Fructose-1,6-bisphosphatase; Pgi Glucose-6-phosphate isomerase; Zwf-1 Glucose-6-phosphate 1-dehydrogenase; Edd Phosphogluconate dehydratase; Eda Keto-hydroxyglutarate-aldolase/keto-deoxy-phosphogluconate aldolase; Fda fructose-1,6-bisphosphate aldolase; TpiA Triosephosphate isomerase; Gap Glyceraldehyde-3-phosphate dehydrogenase; Pgk phosphoglycerate kinase; Eno phosphopyruvate hydratase; Pcc phosphoenolpyruvate carboxylase; MaeB Malic enzyme; Pyk pyruvate kinase; Mdh malate dehydrogenase; AceE Pyruvate dehydrogenase subunit E1; AceF dihydrolipoamide acetyltransferase; LpdA lipoamide dehydrogenase; AccC-2 pyruvate carboxylase subunit A; OadA pyruvate carboxylase subunit B; FumC fumarate hydratase; SdhABCD succinate dehydrogenase; SucA 2-oxoglutarate dehydrogenase E1 component; KgdB; SucC succinyl-CoA synthetase subunit beta; SucD succinyl-CoA synthetase subunit alpha; KgdB dihydrolipoamide succinyltransferase; AcnA aconitate hydratase; AcnB bifunctional aconitate hydratase 2/2-methylisocitrate dehydratase; Icd isocitrate dehydrogenase; GltA type II citrate synthase.

(Edd), catalyzes a dehydration of 6-phosphogluconate to form 2-keto-3-deoxy-6-phosphogluconate (2K3D6P), then 2K3D6P aldolase (Eda), catalyzes an aldol cleavage to form pyruvate and glyceraldehyde 3-phosphate (GA3P). Finally, the triose phosphates intermediates is further metabolized by the glycolytic pathway to provide energy through TCA cycle (Peekhaus *et al*, 1998).

Mutants deficient in activities of the two ED pathway enzymes have been isolated in *P. putida*, *P. aeruginosa*, *E. coli*, etc (Lessie and Phibbs, 1984). In *Pseudomonas* species, mutants blocked in the ED pathway were unable to utilize glucose or gluconate. These phenotypic observations are in agreement with the absence of the 6-phosphofructokinase discussed above. In contrast, *E. coli* mutants grow normally on glucose and retained the capacity to utilize gluconate *via* the PP route. That reflects in part the large differences between *E. coli* and *Pseudomonas* species (Lessie *et al*, 1984).

Although the catabolism of carbohydrates in *P. putida* has been studied since the 70`s, there are many phenomena that depend on carbon source and metabolic pathways involved in its degradation that have not been properly explained. Thus, one of the aims of this Thesis was to determine at a quantitative level the metabolic steps involved in the degradation of carbohydrates in *P. putida* so establishes the basis for understanding other phenomena dependent on carbon source.

2. Transcriptional factors involved in regulation of central carbon metabolism of bacteria

2.1. Transcriptional factor *vs* central metabolism

The genome of *E. coli* possesses more than 300 potential regulators that can control cell activity at the transcriptional level. However, only half of these have been studied and experimentally verified (Browning and Busby, 2004). Some of these transcriptional factors simultaneously regulate large numbers of genes (global regulators), while others control just one or two genes (local regulators). There are seven specific transcriptional factors called global regulators (Crp, Fnr, IHF, Fis, ArcA/ArcB ,NarL and Lrp) since they control 50% of all the regulated genes in the cell. On the other hand, around 60 transcriptional factors control only a single promoter (Browning *et al*, 2004).

The mechanism of regulation of the transcriptional factors involves the binding of the protein to one or more operators in the promoter region, which makes transcription be activated or repressed. In fact, some transcription factors works exclusively as activators or repressors, while others can function as dual regulators. A computational analysis of the model species *E. coli* suggests that of the 300 potential regulators found in its genome 35% are activators, 43% repressors and 22% dual regulators (Zhou and Yang, 2006). Despite many studies of the use of metabolic pathways and central enzymes, their regulation is still poorly understood (Blencke *et al*, 2003). Nowadays, it is known that central metabolism in bacteria is controlled through the interplay of global and local regulators, the outcome of which depends on the nature of the carbon and energy sources and the specific culture conditions. In past years several works have been published that report regulation of gene expression of central metabolic genes due to different transcripcional factors. Some of the most important are briefly described below:

[i] the ArcB/ArcA two-component signal transduction system that functions as the aerobiosis-sensing device that regulate the activity of catabolic pathways depending of the redox conditions. Upon signal perception, ArcB is phosphorylated, and the phosphoryl group is subsequently transferred to ArcA (Georgellis *et al*, 1997). The extent of phosphorylation of ArcA determines the expression of operons involved in a wide variety of (mostly) catabolic pathways that are operative under different redox growth conditions (Bekker *et al*, 2010);

[ii] The catabolic repressor Crp that is a global transcriptional regulator that is involved in the regulation of an important number of genes (*e.g. pts* genes in *E. coli*); it is activated by adenylate cyclase (Cya)-synthesized cAMP (Gosset *et al*, 2004);

[iii] Fnr is a global regulator that controls transcription of genes whose functions facilitate adaptation to growth under O_2 limiting conditions (Unden *et al*, 2002; Unden and Schirawski, 1997);

[iv] the cAMP-independent catabolite repressor-activator Cra which is a dual transcriptional regulator that controls the carbon flow in *E. coli* (Saier and Ramseier, 1996) and,

[v] the global repressor Mlc that controls transcription of genes involved in carbohydrate utilization, such as the phosphoenolpyruvate PEP:glucose phosphotransferase (PTS) system (Plumbridge, 2002).

As the regulation by Cra in *P. putida* is studied in this work, there will be a more detailed

description of the role that this regulator exerts in bacteria in the next section.

2.2. Regulatory duties of the catabolite repressor/activator (Cra) protein in central carbon metabolism of bacteria

The catabolite repressor/activator (Cra) protein (also known as FruR) is a pleiotropic regulatory protein that plays a key role in the control of carbon flow in *E. coli* and *Salmonella typhimurium* (Saier *et al*, 1996). This factor was first identified as a repressor that inhibited expression of the fructose operon of these two bacteria when the sugar was not available -thereby the earlier name FruR (Ramseier *et al*, 1993). Later work, however, revealed that the same protein represses genes for many other enzymes of the central metabolism (*pfkA*, *pykA*, *pykF*, *acnB*, *edd*, *eda*, *mtlADR* and *gapB*; (Bledig *et al*, 1996; Ow *et al*, 2007; Saier *et al*, 1996; Sarkar *et al*, 2008) and activates others (*ppsA*, *fbp*, *pckA*, *acnA*, *icd*, *aceA*, and *aceB*; (Cortay *et al*, 1994; Negre *et al*, 1998; Prost *et al*, 1999; Ramseier *et al*, 1996; Saier *et al*, 1996), suggesting a dual character of Cra as both a transcriptional repressor and an activator. Therefore, Cra apparently controls the direction of carbon flow in *E. coli* and consequently influences the rates of utilization of dozens of exogenous carbon sources.

From a structural point of view, the Cra protein has been classified as a member of the GalR-LacI superfamily of DNA-binding transcriptional regulators (Penin *et al*, 1997; Scarabel *et al*, 1995). In *E. coli*, the Cra monomer is organized in two functional domains. The N-terminal helix-turn-helix module accounts for the binding of the protein to the cognate DNA operator sequence, while the C-terminal portion mediates the interactions between subunits and triggers changes in the protein upon effector binding (Scarabel *et al*, 1995). Earlier studies on the Cra proteins of *E. coli* and *S. typhimurium* suggested that the regulator is a tetramer (see Fig. 2) that recognizes an imperfect palindromic DNA sequence to which it binds asymmetrically (Saier *et al*, 1996).

It is generally believed that promoters containing a Cra operator upstream of the RNAP binding site might become activated by the factor, thereby stimulating transcription of downstream genes. In contrast, Cra binding sites overlapping those bound by RNA polymerase originate a typical negative regulation scenario (Saier *et al*, 1996). Whether positive or negative, the effects of Cra on transcription can be counteracted *in vitro* by

micromolar concentrations of fructose-1-phosphate (F1P) or millimolar concentrations of fructose-1,6-bisphosphate (FBP; Ramseier *et al*, 1995). In fact, the nature of the metabolic effector(s) alleged to make(s) Cra release target DNA sites is intriguing. This is because F1P and FBP can be originated by different metabolic routes and produced at levels that depend on the consumed carbon source. Furthermore, electronic densities of these two chemicals are not alike, making it improbable that the same effector-recognition pocket can bind both of them.

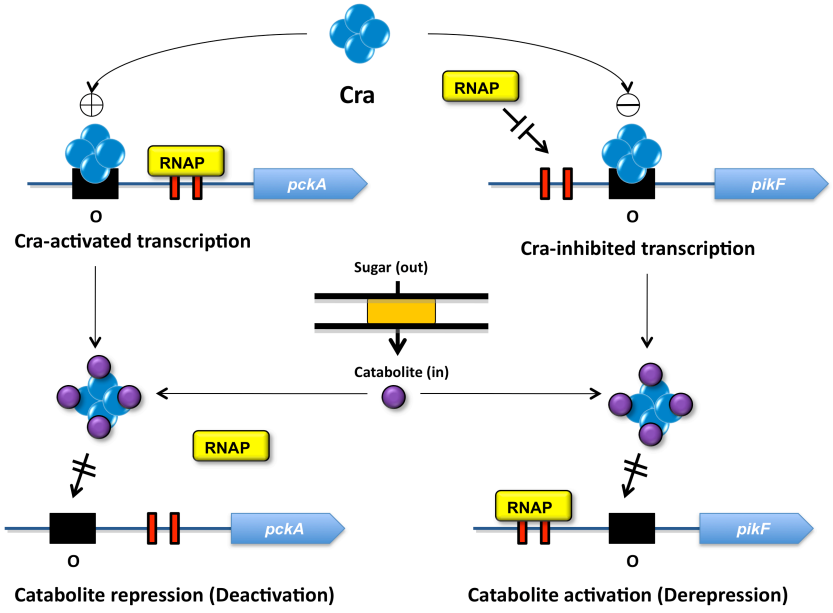

Figure 2. Model of the sensory transduction pathway for Cra-mediated catabolite repression and catabolite activation in *E. coli*. In this species Cra protein binds to the operator as a tetramer, where it can activate or repress the transcription. In presence of the catabolic effector (lower panel), the protein change its conformation and is unable to bind to the operator, which produces deactivation or derepression of the transcription.

Conflicting publications on this matter bear witness of such a problem in the relevant literature. Gel retardation experiments with a labeled DNA fragment bearing a Cra operator (Bledig *et al*, 1996; Ramseier *et al*, 1993) could authenticate F1P as one *bona fide* effector, but not FBP. Some studies suggest that the *in vitro* response of Cra to FBP is due to a possible contamination of FBP with F1P (Ramseier *et al*, 1993). Yet, other authors argue that FBP is an authentic effector of Cra (Bledig *et al*, 1996; Kotte *et al*, 2010). The state of affairs at this point is, therefore, that of uncertainly on the role of FBP as agonist

of the Cra regulator (that F1P is one seems to be beyond question). Besides uncertain role of the FBP, studies of Cra regulation have been reported just in enterobacteria, while in other species such as *P. putida* the Cra regulation remains unknown.

3. Phosphoenolpyruvate PEP:carbohydrate phosphotransferase system (PTS) in bacteria

3.1. Carbohydrate PTS system

The phosphoenolpyruvate PEP:carbohydrate phosphotransferase system (PTS) was discovered in *E. coli* by Kundig, Ghosh, and Roseman as a device that phosphorylates a number of carbohydrates (Kundig *et al*, 1964). Later, it was demonstrated that the PTS is a transport system that catalyzes the intake of several sugars and their conversion to the respective phosphoesters. The common features of this phosphotransferase system included [i] the use of phosphoenolpyruvate (PEP) as the phosphoryl donor for sugar phosphorylation and [ii] the presence of three essential catalytic entities, termed enzyme I, enzyme II, and HPr (heat-stable, histidine-phosphorylatable protein; Saier and Reizer, 1994). Specifically, enzymes I (EI) and HPr are cytoplasmic energy-coupling proteins, which lack sugar specificity, and membranous enzyme II (EII) is specific for one or a few sugars. Actually, the enzyme II is a complex that consist of three proteins or protein domains, namely, EIIA, EIIB, and EIIC. Phosphoryl relay proceeds sequentially from PEP to EI, HPr, EIIA, EIIB, and finally, the incoming sugar, which is transported across the membrane *via* the integral membrane EIIC porter (Fig. 3). Currently, we know that PTS proteins are present in a large number of bacteria where we can find transport systems for glucose, fructose, maltose, mannose and many more sugars (Deutscher *et al*, 2006). It is interesting that the most widely distributed PTS system (see Fig. 4) is the fructose-specific PTS (PTS^{Fru}) or fructose operon. Many evolutionarily divergent genera (*e.g.*, *Azospirillum, Fusobacterium, Lactobacillus, Listeria, Pseudomonas, Rhodobacter, Streptomyces*, etc.) possess the PTS^{Fru} system, but they apparently cannot phosphorylate other sugars *via* the PTS. This would suggest that this PTS system is the ancestral and all the other are derived from it (Saier *et al*, 1996).

The very first function that was asigned to the PTS systems, was its participation in sugar transport and phosphorylation. Today, we know that besides sugar reception, transport, and phosphorylation, this system in involved in several regulatory roles in the

cell including cell division, chemoreception, central metabolism, pathogenesis, flagellar motility, the control of 54-dependent transcription of several metabolic genes and others (Deutscher *et al*, 2006; Postma *et al*, 1993).

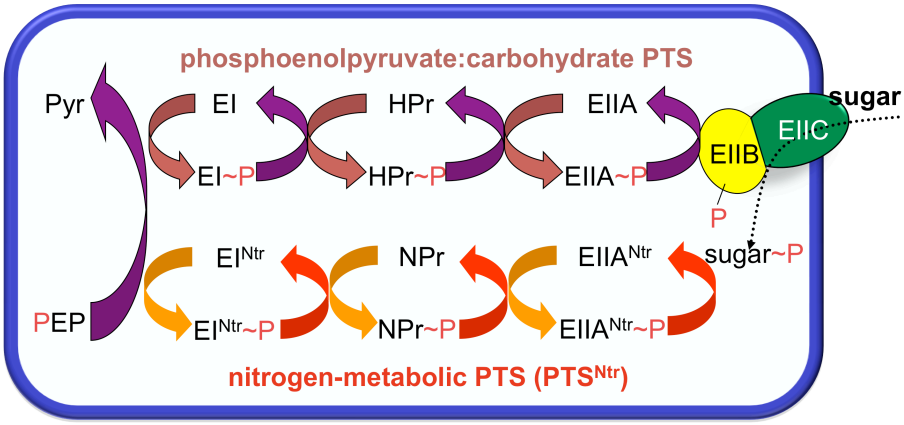

Figure 3. PTS systems in bacteria. The PTS systems are formed by three essential enzymes called EI, HPr an EIIA. Enzymes I (EI) and HPr are cytoplasmic proteins, which lack sugar specificity, and enzyme II (EII) usually is a complex that consist of three proteins or protein domains, namely, EIIA, EIIB, and EIIC. In all cases, PEP acts as phosphoryl donor for sugar phosphorylation. Moreover, many bacteria possess a PTS system that is not involved in sugar transport (PTS^{Ntr}) which is discussed in the next section.

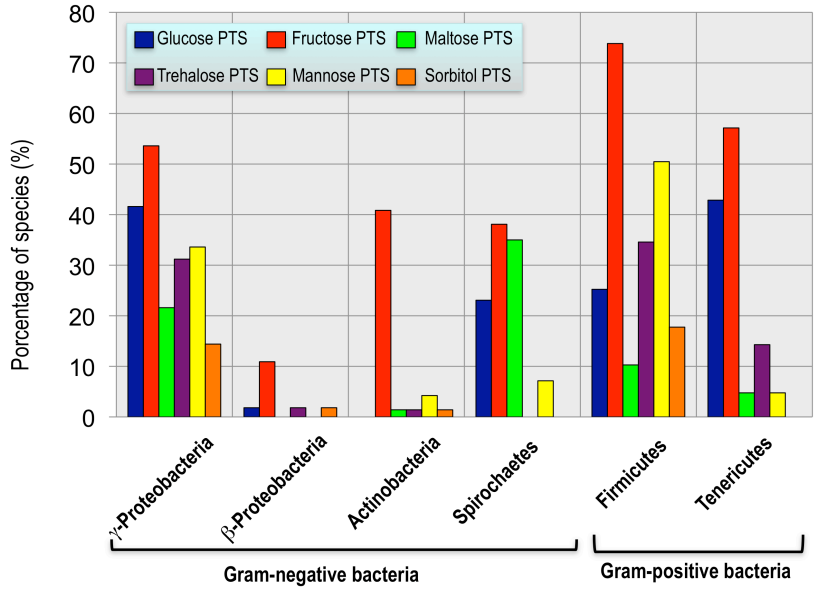

Figure 4. Presence of PTS systems in bacteria. Many evolutionarily divergent genera (but not all) possess the fructose-specific PTS or fructose operon. They may also have the genes for phosphorylate other sugars *via* PTS. It is clear that the PTS^{Fru} is the most conserved PTS system in bacteria. The y-axis represents the porcentage of species in each genera that report the presence of the respective PTS system. The information was obtained from KEGG database.

3.2. Nitrogen PTS (PTS^{Ntr}) system in bacteria

In addition to the carbohydrate PTS, *E. coli* and many other bacteria contain a parallel PTS called nitrogen PTS system (PTS^{Ntr}, see Fig. 3). This system is formed by the EI^{Ntr} (PtsP) protein (Rabus *et al*, 1999), a HPr (Npr or PtsO) homologue (Jones *et al*, 1994; Powell *et al*, 1995) and the $EIIA^{Ntr}$ (PtsN) protein (Powell *et al*, 1995). The phosphorylation chain starting from PEP through EI^{Ntr} → NPr → $EIIA^{Ntr}$ is highly specific. Yet, it has been reported in *E. coli* (Powell *et al*, 1995; Zimmer *et al*, 2008) and other species (Pfluger and de Lorenzo, 2008) that the system exhibits cross-reactivity with the carbohydrate PTS system. A clear difference between the two PTS systems, is that permease components are absent in the nitrogen related set, ruling out its participation in sugar intake (Velazquez *et al*, 2007). Owing that *ptsN* and *ptsO* genes form an operon with the *rpoN* gene (encoding the sigma factor of RNA polymerase, σ^{54}), the involvement of PtsN/PtsO proteins with nitrogen regulation has been suggested, leading to the designation nitrogen PTS (Powell *et al*, 1995). Multiple phenotypes associated to PTS^{Ntr} proteins (specially to PtsN) suggest that the PTS^{Ntr} system strongly participates in regulation of several metabolic functions in the cell (Cases *et al*, 2001a; Cases *et al*, 2007; Lee *et al*, 2007; Luttmann *et al*, 2009; Pfluger and de Lorenzo, 2007; Reizer *et al*, 1992; Velazquez *et al*, 2007). For example, in *E. coli*, the *ptsN* mutant reduced its capabilities to utilize certain amino acids as nitrogen source when glucose was the substrate (Powell *et al*, 1995). Moreover, the *ptsN* strain showed a mucoidy character in the presence of glucose with Arg, His, or Pro which is similar to the observations made in a *ntrC* mutant (Ninfa, 2007). On the other hand, growth experiments with leucine-containing peptides indicated that *ptsP* and *ptsO* mutants tolerate these compounds while wild type strain and *ptsN* mutant are sensitive to their presence (Lee *et al*, 2005). The resistance of *ptsO* and *ptsP* strains was explained by the ability of the nonphosphorylated-PtsN to endure the intracellular accumulation of leucine which is a potent feedback inhibitor of acetolactate synthase (*ilvB*), a key enzyme for the biosynthesis of valine and isoleucine (Lee *et al*, 2005). This result (in addition to the finding that the expression of the *ilvB* depends on the presence of nonphosphorylated-PtsN) strengthens the idea that the nitrogen PTS links the regulation of carbon and nitrogen metabolism (Commichau *et al*, 2006). Furthermore, it has been demonstrated that the dephosphorylated PtsN (but not its phosphorylated form), forms a tight complex with TrkA that inhibits the accumulation of high intracellular concentrations of K^+ (Lee *et al*, 2007). The high K^+ concentration (in the

ptsN mutant) produces the sensitivity of *E. coli* to Leucine or Leucine containing peptides (LCPs) by inhibiting the expression and activity of acetolactate synthase (Lee *et al*, 2007).

Yet, the cases of toxicity of leucine and the regulation of K^+ uptake are just two of the few that have been elucidated: the majority of the mechanisms behind the multiple phenotypes associated to PTS^{Ntr} proteins remain poorly understood. Examples of processes controlled directly or indirectly by PTS^{Ntr}, which the mechanism remains unexplained included: the supression by *ptsN* and the effects of a lethal σ^E mutation in *E. coli* (Powell *et al*, 1995), the effects of PTS^{Ntr} proteins in accumulation of polyhydroxyalkanoates (PHAs) in *P. putida* (Velazquez *et al*, 2007), the involvement of *ptsN* in the utilization of organic nitrogen sources in *P. aeruginosa* (Jin *et al*, 1994), the requirements of *ptsP* for replication in host cells and thereby for virulence in *Legionella pneumophila* (Edelstein *et al*, 1999) and others. Moreover, other key questions remain unanswered, *e.g.* where the phosphate goes after $EIIA^{Ntr}$ or which is the metabolic signals that are recognized by the PTS^{Ntr} system?. In our laboratory, we are working to answer these questions and understand the functions of the PTS in bacteria, specifically in the soil bacterium *P. putida*. Some of our findings in *P. putida* are summarized in the next section.

3.3. PTS systems in *P. putida*

In *P. putida*, one sugar-specific PTS for fructose transport (FruA/EIIBC and FruB/EI-HPr-EIIA) coexists with the PTS^{Ntr} ($PtsP/EI^{Ntr}$, PtsO/NPr, and $PtsN/EIIA^{Ntr}$), which, while keeping the core phosphotransfer domains, lacks the EIIBC modules that make the connection to sugar intake (Fig. 5, Pfluger *et al*, 2007; Velazquez *et al*, 2007). As discussed above, the high energy phosphate is derived in both systems from phosphoenolpyruvate (PEP) and then transferred from EI via HPr/NPr to the EII enzymes (Fig. 5; Postma *et al*, 1993). In *P. putida*, it was shown that the PTS^{Fru} and the PTS^{Ntr} do not represent two completely separated systems, since they do communicate under specific conditions with each other *in vivo* by the exchange of phosphate moieties (Fig. 5; Pfluger *et al*, 2008). This interaction, which was postulated for a long time on the basis of *in vitro* experiments with the purified proteins (Powell *et al*, 1995), is not restricted to the special case of *P. putida*, where one PTS of each type is present, but was also observed *in vivo* in *E. coli* (Zimmer *et al*, 2008) and is probably a common principle.

In *P. putida*, global expression analysis using two-dimensional gel electrophoresis has indicated that *ptsN* affects numerous proteins, comprising 5–9% of all proteins analyzed (Cases *et al*, 2001a). Of these, a small number are regulated by glucose, and, of this small set, some are regulated from σ^{54}-dependent promoters. A much larger number of proteins regulated by *ptsN* were unrelated to control by glucose or σ^{54}. Thus, the broad conclusion is that *ptsN* controls numerous genes, most likely by a variety of different mechanisms.

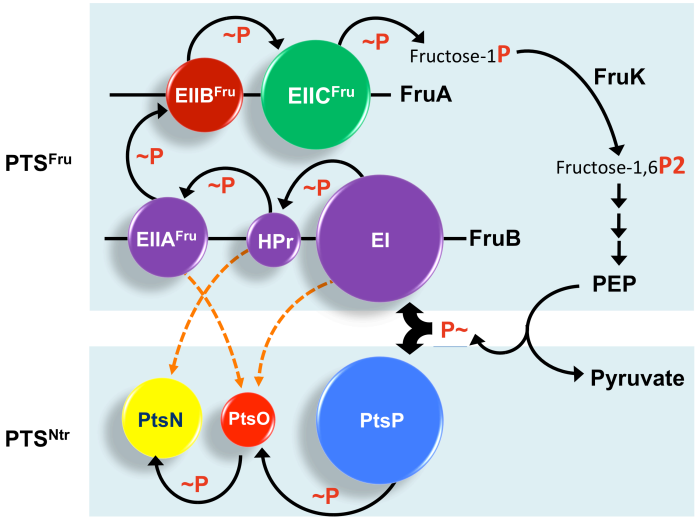

Figure 5. PTS systems in *P. putida*. In *P. putida*, one specif sugar PTS for fructose transport PTS^{Fru} coexists with one PTS^{Ntr}. The PTS^{Fru} is formed by FruA/EIIBC and FruB/EI-HPr-EIIA and FruK while PTS^{Ntr} is formed by PtsP/EI^{Ntr}, PtsO/NPr, and PtsN/$EIIA^{Ntr}$. In both systems the high-energy phosphate is originated in phosphoenolpyruvate (PEP) and then transferred from EI via HPr/NPr to the EII enzymes.

Mutants of *P. putida* lacking one or more PTS^{Ntr} proteins display a number of phenotypes (Cases *et al*, 2001a; Cases *et al*, 1999; Cases *et al*, 2001b; Pfluger *et al*, 2007; Pfluger-Grau *et al*, 2011; Velazquez *et al*, 2007). For instance, the PTS^{Ntr} proteins are involved in regulation of accumulation of PHAs, a storage compound accumulated mainly under conditions of carbon overflow and nitrogen limitation (Velazquez *et al*, 2007). According to the putative sensory function of PTS^{Ntr}, mutants in these proteins show different growth phenotypes when cultivated on various carbon and nitrogen sources (Velazquez *et al*, 2007). On the other hand, the PTS^{Ntr} proteins are involved in regulation of the toluene degradation pathway by tuning the activity of the *m*-xylene responsive *Pu* promoter of the pWW0 plasmid (Cases *et al*, 1999; Cases *et al*, 2001b). More recently, it was shown that the non-phosphorylated form of PtsN directly

downregulates pyruvate dehydrogenase (PDH) activity, an enzymatic complex responsible for the decarboxylation of pyruvate to acetyl-CoA, thereby linking glycolysis to the TCA cycle (Pfluger-Grau *et al*, 2011). In the same way as in other bacteria, most of the mechanisms by which PTS^{Ntr} proteins control some processes remain obscure in *P. putida*. As part of the phenotypes observed in PTS^{Ntr} mutants could be explained by an effect on central metabolism, one of the aims of this Thesis was to analyze the flow distribution in central metabolism in various PTS mutants of *P. putida*.

4. The issue at stake

To take full advantage of living organisms for biotecnological purposes, we need to understand the complex mechanism of life as best as possible. The machinery of life is better understood in some species that have been studied more extensively and that the scientific community called as model organisms (such as *E. coli*). However, other species with very interesting features that can be exploited in bioremediation, biocatalysis or as cell factories are much less known. This is the case of *P. putida*, a bacterium that presents the same advantages that *E. coli* in laboratory handling (no pathogenic, genetic tools available, etc) but also it offers robustness, remarkable adaptability to different environments and a large collection of enzymes in its genome encoding for metabolic pathways that are not included in other bacterial species. These characteristics distinguish *P. putida* as an ideal organism as cell factory.

There is extensive evidence that the environmental niche of each bacterium has shaped the metabolism, sensory systems, regulators, etc, to co-adapted to requirements and lifestyle of each organism. Therefore, to use *P. putida* efficiently in biotechnological process we need to study the performance of its metabolic machinery without generalizing the observations made in model organisms. With this idea in mind, we have focused on investigating possible regulatory effects of PTS proteins on carbon central metabolism in *P. putida*. To adress this point, we need a proper understanding of the carbon central metabolism of this bacterium. To this end, we have investigated the regulation exerted on PTS systems by the catabolic repressor/activator (Cra) regulator, which is known to control several metabolic genes in *Escherichia coli* and *Salmonella typhimurium*. In this context, in this work we have addressed the following objectives.

II. OBJECTIVES

General objetive:

To investigate the regulation of PTS systems (PTS^{Fru} and PTS^{Ntr} systems) of *P. putida* as well as its conection with central carbon metabolism.

Through the following specific objetives:

1. To analyze the main metabolic routes and carbon flow in central metabolism of *P. putida*.

2. To study the interplay between the PTS systems and carbon central metabolism.

3. To study the regulation exerted by the catabolic repressor/activator (Cra) regulator on PTS systems of *P. putida*.

III. MATERIALS AND METHODS

1. General procedures

1.1. Bacterial strains

Strains of *Pseudomonas putida* and *Escherichia coli* used in this study are described in Table 1, together with their most relevant characteristics.

Table 1. Strains of *P. putida* and *E. coli*.

Strain	Relevant characteristics	Source/Reference
***P. putida* strains**		
mt-2	*P. putida* wild type with TOL (pWW0) plasmid	Williams and Murray, 1974
KT2440	Strain derived of *P. putida* mt-2 without the pWW0 plasmid	Nelson *et al*, 2002
MAD2	Tel^R, Rif^R. Variant of *P. putida* KT2440, with a *Pu-lacZ* transcriptional fusion along with the constitutive *xylRΔA*$^+$ allele of the *xylR* regulator of the pWW0 plasmid assembled in a mini-*Tn5* vector	Fernandez *et al*, 1995
MAD2 *fruB::xylE*	Tel^R, Rif^R. Derivative of *P. putida* MAD2 carrying a directed chromosomal insertion of the *xylE* marker in *fruB*, replacing a 1.5 kb internal fragment	Cases *et al*, 2001
MAD2 *ptsO::km*	Tel^R, Rif^R, Km^R. Derivative of *P. putida* MAD2 carrying a directed chromosomal insertion of a Km resistance cassette in *ptsO*	Cases *et al*, 2001
MAD2 *ptsP::km*	Tel^R, Rif^R, Km^R. Derivative of *P. putida* MAD2 carrying a directed chromosomal insertion of a Km resistance cassette in *ptsP* replacing a 249 bp internal fragment	Cases *et al*, 2001
MAD2 *ptsN::km*	Tel^R, Rif^R, Km^R. Derivative of *P. putida* MAD2 carrying a directed chromosomal insertion of a Km resistance cassette in *ptsN*	Cases *et al*, 1999
MAD2 *ptsN::xylE, ptsO::km*	Tel^R, Rif^R, Km^R. Derivative of *P. putida* MAD2 carrying a directed chromosomal insertion of a *xylE* marker in *ptsN* and Km resistance in *ptsO*	Cases *et al*, 2001

MAD2 *ptsP::km, fruB::xylE*	Tel^R, Rif^R, Km^R. Derivative of *P. putida* MAD2 carrying a directed chromosomal insertion of a Km resistance cassette in *ptsP* and a *xylE* marker in *fruB*	Cases *et al*, 2001
MAD2 *ptsNHA*	Tel^R. Derivative of *P. putida* MAD2 in which His in position 68 has been replaced by an Ala (A68) residue in the amino acid sequence of PtsN protein	Pfluger-Grau *et al*, 2011
MAD2 *ptsNHE*	Tel^R. Derivative of *P. putida* MAD2 in which His in position 68 has been replaced by a Glu (E68) residue in the amino acid sequence of PtsN protein	Pfluger-Grau *et al*, 2011
MAD2 *eda::xylE*	Tel^R, Rif^R. Derivative of *P. putida* MAD2 carrying a directed chromosomal insertion of the *xylE* marker in *eda*	Velazquez *et al*, 2004
KT2440 Δ*cra*	Derivative of *P. putida* KT2440 with a complete deletion of *cra* gene	This work
KT2440 Δ*cra* Δ*ptsP*	Derivative of *P. putida* KT2440 with a complete deletion of *cra* and *ptsP* genes	This work
KT2440 Δ*ptsP*	Derivative of *P. putida* KT2440 with a complete deletion of *ptsP* gene	This work
KT2440 Δ*fruB*	Derivative of *P. putida* KT2440 with a complete deletion of *fruB* gene	This work
KT2440 *eda::km*	Km^R, Rif^R. Derivative of *P. putida* KT2440 carrying a chromosomal insertion of a mini-*Tn5* Km in *eda*	Duque *et al*, 2007
KT2440 *tpiA::km*	Km^R. Derivative of *P. putida* KT2440 carrying a chromosomal insertion of a mini-*Tn5* Km in *tpiA*	V. dos Santos
KT2440 *zwf-1::km*	Km^R, Rif^R. Derivative of *P. putida* KT2440 carrying a chromosomal insertion of a mini-*Tn5* Km in *zwf-1*	Duque *et al*, 2007
KT2440 *pgi::km*	Km^R, Rif^R. Derivative of *P. putida* KT2440 carrying a chromosomal insertion of a mini-*Tn5* Km in PP1808 (*pgi*)	Duque *et al*, 2007
KT2440 *pgi2::km*	Km^R, Rif^R. Derivative of *P. putida* KT2440 carrying a chromosomal insertion of a mini-*Tn5* Km in PP4701 (*pgi*)	Duque *et al*, 2007
KT2440 *edd::km*	Km^R, Rif^R. Derivative of *P. putida* KT2440 carrying a chromosomal insertion of a mini-Tn5 Km in *edd*	Duque *et al*, 2007

KT2440 *gnd::km*	Km^R, Rif^R. Derivative of *P. putida* KT2440 carrying a chromosomal insertion of a mini-Tn5 Km in *gnd*	Duque *et al*, 2007
***E. coli* strains**		
CC118	Δ(*ara-leu*), *araD*, Δ*lacX74*, *galE*, *galK*, *phoA*, *thi1*, *rpsE*, *rpoB*, *argE*, *recA1*	Manoil and Beckwith, 1985
CC118λ*pir*	CC118 λ*pir* phage lysogen	Herrero *et al*, 1990
DH5α	F^- Φ80 *lacZ*ΔMΔ15 (*lacZYA-argF*), U169, *recA1*, *endA1*, *hsdR17*, *R-M+*, *supE44*, *thil*, *gyrA*, *relA1*	Hanahan, 1983
DH5αλ*pir*	DH5α λpir phage lysogen	Lab collection
W3110	K12, F^-, IN (*rrnD-rrnE*)	Bachmann, 1987
BL21 (DE3)	$F^–$ *ompT gal dcm lon hsdSB* (rB^- mB^-) λ (DE3 [*lacI lacUV*5-T7 gene 1 *ind1 sam7 nin5*])	Novagen

1.2. Media and culture conditions

P. putida and *E. coli* strains were cultured at 30 °C and 37 °C, respectively, in an orbital shaker at 170 rpm. The rich medium used to grow all strains of this study was Luria-Bertani (LB) as described in Sambrook *et al.* (1989). Cultures on solid medium were performed with LB medium supplemented with Bacto Agar (Pronadisa) 1.5% (w/v). When needed, we added 5-bromo-4-chloro-3-indolyl-β-D-galactopyranoside (X-gal) at a concentration of 0.08 mM, and isopropyl-1-thio-β-galactopyranoside (IPTG) to a concentration between 0.5 and 1 mM. Moreover, different strains of *P. putida* were also cultivated, when it was appropriate in minimal medium M9 (Miller, 1972), supplemented with glucose, fructose or succinate as carbon source (0.2% w/v).

Concentrated solutions of different carbon sources were sterilized by autoclaving and added to the medium aseptically. The solid minimal medium cultures were performed by supplementing the M9 medium and carbon source (0.2% w/v) with 1.5% Bacto Agar (w/v). Antibiotics were prepared in concentrated solutions (1000x), were sterilized by filtration and stored at -20 °C. The final concentrations of each antibiotic were: ampicillin (Ap, 150 μg/ml, or 500 μg/ml for *P. putida*), kanamycin (Km, 50 μg/ml), potassium tellurite (Tel, 80 μg/ml) and tetracycline (Tc, 10 μg/ml).

During periods of less than one month, the strains were stored at 4 °C on LB or minimal medium agar plates. For long-term preservation, the bacteria were frozen in the culture medium corresponding to 20% glycerol (v/v) and kept at -80 °C. Growth in liquid medium was followed by turbidometry at 600 nm (OD_{600}) using an Ultrospec-3000 pro or to 595 nm in a Victor 2 multichannel spectrophotometer (Perkin Elmer).

1.3. Plasmids

Table 2 shows the plasmids used in this Thesis and its main features.

Table 2. Plasmids used in this work.

Plasmid	Characteristics	Reference
pVLT31	Tc^R, Broad-host-range plasmid based on lacIq/Ptrc	de Lorenzo *et al*, 1993
pVLT31*pfkA*	Tc^R, pVLT31 plasmid with *pfkA* sequence from *E. coli* W3110 cloned in the polylinker as a 963 bp KpnI-HindIII fragment. The cloned sequence included the Ribosomal Binding Site (RBS) from pTrc99A vector (AGGAAA)	This work
pVLT31*ptsN_Etag*	Tc^R. The plasmid carries a variant of the *ptsN* gene with a short E-tag epitope added in its C-terminus	Pfluger and de Lorenzo, 2007a
pET28a(+)	Km^R. The plasmid carries a N-terminal His-Tag/thrombin/T7-Tag configuration in addition to an optional C-terminal His-Tag sequence	Novagen
pET28a(+)*cra*	Km^R. pET28a(+) plasmid with *cra* sequence from *P. putida* KT2440 cloned as NdeI/XhoI fragment	This work
pSW	Ap^R, *ori*RK2, *xylS*, *Pm*→*I-sceI*	Wong and Mekalanos, 2000
pEMG	Km^R, *ori*R6K, *lacZ*α with two flanking I-SceI sites	Martínez-García and de Lorenzo, submitted

pEMGΔ*cra*	pEMG bearing a 1000 bp TS1-TS2 EcoRI-BamHI insert for *cra* deletion	This work
pEMGΔ*ptsP*	pEMG bearing a 1600 bp TS1-TS2 BamHI-XbaI insert for *ptsP* deletion	This work
pEMGΔ*fruB*	pEMG bearing a 1000 bp TS1-TS2 EcoRI-BamHI insert for *fruB* deletion	This work
pSEVA221	Km^R, *oriRK2, oriT*. Standard broad-host range cloning plasmid	Lab collection
pUJ9	Ap^R, *ori*ColE1, promoter probe vector, *lacZ* fusion	de Lorenzo *et al*, 1990
pUJ9P_{fruB}	Vector derivative from pUJ9 with *fruB* promoter cloned as an 586 bp EcoRI/BamHI fragment	This work
pMCH1	Km^R, *oriRK2, oriT*, *lacZ*. pSEVA221 inserted with a EcoRI-HindIII fragment from pUJ9P_{fruB} bearing a P_{fruB}-*lacZ* translational fusion	This work
pMCH2	Km^R, *oriRK2, oriT, lacZ*. Plasmid derivative from pMCH1 in which EcoRI-BamHI fragment (*fruB* promoter, 586 bp) was replaced by *cra* promoter fragment (376 bp) bearing a P_{cra}-*lacZ* translational fusion	This work
pMCH3	Km^R, *oriRK2, oriT, lacZ*. pSEVA221 inserted with a BamHI-HindIII fragment from pUJ9. This plasmid corresponds to the negative control for experiments with pMCH1 and pMCH2 plasmids.	This work

1.4. Cell transformation

Cells of *E. coli* were made competent for transformation with the RbCl method (Sambrook, 1989) or by electroporation (Wirth *et al*, 1989). For *P. putida* strains, electrocompetent cells were produced by washing them at room temperature with 300 mM sucrose (Choi *et al*, 2006). Electroporation was performed with a Gene Pulser/Pulse Controller (Bio-Rad) system using the following conditions: 2.5 kV, 25 μF, 200 ohms.

1.5. DNA manipulation methods

Techniques used for preparation and manipulation of DNA have been described by Sambrook *et al.* (1989). Restriction endonucleases were purchased from New England

Biolabs. Digestions were always conducted at 37 °C for 2 h. For DNA ligation, enzymes T4 ligase (incubation by 12 h at 16 °C) or Quick Ligase (incubation by 5 min to room temperature) were used. In both cases a ratio 3/1 insert/vector was used. All enzymes were used according to manufacturer's specifications. The DNA fragments were purified using agarose gels, and the commercial kit QIAEX®II Gel Extraction, QIAGEN (Cat. # 20021). Genomic DNA from *P. putida*, used in PCR amplifications was obtained according to the protocol described by Murray and Thompson (1980) which uses extraction with cetyl trimethyl ammonium bromide (CTAB)/NaCl. Plasmid DNA was obtained with alkaline lysis with the QIAprep Spin Miniprep Kit QIAGEN (Cat. # 27106), according to the manufacturer's protocol.

1.6. Design of oligonucleotides

Polymerase Chain Reaction (PCR) primers were designed from the DNA sequence of interest using the analysis software Ape-A Plasmid Editor v1.12 (Copyright © 2003-2005, M. Wayne Davis). The hybridization temperature (Tm) in all cases was above 55 °C. The synthesis was carried out by Sigma-Genosys. All oligonucleotides used are listed in Table 3.

Table 3. Synthetic oligonucleotides used in this work for amplification of PCR products. The underlined sequences correspond to the restriction enzyme introduced in each case

Oligonucleotide	Sequence (5´-3')
PfkA-F (KpnI)	CGCGGGGTACCAGGAAAGATATAATGATTAAGAAAATCGGT
PfkA-R (HindIII)	CGCGGAAGCTTTTAATACAGAAAAAACGCGCAGTC
Cra-F (NdeI)	GGGAATTCCATATGAAACTCAGCGATA TCGCCCGT
Cra-R (XhoI)	CCGGCTCGAGTCAGGCCACTGAGAT
cra-TS1F (EcoRI)	CGGAATTCGGCCTCTTCGTAGCTGCCGGC
cra-TS1R	CAGCCCCGGTAATAACAAGGAAAATTCGACATGCGCCTGAT CGACACC
cra-TS2F	CGAATTTTCCTTGTTATTACCGGGGCTG
cra-TS2R (BamHI)	CGGGATCCATACACCAGGTCACGTGTTTGCG
cra/fruB-F	TCAGATTAAACGTTTCAGCTGC
cra/fruB-R	GCAGCTGAAACGTTTAATCTGA

ptsP-TS1F (BamHI)	CGGGATCCCCGCCCCACTCAGCCCCTGG
ptsP-TS1R	ACGGAGTTCGACCCCGAGCCGGGTGATGCTGTTTGTGCCG
ptsP-TS2F	GGCTCGGGGTCGAACTCCGT
ptsP-TS2R (XbaI)	GCTCTAGACCAGGGTGCCATTGAGGTAA
fruB-TS1F (EcoRI)	CGGAATTCCTCCAGATCCGGGAGAATGAAGCC
fruB-TS1R	AGAGTGAGGATCTTGGCCATGACCTTCTCCTTTTGCAGTT
fruB-TS2F	ATGGCCAAGATCCTCACTCT
fruB-TS2R(BamHI)	CGGGATCCCTGTCCAGGACTACCTTGAGGCC
pSW-F	GGACGCTTCGCTGAAAACTA
psW-R	AACGTCGTGACTGGGAAAAC
P*fruB*-F (EcoRI)	CGGAATTCCGAATTTTCCTTGTTATTACCGGGG
P*fruB*-R (BamHI)	CGGGATCCGCGGCAATACCAATGGC
P*cra*-F (EcoRI)	CGGAATTCGACCTTCTCCTTTTGCAGTTCCCGTTCGGG
P*cra*-R (BamHI)	CGGGATCCCTGATGCGCTGCTGTTCAGCCTTG

1.7. Design of *P. putida* mutants

Strains Δ*cra*, Δ*ptsP*, Δ*cra*Δ*ptsP* and Δ*fruB* were constructed using the method developed by Martínez-García and de Lorenzo (submitted). Primers *cra*-TS1F (EcoRI)/ *cra*-TS1R/ *cra*-TS2F/ *cra*-TS2R (BamHI)/ *fruB*-TS1F (EcoRI)/ *fruB*-TS1R/ *fruB*-TS2F/ *fruB*-TS2R (BamHI)/ *ptsP*-TS1F (BamHI)/ *ptsP*-TS1R/ *ptsP*-TS2F and *ptsP*-TS2R (XbaI) were used (Table 3) to amplify flanking regions (TS1, upstream and TS2, downstream) of genes *cra*, *ptsP* and *fruB* respectively. TS1 and TS2 regions of homology of 500-800 bp length were amplified with Vent DNA polymerase (Promega) and both fragments (TS1 and TS2) joined together by overlap extension (SOE)-PCR (Horton *et al*, 1989). The resulting 1.0-1.6-kb segments were purified as EcoRI-BamHI fragments (BamHI-XbaI for *ptsP*), ligated into the pEMG and transformed into *E. coli* DH5αλ*pir*. Candidate clones were confirmed by PCR and sequencing the entire TS1-TS2 insert. The resulting pEMGΔ*cra* pEMGΔ*ptsP*, pEMGΔ*fruB* vectors were isolated and electroporated in *P. putida* KT2440 (pSW).

The cointegrated Km^R clones were grown overnight in a 5 ml tube with LB medium, Ap 500 μg/ml and 15 mM 3-methylbenzoate as inducer and plated in LB. The individual colonies were restreaked in LB and LB+Km to check the lost of the cointegrated plasmid. Kanamycin-sensitive clones were analyzed by colony PCR for

identification of *cra*, *ptsP* and *fruB* deleted clones. Finally, pSW plasmid was eliminated after three consecutive passes in liquid LB. Elimination of the plasmid was verified in all the cases by direct colony PCR amplification, using the primers pair pSW-F and pSW-R.

1.8. Construction of *lacZ*-translational fusions

For gene expression studies, plasmids were constructed as follows. First, the sequence of the regulatoy region of *fruB* (284 bp before ATG), plus 100 aminoacids of the FruB protein was amplified by PCR using P*fruB*-F (EcoRI) and P*fruB*-R (BamHI) primers (Table 3). The 586 bp DNA fragment was digested as EcoRI-BamHI, ligated to the polylinker of the pUJ9 and the vector subsequently transformed in *E. coli* DH5α. Then, the vector was isolated, digested with EcoRI-HindIII enzymes, and the DNA band corresponding to fragment P_{fruB}*lacZ* was purified, cloned in the pSEVA221 and transformed in *E. coli* DH5α to obtain the vector pMCH1. This vector corresponds to a translational fusion P_{fruB}::*lacZ* which was electroporated in *P. putida* KT2440 and its mutant Δ*cra*.

On the other hand, to obtain the P_{cra}::*lacZ* translational fusion, the regulatory region of *cra* (284 bp before ATG), plus 30 aminoacids of Cra protein was amplified by PCR using P*cra*-F (EcoRI) and P*cra*-R (BamHI) primers (Table 3). The 376 bp DNA fragment was digested as EcoRI-BamHI, ligated to the polylinker of pMCH1 and the vector subsequently transformed in *E. coli* DH5α. This procedure replaced the P_{fruB} promoter from pMCH1 by P_{cra} promoter bearing the pMCH2 vector. Finally, this vector was electroporated in *P. putida* KT2440.

2. Metabolic Flux analysis

2.1. Determination of physiological parameters for metabolic flux analysis

For determination of physiological parameters, bacteria were grown at 30 °C in 500 ml baffled shake flasks with 50 ml synthetic M9 medium with glucose or fructose as C-source. Cell growth was monitored spectrophotometrically at 600 nm (OD_{600}) and glucose or fructose concentrations were determined enzymatically with the glucose (HK) assay kit (Sigma-Aldrich) or and the fructose kit (Enzytec) according to the suppliers' manuals, respectively. The following physiological parameters were determined by regression analysis during the exponential growth phase in the batch culture, as described elsewhere (Sauer *et al*, 1999): maximum specific growth rate, biomass yield on

glucose (or fructose, respectively), specific glucose (or fructose, respectively) consumption. The correlations factors (k) between cellular dry weight (CDW) and OD_{600} were determined from batch cultures of each mutant. Therefore, CDW was measured from at least four parallel 10 ml cell suspensions by harvesting the cells by fast filtration through pre-weight nitrocellulose filters (0.45 μm), which were subsequently washed with 0.9% NaCl and dried at 105 °C for 24 h to a constant weight.

2.2. Metabolic flux ratio analysis by GC-MS

For labelling, either 100% [1-^{13}C]-glucose (or [1-^{13}C]-fructose, respectively, Sigma-Aldrich), or a mixture of 20% (wt/wt) [U-^{13}C]-glucose (or [U-^{13}C]-fructose, respectively, Sigma-Aldrich) and 80% (wt/wt) natural glucose (or fructose, respectively) were used. 5 ml cell aliquots were harvested in mid-exponential growth by centrifugation at 1,200 x g and 4 °C for 10 min. The pellet was washed twice with 1 ml of 0.9% NaCl, then hydrolyzed in 1 ml 6 M HCl for 24 h at 110 °C in sealed 2 ml Eppendorff tubes, and desiccated overnight in a heating block at 85 °C under a constant air stream. The hydrolysate was dissolved in 30 μl of 99.8% pure dimethyl formamide. For derivatization, 20 μl of N-methyl-N-(tert-butyldimethylsilyl)-trifluoroacetamide was added and the mixture was incubated at 85 °C for 60 min. The GC-MS-derived mass isotope distributions of proteinogenic amino acids was analyzed injecting 1 μl of the derivatized sample into the gas chromatograph 6890N (Agilent Technologies) combined with the Mass selective Detector model 5973 (Agilent Technologies) and analyzed as described previously (Dauner and Sauer, 2000; Fischer and Sauer, 2003).

The corrected mass distributions were related to the *in vivo* metabolic activities obtained with previously described algebraic equations and statistical-data treatment of metabolic-flux ratio analysis (Fischer *et al*, 2003) using the program ratio of Fiat Flux software (Zamboni *et al*, 2005).

2.3. ^{13}C-constrained metabolic net flux analysis

The metabolic model used for net-flux analysis was based on the master reaction network (Fuhrer and Sauer 2005), which included 45 reactions and 33 metabolites. To adapt the metabolic reaction network to growth on fructose, it was necessary to modify the upper metabolism as follows: fructose is taken up by the PTS^{Fru} system and thereby activated to F1P, which is then converted to FBP by the activity of the 1-Phosphofructokinase (Lessie and Phibbs, 1984; Sawyer *et al*, 1977; Schleissner *et al*,

1997; Van Dijken and Quayle, 1977; Velazquez *et al*, 2004; Vicente, 1975; Vicente *et al*, 1975). Net fluxes were then calculated using [i] the stoichiometric reaction matrix, [ii] the METAFoR analysis-derived flux ratios, [iii] physiological data, and [iv] precursor requirements for biomass synthesis, as described previously (Zamboni *et al*, 2005). Specifically, the following flux ratios were used: serine derived through the EMP pathway, pyruvate derived through the ED pathway, oxaloacetate (OAA) originating from pyruvate, PEP originating from OAA, the lower and upper bounds of pyruvate originating from malate, and the upper bound of PEP derived through the PP pathway. The stoichiometric matrix was then solved with the MATLAB-based program Netto of Fiat Flux software (Zamboni *et al*, 2005) by minimizing the sum of the weighted square residuals of the constraints from both metabolite balances and flux ratios to obtain estimated net fluxes.

3. Metabolic measurements

3.1. Determination of metabolite concentrations by Liquid Chromatography Mass spectrometry (LC-MS)

For metabolite quantification fresh medium (M9 medium with glucose, fructose or succinate) was inoculated to a starting OD_{600} of 0.05 from a *P. putida* wild type culture grown on the same medium. The biomass corresponding to 0.5-0.6 mg of cellular dry weight (CDW, 4 ml of culture to OD_{600} = 0.5-0.6) of each of the samples (five independent replicates) were separated of its supernatant by fast centrifugation (13 000 x g, 30 sec) and the cell pellet frozen in liquid nitrogen until extraction. Then, the samples were extracted three times with 0.5 ml 60% (v/v) ethanol buffered with 10 mM ammonium acetate pH 7.2 at 78 °C for 1 min as described previously (Buescher *et al*, 2010; Fuhrer and Sauer, 2009). After each extraction step, biomass was separated by centrifugation for 1 min at 13 000 x g. The three liquid extracts of each sample were pooled prior to drying at 120 µbar to complete dryness and then stored at -80 °C until resuspension. Prior to analysis, the dry extracts were resuspended in 500 µl of MilliQ water. The samples were sealed in 96-well plates for LC-MS analysis. Quality control and carry-over checks were included in the analysis series by injection of a mixture of standard compounds and water, respectively. Liquid chromatography, mass spectrometer conditions and data analysis were carried out as described previously (Buescher *et al*, 2010).

3.2. Determination of total ATP

ATP was measured in wild type and *pfkA*$^+$ strains using an ATP bioluminiscence kit (Proteinkinase, Biaffin GMBH & Co KG). Cultures of *P. putida* MAD2 (pVLT31) and *P. putida* MAD2 (pVLT31*pfkA*) were diluted to an OD_{600} of 0.05 in fresh medium (M9 medium with glucose or fructose, Tc and IPTG 0.5 mM) and grown at 30 °C until exponential phase (OD_{600} = 0.2-0.5). For ATP extraction, we used the trichloroacetic acid protocol (Bagnara and Finch, 1972) which is considered the best method for microorganisms. This is because it inactives enzymes that might quickly degrade the ATP before measurement (Lundin and Thore, 1975). For this procedure 100 µl of cell culture was mixed with 100 µl of a solution of 5% trichloroacetic acid with 4 mM EDTA and cooled in ice bath by 15 min (Lundin *et al*, 1975). Then, samples were diluted 20-fold with buffer Tris 20 mM, EDTA 2 mM pH = 7.75 and 50 µl of this solution was mixed with 50 µl of bioluminiscence reagent according to manufacturers' instructions. The bioluminiscence signal was measured in a Victor2 (Perkin Elmer) recording spectrophotometer after 10 min of incubation.

4. Expression of enzymes and measurements of their activity

4.1. Expression of 6-phosphofructokinase

The broad-host-range expression vector pVLT31 was employed to express the protein PfkA in the wild type *P. putida* MAD2 and its *eda* mutant. Cultures of *P. putida* MAD2 (pVLT31) and *P. putida* MAD2 (pVLT31*pfkA*) were diluted to an OD_{600} of 0.05 in fresh medium (LB medium, tetracycline and IPTG 0.5 mM) and then grown at 30 °C until exponential phase (OD_{600} = 0.5-0.6). PfkA expression was monitored under denaturing conditions as follows: cells were harvested by centrifugation (2 min, 13 000 x g) such that a cell mass equivalent of 1 ml of culture at an OD_{600} = 1 was adjusted to disperse in 200 µl of denaturing loading buffer (63 mM Tris HCl, 10% glycerol, 2% SDS, 2% mercaptoethanol, 0.0025% Bromophenol Blue, pH 6.8) and boiled at 100 ºC by 5 min. 10 µl of cell suspensions were directly loaded into the wells of a denaturing 10% polyacrylamide SDS-PAGE system.

4.2. Enzymatic assay for 6-phosphofructokinase activity

For determination of PfkA activity, crude cell extracts of *P. putida* MAD2 (pVLT31, as negative control), *E. coli* W3110 (as positive control) and *P. putida* MAD2 (pVLT31*pfkA*) were prepared from pellets of 50 ml cultures. Cells were harvested in the exponential

growth phase (OD_{600} = 0.5-0.6) by centrifugation (15 min, 4000 × g, 4 °C) and the sediments resuspended in Phosphate Buffer Solution 1X (PBS, 1% w/v NaCl, 0.025% KCl, 0.18% Na_2HPO_4, 0.03% KH_2PO_4) such that a cell mass equivalent of 50 ml of culture at an OD_{600} = 0.8 was adjusted to disperse in 2 ml of PBS. Afterwards, cells were lysed by sonication in the cold (5 pulses of 30 sec) and spun down for 30 min at 14,000 × g to collect cell debris. The supernatant was used for protein determination by Bradford analysis (Bradford, 1976) and enzymatic assays for 6-phosphofructokinase activity. The enzymatic assays were performed according to the protocol described by Steinbuchel *et al.* (1986) by following the decrease in extinction at 340 nm at 25 °C due to NADH consumption during 5 minutes in a 200 µl well plate with the use of a Victor2 (Perkin Elmer) recording spectrophotometer.

4.3. Enzymatic assays for malic enzyme and pyruvate carboxylase activities

Crude cell extracts for *in vitro* enzyme assays were prepared from pellets of 50 ml cultures as before. Enzymatic assays (Geer *et al*, 1979; Warren and Tipton, 1974) were run with a spectrophotometric method and the results expressed in micromols of substrate converted per mg protein per min (U/mg protein). NADP-dependent malic enzyme and pyruvate carboxylase were assayed basically as described elsewhere (Geer *et al*, 1979; Warren *et al*, 1974). Briefly, the increase or decrease in extinction at 340 nm at 25 °C due to NADPH production or NADH consumption was followed for 10 minutes in a 200 µl well-plate with the Victor2 multi-tasking plate reader (Perkin Elmer). For the malic enzyme assay a volume equivalent to 25 µg of protein in the cells extracts was used. The final concentrations in the reaction mix were 67 mM triethanolamine, 3.3 mM L-malic acid, 0.3 mM β-nicotinamide adenine dinucleotide phosphate and 5.0 mM magnesium chloride. For the pyruvate carboxylase assays, a volume equivalent to 75 µg of protein in the cells extracts was used and the final concentrations in the reaction mix were 134 mM triethanolamine, 5 mM magnesium sulfate, 7 mM pyruvic acid, 0.12% (w/v) bovine serum albumin, 0.23 mM β-nicotinamide adenine dinucleotide (reduced form), 0.05 mM acetyl coenzyme A, 2.63 units malic dehydrogenase, 1 mM adenosine 5'-triphosphate, 15 mM potassium bicarbonate, 0.05% (v/v) glycerol, 0.002 mM magnesium acetate, 0.001 mM ethylenediaminetetraacetic acid and 0.05 mM Tris-HCl.

5. Cloning, expression and purification of Cra

The DNA sequence encoding the Cra protein of *P. putida* KT2440 (PP0792) was amplified from the chromosome of this bacterium with primers Cra-F and Cra-R (see Table 3). The resulting PCR product was digested with NdeI/XhoI and cloned into the bacterial expression vector pET28a (see Table 2), which adds six histidines to the N-terminus of the encoded protein. Note that we included a stop codon (TCA) in the Cra-R primer inmediatly after of XhoI enzyme sequence to avoid that the vector adds His residues in the C-terminus. The resulting plasmid (pET28a*cra*) was transformed into the specialized host strain *E. coli* BL21 (DE3). For expression of the His_6-tagged protein, the transformed strain was grown at 37 °C in LB to OD_{600} = 0.5 and added with 0.5 mM of IPTG, after which the cultures were grown for 3 more hours. Cells were then harvested by centrifugation and the pellets frozen at -80 °C until further use.

For purification, cells were thawed, resuspended in 50 mM sodium phosphate buffer pH 7.0, 200 mM NaCl (1 ml of culture OD_{600} = 0.5 in 50 µl), and mechanically lysed using a French press (Thermo Electron corporation). Cell debris was removed by centrifugation (20 000 x g for 30 min at 4 °C) and the native His_6-Cra protein isolated to apparent homogeneity from the supernatant of the cell lysate using TALON Metal Affinity Resin (Clontech) according to manufacturers' instructions. The resin was equilibrated with 20 bed volumes of 50 mM sodium phosphate buffer pH 7.0, 200 mM NaCl (equilibration buffer 1X). The clarified sample was passed through the column and then washed successively with 10 bed volumes of equilibration buffer 1X, 10 bed volumes of equilibration buffer 1X plus 5 mM of imidazol, 10 bed volumes of equilibration buffer 1X plus 10 mM of imidazol and finally with 10 bed volumes of equilibration buffer 1X plus 20 mM of imidazol. The pure protein elution was done with equilibration buffer 1X plus 150 mM of imidazol.

The purified protein was kept in the elution buffer at 4 °C until its utilization as indicated in each case. On the other hand, Selenium-methionine (Se/Met)-derivatized *P. putida* Cra was purified as before from cells grown in M9 minimal medium in the presence of 0.2% glucose, seleno-methionine and other amendments known to inhibit methionine biosynthesis (Van Duyne *et al*, 1993). All buffers for (Se/Met)-Cra purification were supplemented with 5 mM dithiothreitol, but the isolation procedures were otherwise identical to those employed for the non-derivatized protein.

6. Identification and synthesis of the Cra operator

The reference *E. coli* consensus sequence for Cra binding sites was retrieved from the PRODORIC database (Munch *et al*, 2003). The resulting DNA motif was then searched in the genome of *P. putida* KT2440 by means of the Virtual Footprint software (version 3.0; Munch *et al*, 2005). One of the identified Cra binding site happened to occur within the intergenic and divergent promoter region of the *cra/fruBKA* (5'TTAAACGTTTCA3') gene cluster (*P. putida* chromosomal coordinates 908211-915030). This plausible operator was synthesized as part of a 22 bp double-stranded DNA fragment and employed in the mobility shift and isothermal microcalorimetry (ITC) assays. The 22-bp DNA fragment used for EMSA with the Cra protein was prepared by heating an equimolar (50 nmol) mixture of complementary oligonucleotides containing the presumed Cra binding site of the *cra/fruBKA* promoter region (primers *cra/fruB*-F and *cra/fruB*-R in Table 3) in 1 ml of TE buffer at 95 °C for 10 min and then keeping the annealed product chilled on ice until further use.

7. Non-radioactive electrophoretic mobility shift assays (EMSA)

The Cra-DNA binding reaction was assembled in a final volume of 20 μl containing 2 μl of TGED binding buffer 10X (final concentrations: 10 mM Tris-HCl pH 8.0, 5% vol/vol glycerol, 0.1 mM EDTA, 1 mM dithiothreitol, 20 μg/ml of poly (dI-dC), 200 μg/ml of bovine serum albumin, 0.75 μM of the Cra-site containing DNA fragment and increasing amounts of the pure Cra. Mixtures were incubated for 15 min at 30 °C and electrophoresed in a non-denaturing 10% (w/v) polyacrylamide: bisacrylamide gel in Tris-glycine buffer 1X pH 8.9. Finally, the gels were stained with ethidium bromide and visualized using a Gel Doc XR (Bio-Rad). In the experiments for identification of potential effectors, Cra was incubated with the DNA fragment in the presence of 1 mM of each of the following compounds: fructose (Fluka, 99% purity), fructose-1-phosphate (F1P, Sigma, 100%), fructose-1,6-bisphosphate (FBP, Sigma, 98%), fructose-6-phosphate (F6P, Sigma, 98%), glucose-6-phosphate (G6P, Sigma, 100% purity) and the samples run in a gel and analyzed as described before.

8. Isothermal Titration Microcalorimetry (ITC)

ITC experiments were performed on a VP microcalorimeter (MicroCal, Northampton, MA, USA) at 25 °C. Prior to experiments, Cra was thoroughly dialyzed in 25 mM Tris-HCl, 50 mM NaCl, 1 mM DTT, pH 8.0. After dialysis, protein solution was filtered through a 0.45 μm filter and its concentration was determined by UV absorption spectroscopy using and extinction coefficient of 1.217 x 10^5 cm M^{-1} at 280 nm (Gasteiger *et al*, 2005). Effectors were prepared by diluting pure powdered products in filtered dialysis buffer so that the ligand and protein solvent were the same. Each titration involved a single 1.6 μl injection and a series of 4.8 μl injections of 250 μM of each of the effectors into a 7.5 μM protein solution. For DNA binding studies, the 22-bp DNA fragment used in EMSA experiments (see above) was dialyzed so that the DNA and protein solvent were the same. In this case, the assays consisted of the injection of 4.8 μl aliquots of 60 μM DNA into a protein solution of 10 μM. The mean enthalpies measured from injection of the ligands into the buffer were subtracted from raw titration data prior to data fitting using the one binding site model of the MicroCal version of the ORIGIN software. From the curves thus fitted, the parameters ΔH (reaction enthalpy), K_A (binding constant, $K_A = 1/K_D$), and n (reaction stoichiometry) were determined. From the values of K_A and ΔH, the change in free energy (ΔG) and in entropy (ΔS) were calculated with the equation: $\Delta G = -RT \ln K_A = \Delta H - T\Delta S$, where R is the universal molar gas constant and T is the absolute temperature.

9. Analysis of Cra oligomerization state

Analytical ultracentrifugation experiments were performed in a Beckman Optima XL-A analytical ultracentrifuge with a UV-visible absorbance detection system. Sedimentation velocity measurements were carried out an An50Ti eight-hole rotor in phosphate buffer with 150 mM Imidazol, 200 mM NaCl, pH 7.0 (elution buffer in protein purification) at 45000 rpm, with 400 ml of protein solution (0.5, 1, and 1.3 mg/ml) in each cell, using double sector Epon-charcoal centrepieces. Differential sedimentation coefficient distributions c(s) were calculated by least squares boundary modelling of sedimentation velocity data using the program SEDFIT (Schuck, 2000, 2004). From this analysis, the experimental sedimentation coefficients (s) were corrected for solvent composition and temperature to obtain the corresponding standard s-values ($s_{20,W}$, standard solvent conditions: pure water at 20 °C) using the SEDNTERP program (Lebowitz *et al*, 2002).

Partial specific volume of 0.7312 mlg^{-1} at 20 °C was calculated from the amino acid composition (Laue *et al*, 1992).

Sedimentation equilibrium experiments were performed at 20 °C by centrifugation of 80 ml samples of Cra at 11000, 13000 and 19000 rpm in the Optima XL-A ultracentrifuge. Conservation of mass in the cell was verified in all the experiments. After the equilibrium scans a high-speed centrifugation run (45000 rpm) was done to estimate the corresponding baseline offsets. Weight-average buoyant molecular weights were determined by fitting a single species model to the experimental data using the Hetero-Analysis program (Cole, 2004). The absolute molecular weight of Cra potein was determined using the partial specific volume (0.7312 ml g^{-1}) and the solvent density (1.0207 mg/ml). In addition, the oligomerization form of *P. putida* Cra was confirmed by size-exclusion chromatography. To this end, a protein solution of 1.0 mg/ml was run through a Superdex 200 column (Amersham Biosciences) in 25 mM Tris-HCl, 50 mM NaCl, pH 8.0. The molecular weight markers were run under the same conditions. Proteins in the eluted fractions were monitored by SDS-PAGE.

10. Cra X-Ray structure

10.1. Cra crystallization

The affinity-purified His-tagged Cra protein was concentrated to 15 mg/ml for its crystallization. During concentration, the sample buffer was diluted approximately 50 times against 25 mM Tris pH 8.0, 50 mM NaCl and 1 mM DTT. This procedure allowed a high concentration of the protein and avoided amorphous precipitation while simultaneously clearing the samples of the potentially disturbing imidazol left after eluting the protein from the metallo-affinity column. Crystals of the native Cra protein were then generated from a 15 mg/ml protein sample by the sitting-drop vapor-diffusion method. Drops were prepared by mixing 150 nl of protein with 150 nl of crystallization solution and equilibrated against 100 μL of the crystallization solution in Greiner plates. Crystals appeared after two days in drops prepared with a solution containing 15% (w/v) of PEG8000, 0.2 M sodium acetate and 0.1 M MES buffer, pH 6.5. Seleno-methionine (Se/Met)-derivatized Cra protein was crystallized using identical conditions. The resulting crystals were dialyzed against the same solution supplemented with 20% glycerol before cryofreezing in liquid nitrogen (see below). For the ligand binding experiments, native Cra protein crystals were soaked for 4 to 7 hours in the

cryofreezing solution containing 1 mM of each tested candidate effectors (F1P, FBP, F6P, G6P and fructose).

10.2. Data collection and structure resolution of Cra

Datasets from the native, effector-less Cra protein, its (Se/Met)-derivatized variant and the ligand-containing complexes F1P and FBP were collected at the European Synchrotron Radiation Facility (ESRF, Grenoble) at beamlines ID14-1, ID23-1 and ID14-2 (crystals soaked with the F6P, G6P and fructose did not show any diffraction). The crystals, which belonged to the space group P_{21}, contained two Cra molecules in the asymmetric unit and a solvent content around 43%. Diffraction data was processed with XDS (Kabsch, 1993) and scaled with SCALA (Collaborative computational project number 4, 1994). The structure of the protein without effector was solved first by the SAD method using the Autorickshaw Server (Panjikar *et al*, 2005) and diffraction data extending up to 2.5 Å resolution.

Structure resolution and phasing in the Server was carried out by SHELX programs (Sheldrick, 2002). The initial model built by RESOLVE (Terwilliger, 2000) gave R-factor/R-free values of 22% and 28% respectively. The model was manually adjusted using Coot (Emsley *et al*, 2010) and refined using PHENIX 1.6-289 (Adams *et al*, 2010) with data up to 2.0 Å resolution to a final R-factor and R-free of 18.4 and 21.8, respectively. Crystal structures of the Cra protein in complex with the F1P and FBP were determined by the molecular replacement method using the effector-less structure and the PHASER program (McCoy *et al*, 2007), followed by refinement with PHENIX 1.6-289 (Adams *et al*, 2010). The structure of the Cra protein prepared by crystal soaking with FBP gave an electron density map in the effector-binding site, which was indistinguishable from the Cra-F1P complex and therefore has not been included separately (not shown). All residues are in the most favored region (91.7%) or the additional allowed regions (7.9%) of the Ramachandran plot, except the effector-binding Asp148 that lies in a disallowed region in all structures.

11. Measurements of β-Galactosidase activity

For measuring promoter activity, we used the protocol described by Miller (1972). For that, pre-inocula of each strain were grown in mineral minimum medium with fructose, glucose or succinate as carbon source. The cultures were diluted to an optical density at

600 nm of approximately 0.05 in fresh medium and then grown at 30 °C until exponential phase (OD_{600} = 0.3-0.6). 1 ml of each sample was collected and promoter activity was measured by assaying the amount of β-galactosidase in cells made permeable with chloroform and sodium dodecyl sulfate. All the enzymatic measurements were performed at least with six biological replicates.

12. Measurements of β-Galactosidase activity with the Galacton-Light Plus™ system (Applied Biosystems)

Low β-Galactosidase activity was measured with the extremely sensitive Galacton-Light Plus™ system (Applied Biosystems). This protocol quantifies low levels of galactosidase, and it is based on a chemiluminescent substrate of the enzyme (Galacton-Plus®, Tropix). In this case, 500 µl of cells (OD_{600} = 0.3-0.6) were separated of its supernatant by centrifugation (14000 x g, 2 min, room temperature) and the cell pellet resuspended in 200 µl of lysis buffer (100 mM potassium phosphate pH 7.8, 0.2% Triton X-100). The lysis mixture was subjected to two freeze-thaw cycles and finally centrifuged 1 min 14000 x g at room temperature to eliminate the cell debris. 20 µl of lysed supernatant were then incubated for 30 min with 80 µl of reaction buffer (100 mM sodium phosphate, pH 8.0, 1 mM $MgCl_2$, 1X Galacton-Plus®). These reactions were run in triplicate in 96-well plates and recorded in a luminometer for 30 sec immediately after the addition of 125 µl of a light emission accelerator (Accelerator-II Sapphire-II™) following the instructions of the commercial supplier.

13. Sample preparation and processing for native PAGE and western blotting

To obtain samples for analysis of PtsN phosphorylation in the native PAGE system, preinocula of *P. putida* KT2440, and mutants, *Δcra*, *ΔptsP*, *ΔcraΔptsP*, containing the plasmid pVLT31*ptsN_Etag* were grown in M9 medium with fructose, glucose or succinate with tetracycline and IPTG 0.5 mM. The cultures were diluted to an OD_{600} of 0.05 in fresh medium and then grown at 30 °C until exponential phase (OD_{600} = 0.4-0.6). The cells were then harvested by centrifugation (2 min, 14000 x g, 4 °C) and the pellets resuspended in a non-denaturing loading buffer (10% glycerol, 40 mM glycine, 5 mM Tris, pH 8.9, and 0.005% w/v bromphenol blue) such that a cell mass equivalent of 1 ml of culture at an OD_{600} of 1.0 was adjusted to disperse in 200 µl of the native

loading buffer. 10 µl of such intact cell suspensions were directly loaded into the wells of the non-denaturing gel system (Pfluger *et al*, 2007a; Pfluger *et al*, 2007b) as was described previously. The non-denaturing gel electrophoresis system consisted of a 10% polyacrylamide gel [10% v/v acrylamide/bis-acrylamide solution (29:1) polymerized with 0.05% v/v TEMED and 0.05% ammonium persulfate in 1X running buffer (200 mM glycine, 25 mM Tris, pH = 8.9)] and casted in a mini-Protean gel box (Bio-Rad). Electrophoresis was carried out with a fixed current of 12.5 mA/gel (8.5 cm, W x H) at 4 ºC for 35 min. The proteins were transferred onto a polyvinylidene difluoride membrane (Immobilon-P, Millipore) using a semidry transfer apparatus (Bio-Rad) as was described previously (Jurado *et al.* 2002). The anti-E-tag monoclonal antibody (MAb)-peroxidase (POD) conjugate (Amersham Pharmacia Biotech) was applied for luminescent detection of the PtsN-E-tag fusion proteins (Jurado *et al.* 2002).

IV. RESULTS

CHAPTER 1

Central carbon metabolism and its interplay with PTS systems in *P. putida**

**** Manuscripts in preparation:***

Max Chavarría, Tobias Fuhrer, Danilo Perez, Javier Tamames, Uwe Sauer & Víctor de Lorenzo. *(2011)* An atypical metabolic cycle formed by Embden-Meyerhoff-Parnas and Entner-Doudoroff enzymes empowers *Pseudomonas putida* to endure environmental stress.

Max Chavarría, Roelco J. Kleijn, Uwe Sauer, Víctor de Lorenzo & Katharina Pfluger-Grau. *(2011)* The regulatory duties of the phosphotransferase system (PTS^{Ntr}) on Central carbon Metabolism of *Pseudomonas putida.*

---

1. Central carbon metabolism in *P. putida*

1.1. Pathways involved in glucose and fructose degradation

Due to comprehensive reasons, the central carbon metabolism (see Fig. 1) was divided in this Thesis into the *upper* metabolism, comprising the degradation of the internalized sugar to C_3 components *via* the ED pathway, the PP pathway, or the EMP pathway, and the *lower* metabolism, formed by the PEP-Pyr-OAA node and the TCA cycle. By evaluating the first module (*upper* metabolism), we can obtain information about metabolic steps, which bacteria use to degrade the main sugars. This is not trivial as different microorganisms use diverse catabolic pathways for sugar consumption, which reflects the phylogeny and evolution of each bacterium. Regarding the carbon source, major differences in the *upper* metabolism can be observed as represented by the net fluxes (Fig. 6). These are relative values and represent the estimated fluxes normalized to the amount of carbon source taken up. When *P. putida* was grown on glucose, 96% of this carbon source was degraded *via* the ED pathway to pyruvate, only about 4% was degraded *via* the PP pathway and no activity of EMP pathway was observed (Fig. 6). When cells were grown on fructose, the ED pathway was still the major carbon degradation pathway, with 52% of the fructose being degraded *via* this pathway. However, about 34% of the internalized fructose is degraded *via* the energetically more

favourable EMP pathway. The rest is degraded *via* the PP pathway.

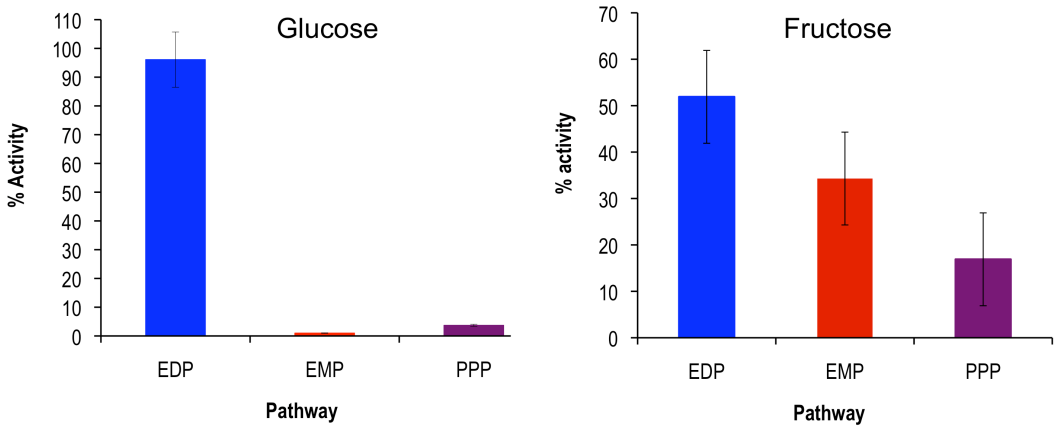

Figure 6. Pathway activity for catabolism of (a) glucose and (b) fructose in *P. putida*. % activity in *y*-axis are represented by the net fluxes calculated by metabolic flux analysis of *P. putida* MAD2 strain.

Therefore, metabolic flux analysis of sugar catabolism in the environmental bacterium *P. putida* showed that the ED pathway is the most prevalent route in the *upper* central metabolism. Using radioactivity experiments with ^{14}-C in *P. putida*, *P. aeruginosa*, and *P. stutzeri* Sawyer *et al.* (1977) reported similar results regarding the pathways involved in degradation of glucose and fructose.

1.2. ED pathway is essential for glucose catabolism in *P. putida*

Following our studies about the carbon central metabolism, we investigated whether *P. putida* was able to grow with glucose as substrate using a metabolic pathway distinct from ED pathway. This would allow us to understand the importance of the ED pathway in the physiology and regulation of other processes. Therefore, we set to study the physiological and metabolic impact of redirecting the metabolism of this bacterium from the ED pathway towards EMP pathway. Using a metabolic engineering approach, we expressed the PfkA enzyme (the missing metabolic enzyme of EMP pathway in *P. putida*) from *E. coli* in a wild type *P. putida* strain as well as its *eda* mutant (mutant unable to use the ED pathway). The enzyme was successfully expressed and remained active in cell extracts of *P. putida* (Figs. 7a and 7b). However, growth experiments in which glucose was the only substrate revealed that the *eda pfkA*$^{+}$ strain was unable to grow on this carbon source suggesting that the PfkA enzyme cannot completely switch the carbon flux into EMP pathway (Fig. 7c). This key observation suggests that the ED

pathway is essential for glucose degradation in *P. putida*. Futhermore, it suggests that a functional EMP pathway cannot be established in the metabolic network of *P. putida* to replace the ED pathway for glucose degradation simply by overexpressing PfkA from *E. coli*.

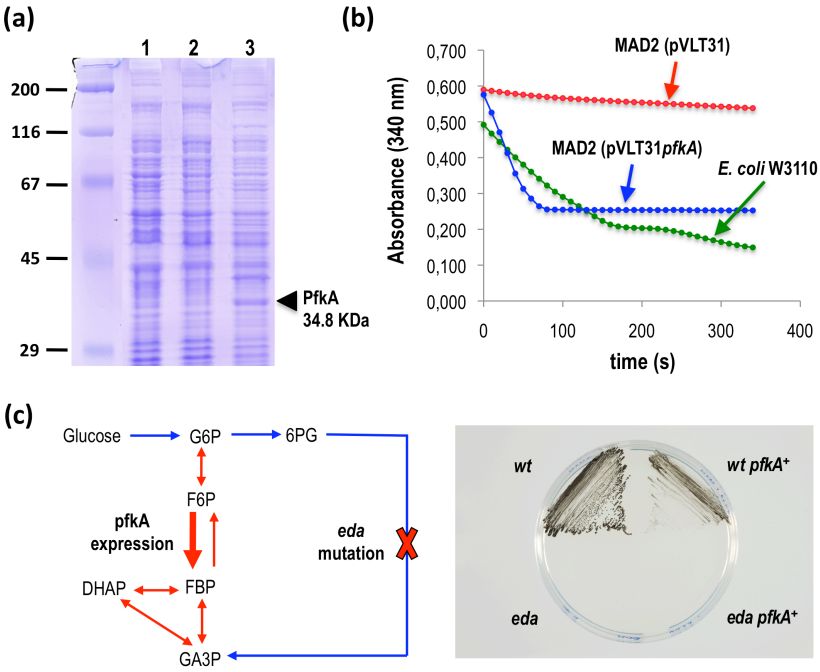

Figure 7. Expression of the PfkA enzyme in *P. putida*. **(a)** SDS gel stained with Coomassie showing the expression of *E. coli* PfkA (34.8 KDa) in *P. putida*. Lane1- MAD2 (pVLT31); Lane 2- MAD2 (pVLT31*pfkA*) –IPTG; Lane 3- MAD2 (pVLT31*pfkA*) +IPTG. **(b)** Enzymatic assays for 6-phosphofructokinase in *E. coli* W3110 (green), MAD2 (pVLT31) (red) and MAD2 (pVLT31*pfkA*) +IPTG (blue). PfkA enzyme was successfully expressed and remained active in cell extracts of *P. putida*. **(c)** Growth experiments with glucose as the only substrate revealed that *eda pfkA*$^+$ strain is unable to grow in this carbon source and therefore the PfkA enzyme cannot switch the carbon flux into EMP pathway.

Surprisingly, the expression of PfkA in the wild type strain had a strong negative effect in bacterial growth (Fig. 8). Growth comparison of wild type and *pfkA*$^+$ showed that the cell growth decreased dramatically with the PfkA expression in all substrates tested (glucose, fructose, and succinate; Fig. 8). The negative effect of the PfkA in *P. putida* is intriguing because based on current metabolic models (Nogales *et al*, 2008; Puchalka *et al*, 2008), it is accepted that this enzyme should cooperate at least partially to the degradation of hexoses, increasing the metabolic efficiency to catabolize these carbon sources (Baart *et al*, 2010). The negative impact on growth can be ordered as follows: fructose > glucose ≈ succinate. The effect in fructose-grown cells is particularly dramatic (Fig. 8c).

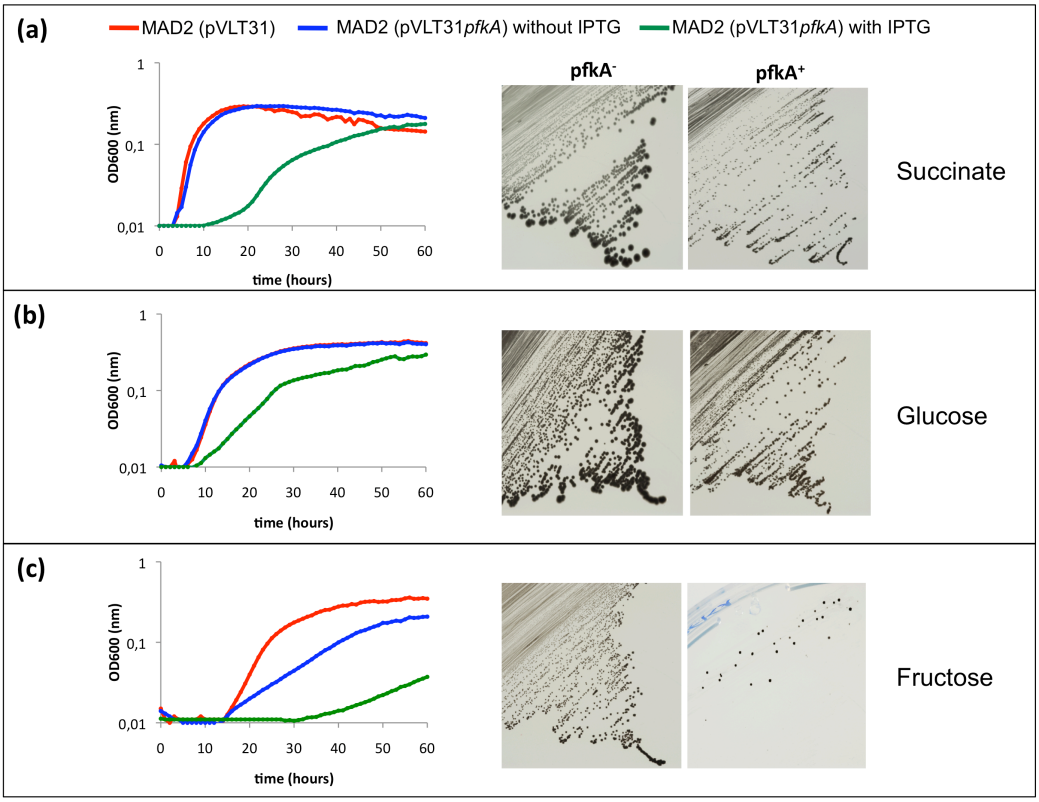

Figure 8. Growth experiments of *P. putida* MAD2 (pVLT31, red) and MAD2 (pVLT31*pfkA*) strains in absence (blue) and presence (green) of IPTG with (a) succinate (b) glucose and (c) fructose as the only carbon substrate. Growth experiments were performed in liquid (left panel) and solid (right panel) media. These experiments showed that when PfkA was expressed in *P. putida* (*pfkA*$^+$ in presence of IPTG) the cell growth was reduced in all the tested carbon sources. The impact on growth can be ordered as follows: fructose > glucose ≈ succinate where the effect in fructose-grown cells is the most drastic.

Knock-in of *pfkA* in *P. putida* apparently unbalances the metabolic network thus affecting the primary biological functions involved in biomass production. Since these observations cannot be explained using existing metabolic models for *P. putida*, we examined in depth the *upper* central metabolism in this bacterium through a metabolomic approach.

1.3. Metabolomic analyses suggest a cyclic operation of the ED pathway in *P. putida*

In order to better understand the central metabolism in *P. putida*, we quantified concentrations of key metabolites when the bacterium was grown on three different carbon sources (Fig. 9): glucose, fructose, (glycolytic conditions) and succinate

(gluconeogenic conditions). In glucose we observed the highest concentrations of glucose 6-phosphate (G6P) and 6-phosphogluconate (6PG), 1167 ± 128 and 2300 ± 1178 μM respectively, as expected from metabolic models. This evidence indicates that *P. putida* channels the glucose directly to G6P (del Castillo *et al*, 2007), which is transformed to 6PG through glucose-6-phosphate dehydrogenase (Zwf). Subsequently this product is catabolized by ED pathway *via* the Eda/Edd enzymes (Fuhrer *et al*, 2005).

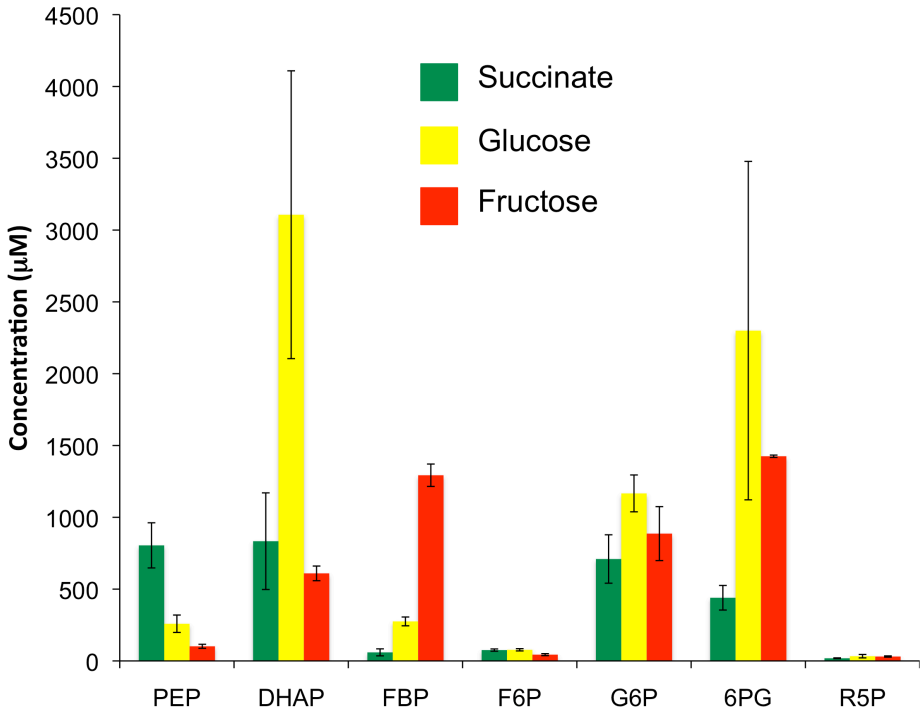

Figure 9. Concentrations of intracellular metabolites in *P. putida* wild type measured by HPLC-MS on succinate (green column), glucose (yellow column) and fructose (red column) cultures. Metabolome data showed that in all the conditions, metabolites of upper metabolism are produced in micromolar concentrations. The metabolic measurements support the occurrence of a cyclic ED pathway, where triose phosphates are recycled to FBP/F6P/G6P/6PG. Metabolite concentrations were expressed in micromols in the intracellular volume.

Alternatively, other authors (Schleissner *et al*, 1997) have suggested that glucose could be converted extracellularly to gluconate and degraded through the ED pathway. Our current results cannot distinguish which of these convergent pheripheral pathways is preferred for glucose uptake in this bacterium. In any case, G6P and 6PG concentrations indicate the preference of the ED pathway in glucose degradation over EMP pathway, which is in agreement with our results obtained through metabolic flux analysis. According to the literature, Zwf/Edd/Eda enzymes carry out irreversible

reactions (Conway, 1992) for C_6 sugar conversion to pyruvate (Pyr) and glyceraldehyde 3-phosphate (GA3P). After these biochemical steps, most *P. putida* metabolic models (Nogales *et al*, 2008; Puchalka *et al*, 2008) consider that triose phosphates are mainly directed towards the TCA cycle (*lower* metabolism, Fig. 1) in order to produce ATP, amino acids and other building blocks necessary for the synthesis of macromolecules. However, our metabolomic analysis in combination with enzymatic activity information provide a new vision of central metabolism in *P. putida,* since it can be deduced that an important fraction of triose phosphates are recycled to DHAP/FBP/F6P/G6P *via* the gluconeogenic enzymes glyceraldehyde 3-phosphate dehydrogenase (Gap), triose phosphate isomerase (TpiA), fructose bisphosphate aldolase (Fda), fructose-1,6-bisphosphatase (Fbp) and glucose phosphate isomerase (Pgi). The quantification of significant concentrations of DHAP, FBP, and F6P in glucose (3107 ± 1002, 275 ± 31 and 77 ± 8 μM respectively; Fig. 9) allows us to entertain about the presence of an operative cycle in the metabolic core formed by the enzymes Gap, TpiA, Fda, Fbp, Pgi, Zwf, Pgl, Edd, and Eda, which are capable of recycling triose phosphates to phosphorylate hexoses. The possibility that these metabolites (DHAP, FBP and F6P) would be formed from the EMP pathway is discarded by the absence of any 6-phosphofructokinase as discussed in the Introduction.

Metabolic data in fructose and succinate allowed us to come to similar conclusions about the direction of the carbon flux in the central metabolism of *P. putida*. In fructose as substrate we observed the highest levels of FBP (Fig. 9). This value is consistent with the pheripheral pathway reported for this carbon source in *P. putida*; involving the phosphoenolpyruvate PEP:phosphotransferase system, PTS^{Fru} system (Velazquez *et al*, 2007), encoded by *fruBKA* where the fructose is phosphorylated to F1P and subsequently diphosphorylated to FBP. On the other hand, the presence of significant FBP levels when using glucose and succinate as substrates suggest that this compound is generated by Fda *via* the proposed cyclic ED pathway.

According to current metabolic models (Nogales *et al*, 2008; Puchalka *et al*, 2008), fructose can be degraded through EMP pathway since this sugar enters this pathway directly to FBP by the action of FruBKA and consequently does not require 6-phosphofructokinase. However, the detected levels on fructose of F6P (44 ± 7 μM), G6P (887 ± 188 μM), and 6PG (1425 ± 8 μM) suggest that this substrate is degraded mainly through the ED pathway, which is consistent with our fluxomic data and previous reports (Van Dijken and Quayle, 1977). The preference of *P. putida* to use the

ED pathway for fructose metabolization is intriguing since that option is energetically less efficient than EMP pathway. Alas, when grown on fructose as carbon source, metabolomic data cannot distinguish whether the concentrations of DHAP are produced by glycolytic activity or the proposed cyclic ED pathway. On the other hand, the measured levels on succinate of FBP (60 ± 24 μM), F6P (76 ± 8 μM), G6P (710 ± 169 μM), and 6PG (440 ± 86 μM) indicates that bacteria can reconstruct the entire metabolic network in gluconeogenic conditions, thus synthesizing the compounds of the *upper* metabolism. Quantification of these metabolites on succinate shows how important it is for the cell the formation of the intermediaries from *upper* metabolism in *P. putida*.

1.4. A cyclic ED pathway is needed under glycolytic and gluconeogenic conditions

The occurrence of a cyclic ED pathway in *P. putida* is strongly suggested by metabolomic data; however an open question is how essential is the operativity of this cycle for the bacterium under different metabolic conditions. In order to answer this standing question we tested the growth in different substrates (glucose, fructose, and succinate) of different *P. putida* mutants bearing inactivated versions of enzymes belonging to the proposed cyclic ED pathway, namely Eda, Edd, Zwf-1, Pgi, Gnd, and TpiA (Fig. 10).

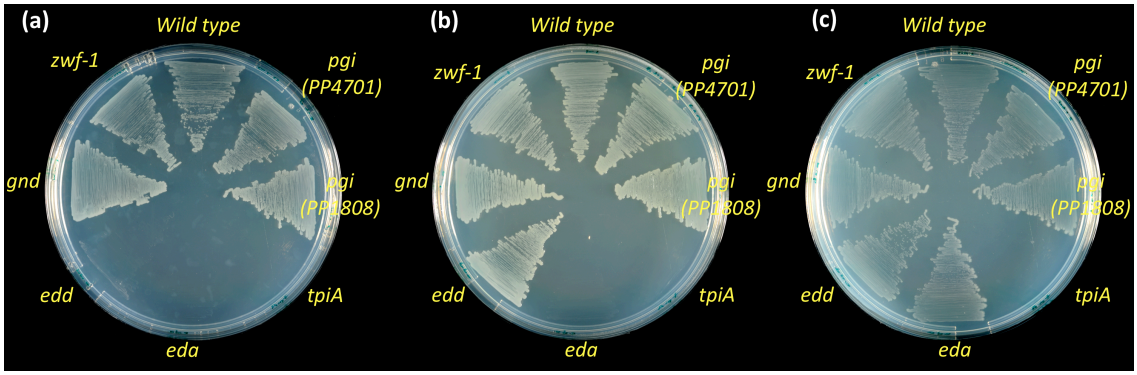

Figure 10. Growth experiments of *P. putida* wild type, *pgi* (PP1808), *pgi* (PP4701), *tpiA*, *eda*, *edd*, *gnd* and *zwf-1* mutants on (a) glucose, (b) fructose and (c) succinate as the only carbon source. Experiments illustrate how the formation of the cyclic ED pathway is physiologically important for cells in glycolytic and gluconeogenic conditions.

The results showed that the *tpiA* mutant was unable to grow in all tested conditions, which suggested that the recycling of triose phosphates to hexoses is physiologically important for the cell in all conditions. On the other hand, *zwf*-1 strain grew in all the

carbon sources but this result would be explained by the existence of two other glucose 6-phosphate dehydrogenase encoding genes, *zwf*-2 (PP4042) and *zwf*-3 (PP5351) in *P. putida* which can be functionally redundant. A similar situation occurs in mutants of glucose 6-phophate isomerase (PP1808 and PP4701) since both enzymes can complement its activity respectively. Assessing the real effect of blocking the operation of the cyclic ED by *zwf* and *pgi* products is hampered by the gene redundancy.

On the other hand, *eda* mutant is unable to grow on fructose and glucose but it grows normally on succinate. A detailed analysis of carbon flux based on gene annotation and reversibility reported for each reaction indicates that the *eda* mutant is able to generate the whole set of metabolites constituting the cycle in succinate. GA3P, DHAP, FBP, F6P, G6P and 6PG are produced by gluconeogenic activity as was shown for the wild type strain (Fig. 9). It should be noted that the *eda* mutant is unable to transform the 2K3D6P to GA3P and Pyr to complete the ED cycle. We think that in *eda* mutant this reaction is not essential since GA3P and Pyr are supplied through gluconeogenic activity. Particulary, the absence of growth in fructose is interesting in this mutant. *P. putida* could degrade this pentose using the EMP pathway. However, the bacterium is unable to grow. One explanation for this observation was given by Vicente and Canovas (1973). They suggested that the *eda* mutant accumulates 2K3D6P at levels that could become toxic on fructose as carbon source. The *edd* mutant can support this hypothesis since it is unable to grow in glucose, but is able to grow well in fructose and succinate. It seems that in absence of any accumulation of 2K3D6P, the EMP pathway can be used by *P. putida* for fructose degradation.

Finally, we included a *gnd* mutant in the growth experiments, which can provide information about the carbon flux through the pentoses pathway *via* G6P. This mutant was able to grow in all the conditions tested, which indicates that this reaction is not essential for growth. These experiments with *gnd* mutant (Fig. 10) correlate well with our fluxomic (Fig. 6) and metabolomic (Fig. 9) data, since they show that the input to the PP pathway through 6PG is low. While our results can ensure that the production of PP metabolites *via* 6PG is low, we can not exclude that part of the demand of C_5 metabolites is produced *via* GA3P and F6P.

It was not possible to evaluate the phenotype of mutants in other genes encoding enzymes of the cycle such as *pgl*, *fda* or *fbp* since they are not available. It should be

noted that several attempts to obtain an *fbp* mutant in *P. putida* were unsuccessful probably indicating an essential role for viability, as it has been suggested for *P. aeruginosa* (Banerjee, 1989). On the other hand, previous studies in *P. aeruginosa* have showed that a mutant lacking Fda is able to grow on fructose but not on other carbon sources such as glucose, gluconate or succinate (Banerjee *et al*, 1985). In this case, the way in which the fructose enters to the central metabolism in the cell allows the *fda* mutant to form all metabolites constituting the cyclic ED. Taken together, all the results about the growth on different c-sources, it can be concluded that biosynthesis of the metabolites of the cycle: DHAP, FBP, F6P and G6P is essential for *P. putida*.

1.5. PfkA expression produces a futile cycle in central metabolism that wastes ATP

In light of metabolomics and growth data of *P. putida* mutants we could argue that *upper* metabolism in *P. putida* is carried out cyclically. With this idea in mind, we can interpret the drastic reduction in the biomass formation when PfkA enzyme was expressed in this bacterium. PfkA expression catalyzes the opossite reaction (F6P→FBP) than the innate carbon flow (FBP→F6P) in the cyclic ED pathway, which gives rise to a futile cycle in the central metabolism. As mentioned above, it seems that the more drastic effect on growth is observed with fructose as carbon source, which can be explained by the proximity of the futile cycle to the imput of the fructose into central metabolism (Fructose → FBP *via* FruBKA). This futile cycle is also produced on glucose and succinate, but the impact on growth is lower because it does not affect the early metabolic steps for these carbon sources. To demonstrate the existence of a futile cycle between the FBP and PfkA we determined the concentrations of ATP in the wt and *pfkA*$^{+}$ strains on glucose and fructose (Fig. 11). As can be observed, the expression of PfkA decreased the pool of ATP in the cell, what is consistent with a waste of ATP by the proposed futile cycle.

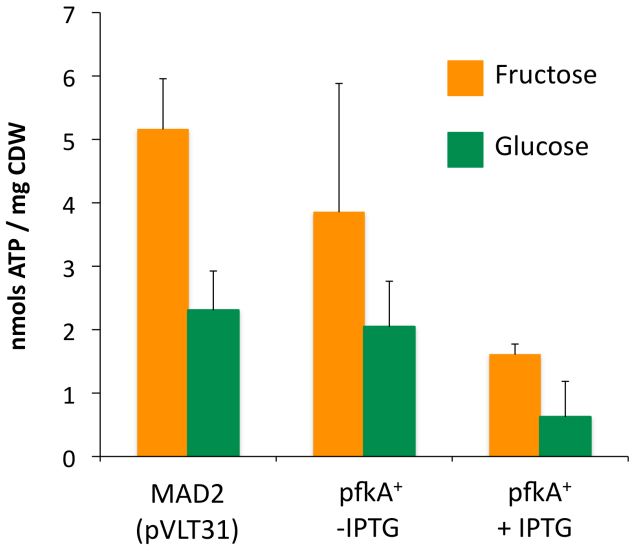

Figure 11. Determination of ATP in *P. putida* MAD2 in absence and presence of PfkA enzyme. Experiments were performed in *P. putida* MAD2 (pVLT31); MAD2 (pVLT31*pfkA*) in absence of presence of IPTG 0.5 mM with fructose (orange columns) and glucose (green columns) as carbon source. Expression of PfkA enzyme reduces the ATP pool in *P. putida*. ATP concentrations were normalized to Cellular Dry Weight (CDW) and expressed in nmols of ATP per milligram of CDW.

2. The regulatory duties of the PTS^{Ntr} system on the central carbon metabolism of *P. putida*

As it was mentioned in the Introduction, *P. putida* KT2440 possesses, like many other bacteria one branch of the phosphotransferase system that is not related to sugar transport, but fulfils various regulatory functions. Recently, we showed that the non-phosphorylated form of one of its proteins, PtsN, directly downregulates the pyruvate dehydrogenase (PDH) activity, an enzymatic complex responsible for the decarboxylation of pyruvate to acetyl-CoA, thereby linking glycolysis to the TCA cycle (Pfluger-Grau *et al*, 2011). On this background, we set out to clarify a possible regulatory role of the PTS^{Ntr} in the central carbon metabolism in this bacterium, as some of the phenotypes described above could be consistent with an alteration in the central metabolism (Velazquez *et al*, 2007). To this end, we analyzed the metabolic fluxes of isogenic strains bearing non-polar directed mutations in each of the corresponding *pts* genes.

2.1. Physiological parameters for growth on different carbon sources

In order to analyze the influence of the PTS^{Ntr} on the central carbon metabolism we compared the metabolic fluxes of cells grown on a non-PTS sugar (glucose) to cells grown on a PTS sugar (fructose) in several *pts* mutants. As a first step, the physiological parameters of the two growth conditions were determined in *P. putida* MAD2 and PTS mutants (Table 4 and 5) in batch cultures.

Table 4. Growth physiology in glucose

Strain	Maximum specific growth rate (μ) [h^{-1}]	Biomass yield on glucose ($Y_{X/G}$) [$g_{CDW}/g_{glucose}$]	Specific glucose consumption rate (q_{glc}) [$mmol_{glc}/g_{biomass}h$]
MAD2	0.25 ± 0.01	0.28 ± 0.03	4.79 ± 0.38
fruB	0.30 ± 0.02	0.29 ± 0.04	4.75 ± 0.43
ptsO	0.30 ± 0.01	0.32 ± 0.02	4.86 ± 0.32
ptsP	0.32 ± 0.03	0.29 ± 0.01	4.90 ±0.43
ptsN	0.23 ± 0.01	0.25 ± 0.04	4.20 ± 0.25
ptsN/ptsO	0.21 ± 0.01	0.31 ± 0.03	4.10 ± 0.11
ptsP/fruB	0.27 ± 0.02	0.31 ± 0.02	4.38 ± 0.10

Table 5. Growth physiology in fructose

Strain	Maximum specific growth rate (μ) [h^{-1}]	Biomass yield on fructose ($Y_{X/F}$) [$g_{CDW}/g_{fructose}$]	Specific fructose consumption rate (q_{Frc}) [$mmol_{Frc}/g_{biomass}h$]
MAD2	0.15 ± 0.05	0.47 ± 0.01	0.85± 0.04
fruB	--	--	--
ptsO	0.12 ± 0.03	0.55 ± 0.01	0.96 ± 0.03
ptsP	0.13 ± 0.02	0.47 ± 0.03	0.80 ± 0.03
ptsN	0.09 ± 0.04	0.49 ± 0.09	0.87 ± 0.02
ptsN/ptsO	0.11 ± 0.03	0.45 ± 0.01	0.90 ± 0.01
ptsP/FruB	--	--	--

We observed 60% reduced growth rate in wild type cells grown on fructose compared to growth on glucose. The final biomass concentration reached however, was comparable between the two growth conditions (1.9 ± 0.09 mg/ml culture on glucose and 1.8 ± 0.08 mg/ml culture on fructose). The lower growth rate observed with fructose comes along with a lower rate of fructose uptake into the cells. Cells grown on fructose internalized 0.75 mmol fructose per g biomass per hour, whereas cells grown of glucose consumed the sugar more than 6 fold faster (4.79 mmol glucose per g biomass per hour). However, growth on fructose seems to be energetically more efficient as reflected by the biomass yield per g sugar consumed. Whereas cells grown on glucose reached 0.28 g CDW (cellular dry weight) per g glucose consumed, cells grown on fructose have a 1.6-fold higher yield (0.47 g CDW/g fructose). Thus, taken together, the non-PTS sugar is degraded more rapidly, but less efficiently than the PTS sugar, a phenomenon that suggests differences in the metabolic fluxes in the central carbon metabolism.

2.2. Metabolic flux analysis of PTS mutants

Analysis of the flux ratios of the upper metabolism (Fig. 12, serine derived from the EMP pathway and pyruvate derived from the ED pathway) revealed that mutation of any of the *pts* genes had no significant influence on the upper pathway, of course with the exception of *fruB* mutations, as these mutants are no longer able to grow on fructose (Velazquez *et al*, 2007).

An interesting picture emerges by analyzing the fluxes around the PEP-Pyr-OAA node in the *pts* mutants (oxaloacetate derived from pyruvate and pyruvate derived from malate). The first striking result is that the only mutation that seems to have a significant influence on the fluxes of the central carbon metabolism is the disruption of *ptsN*, as seen with the *ptsN* or the *ptsN/ptsO* mutant. Therefore, the following analysis is focused these mutants. Both mutants showed higher fluxes in the reactions of the pyruvate shunt (see Figs. 13 and 14, from malate to pyruvate to OAA), independent of the carbon source used. This can be seen in both the flux ratios (Fig. 12) and even better in the net fluxes (Figs. 13 and 14).

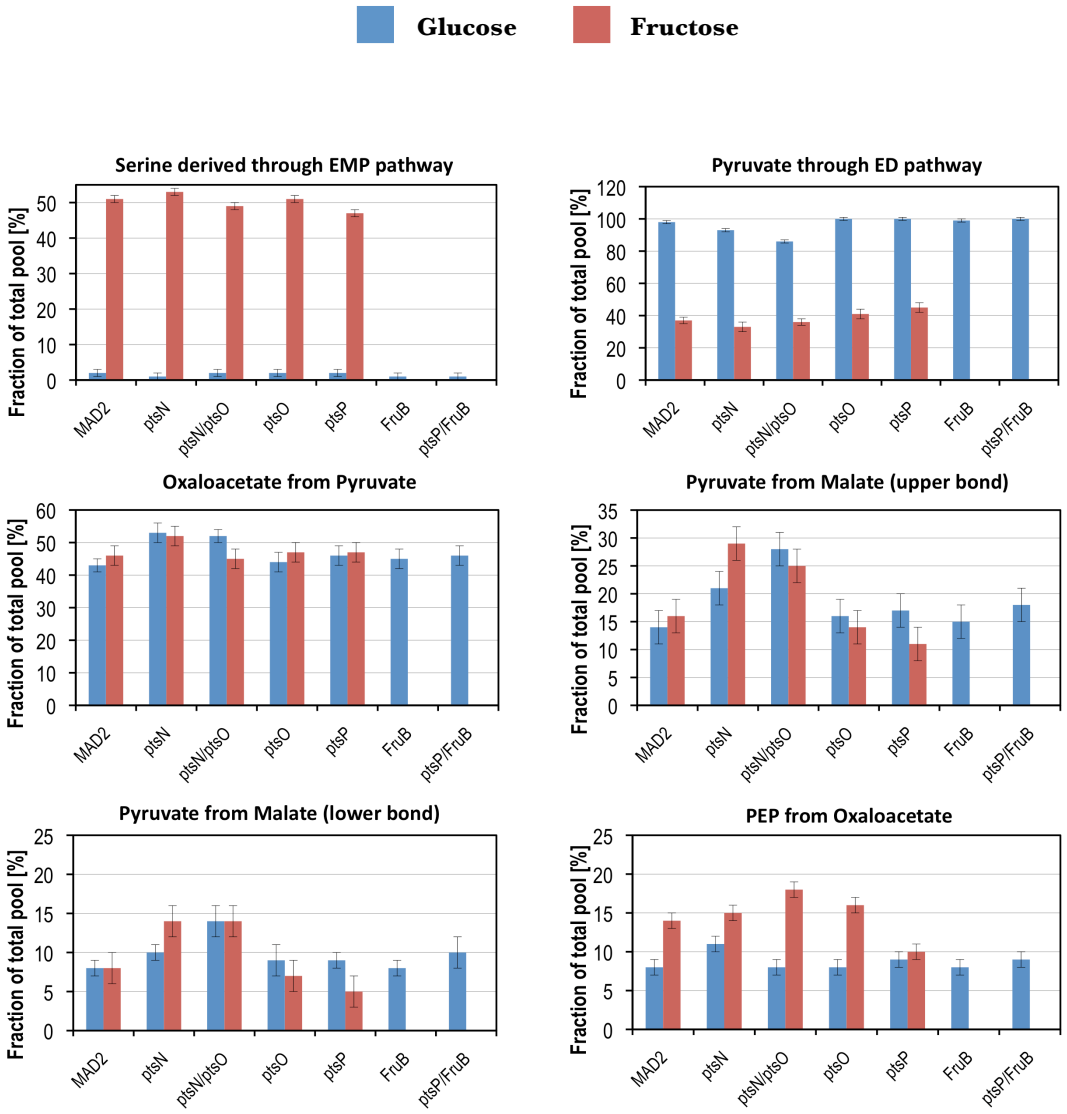

Figure 12. Metabolic flux ratios obtained by METAFoR analysis of experiments with 100% [1-^{13}C]glucose (or 100% [1-^{13}C]fructose), 20% [U-^{13}C]glucose (or 20% [U-^{13}C]fructose), and 80% naturally labelled glucose (or fructose). The data represent the flux ratios (fraction of total pool) for all the *pts* mutants grown on either glucose (blue) or fructose (red) as carbon source. Flux ratios are shown for serine derived from the EMP pathway, pyruvate derived from the ED pathway, oxaloacetate derived from pyruvate, pyruvate derived from malate (upper and lower bond), and phosphoenolpyruvate derived from oxaloacetate. For *fruB* and double mutant *fruB/ptsP* no values are shown growing on fructose, as *fruB* mutants are unable to grow on fructose.

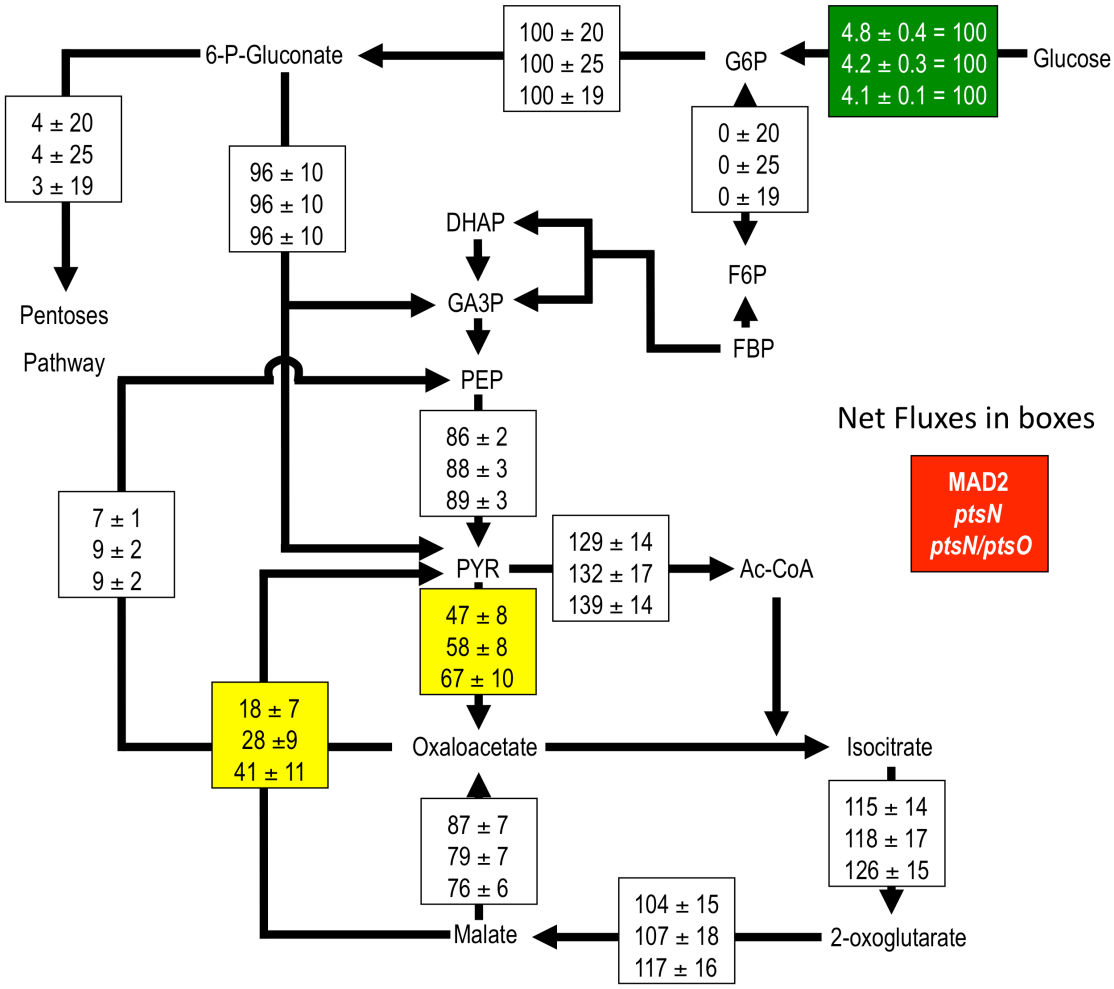

Figure 13. Metabolic net fluxes in the *P. putida* MAD2 reference strain, *ptsN* and *ptsN/ptsO* mutants on glucose as carbon source. Flux values were normalized to the specific glucose uptake rate (shown in the green box). Values shown represent the mean of two independent experiments and the errors indicate their standard deviation. For clarity reasons only the fluxes for the *ptsN* and the *ptsN/ptsO* mutants are shown. Metabolic net fluxes for *ptsO*, and *ptsP* mutants were omitted, as they do not differ significantly in respect to wild type strain. Note the increased net fluxes for *ptsN* and *ptsN/ptsO* mutants in the pyruvate shunt (yellow boxes).

The presentation of the data as net fluxes allows an easy and reliable comparison between various strains grown under the same conditions, because data are normalized to hexose/pentose consumption rates. For the sake of clarity we present in Fig. 13 and 14 only the values for the wild type strain, the *ptsN* and the *ptsN/ptsO* mutants. The flux from pyruvate to OAA catalyzed by the pyruvate carboxylase increased in the *ptsN* mutant 1.2-fold (1.4-fold for *ptsN/ptsO* mutant) on glucose and 1.4-fold (1.5-fold for *ptsN/ptsO* mutant) on fructose. The flux from malate to pyruvate catalyzed by the malic enzyme increased in the *ptsN* mutant 1.6-fold (2.3-fold for *ptsN/ptsO* mutant) on glucose

and 1.5-fold (1.7-fold for *ptsN/ptsO* mutant) on fructose. Thus, the loss of the PtsN protein leads on average to a 1.6-fold increase in the carbon fluxes of the reactions of the pyruvate shunt, independently of the carbon source used. Statistical analysis (t-test) showed that differences between the wild type strain and mutants *ptsN*, *ptsN/ptsO* are all significant at a confidence level of 95% with the exception of the differences observed in the single *ptsN* mutant on glucose. However, similarly to the double mutant *ptsN/ptsO* on glucose, the single mutant *ptsN* is the only strain where these fluxes are higher than wild type strain.

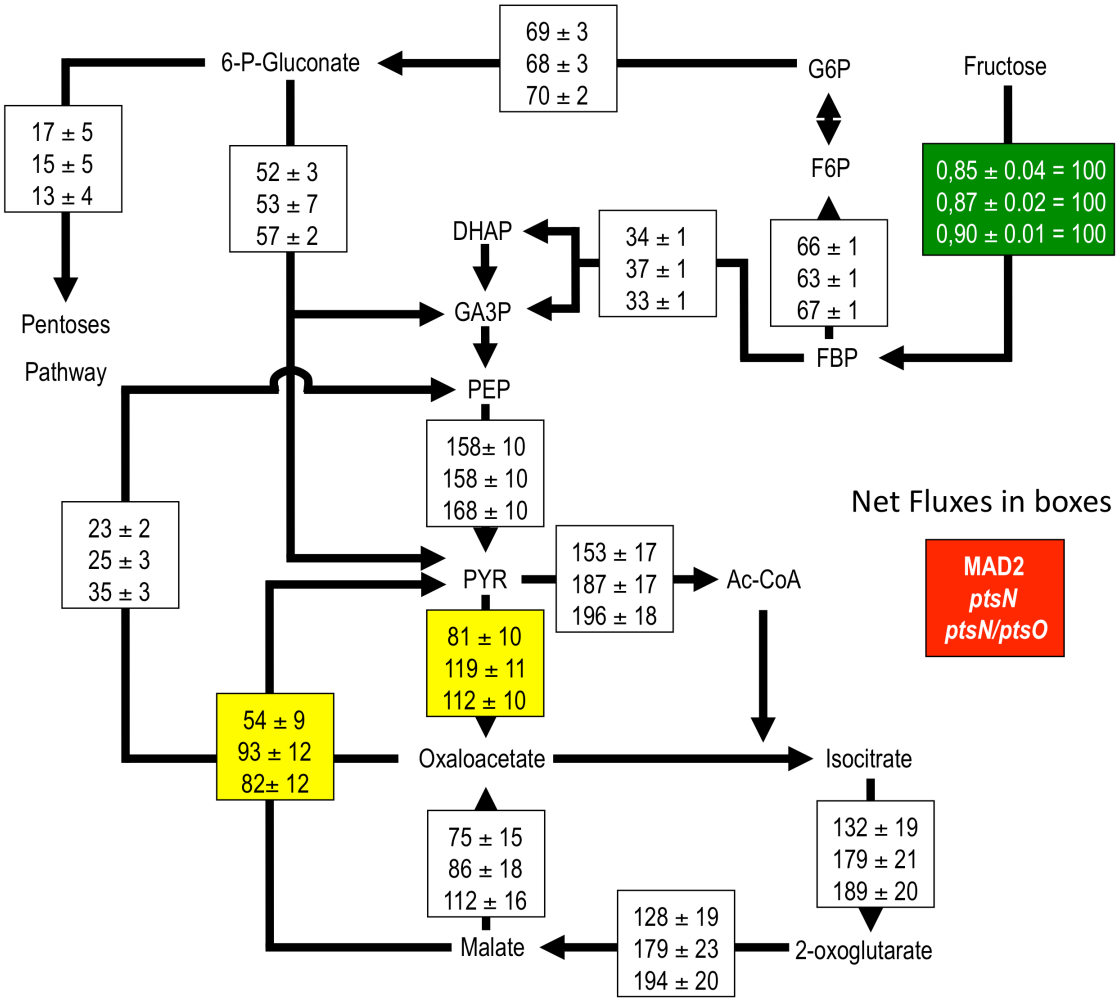

Figure 14. Metabolic net fluxes in the *P. putida* MAD2 reference strain, *ptsN* and *ptsN/ptsO* mutants on fructose as carbon source. Flux values were normalized to the specific fructose uptake rate (shown in the green box). Values shown represent the mean of two independent experiments and the errors indicate their standard deviation. For the sake of clarity only the fluxes for the *ptsN* and the *ptsN/ptsO* mutants are shown. Metabolic net fluxes for *ptsO*, and *ptsP* mutants were omitted, as they do not differ significantly in respect to wild type strain. Note the increased net fluxes for *ptsN* and *ptsN/ptsO* mutants in the pyruvate shunt (yellow boxes).

The fluxomic analysis revealed significantly higher fluxes in the reactions of the pyruvate shunt, which bypasses malate dehydrogenase in the TCA cycle. The pyruvate shunt is a metabolic futile cycle and it comprises the reactions from malate to pyruvate catalized by the malic enzyme and from pyruvate to oxaloacetate by the pyruvate carboxylase. In the *P. putida* chromosome the malic enzyme is encoded by *maeB* (PP_5085) and the pyruvate carboxylase by *accC-2* (PP_5347) and *oadA* (PP_5346). Some bacteria, *e.g. P. aeruginosa*, possess two malic enzymes that differ in cofactor preference (NAD^+ or $NADP^+$-dependent; Eyzaguirre *et al*, 1973). In *P. putida* however, we could only find one gene encoding a putative malic enzyme and obtained measurable enzymatic values only assaying the NADP-dependent but not the NAD-dependent activity (at least *in vitro*, Fig 15). Therefore, *P. putida* seems to have only one malic enzyme encoded by *maeB* (PP_5085). As a next step, we analyzed whether the higher fluxes in the *ptsN* mutants in the shunt can be traced to higher activities of the corresponding enzymes. Thus, cell free extracts of *P. putida* MAD2, *ptsN* and *ptsN/ptsO* were prepared from cultures grown on glucose or fructose, respectively, and assayed for activity of the pyruvate shunt enzymes (Fig. 16).

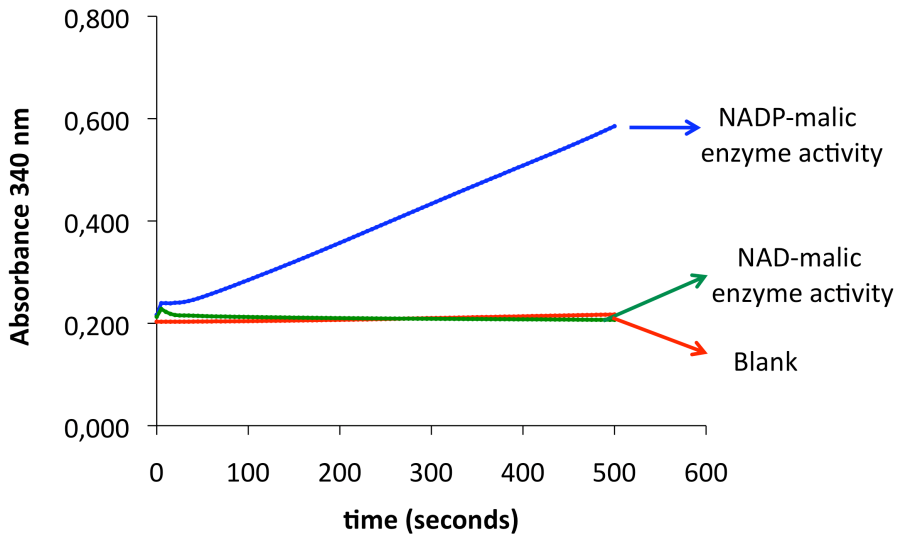

Figure 15. Enzymatic assay for NADP dependent-malic enzyme (blue) and NAD dependent malic enzyme (green) in *P. putida* wild type strain. As can be observed, enzyme activity was obtained only when the cofactor was NADP which suggests that the enzyme MaeB (PP_5085) is NADP-dependent. A blank of the assay (red) was performed with all the components of the enzymatic reaction but lacking proteins.

The activity of the malic enzyme was about 1.4-fold higher in PtsN-less cell extracts with no apparent influence of the presence/absence of PtsO and independent of the carbon

source. These data reflect well the estimated fluxes. When measuring the specific activity of the pyruvate carboxylase, a similar result was obtained (Fig. 16b). In cell extracts of *P. putida ptsN* and *ptsN/ptsO* the enzyme showed higher activity as compared to the wild type, and again, this was independent of the carbon source and the presence of PtsO.

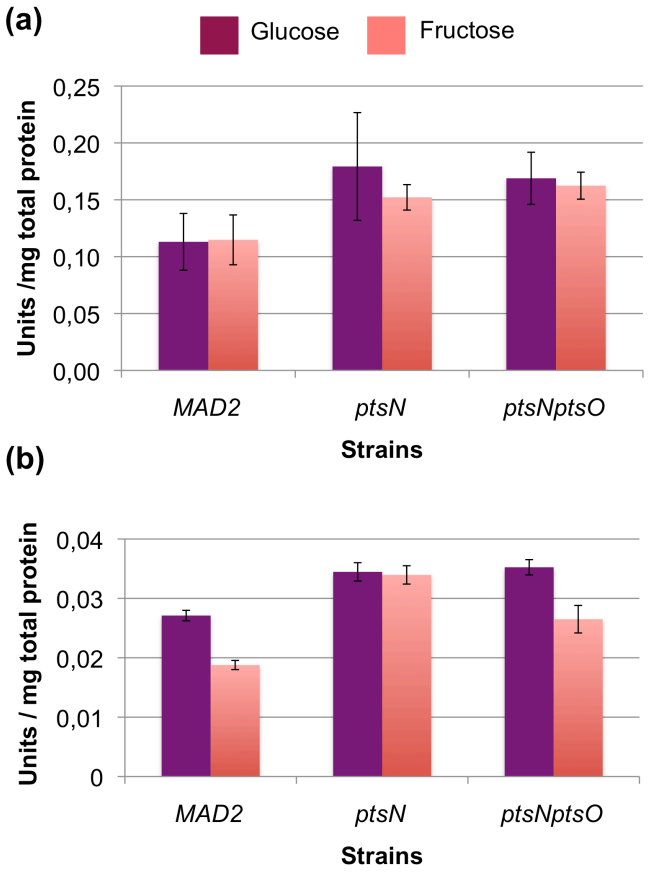

Figure 16. Enzyme activities in crude cell extracts for pyruvate shunt enzymes (a) malic enzyme and (b) pyruvate carboxylase of the *P. putida* MAD2 reference strain, *ptsN* and *ptsN/ptsO* mutants. The enzymatic activities were measured on glucose and fructose as carbon source and the data are show in Units per milligram of protein (U/mg protein). Given values represent the mean of three independent experiments and the error bars indicate their standard deviation.

In a next step, we wondered whether the regulation exerted by PtsN on the pyruvate shunt depend of its phosphoprylation state. To clarify this issue we analyzed the malic enzyme activity in two *P. putida* MAD2 strains altogether isogenic to the wild-type but bearing each an allele of *ptsN* with changes in the triplet corresponding to the phosphorylable position H68 of the EIIA^{Ntr} protein (Pfluger-Grau *et al*, 2011). In one case (*ptsNHA*), the encoded product had a HisxAla substitution that prevented any phosphorylation and thus locked PtsN in a form devoid of any phospho-histidine

(Pfluger and de Lorenzo, 2007). In the other case (*ptsNHE*), the same H68 codon was changed from His to Glu. The addition of a negative charge in the position formerly occupied by a phosphorylable histidine is generally considered to lock the protein in a form that resembles the phosphorylated species (Wittekind *et al,* 1989). The difference is that such a charge cannot be transferred further to another destination. This genetic approach allows to differentiate the effects of PtsN owing to its phosphorylation state. The results are shown in Fig. 17. No significant differences in enzyme activity were observed between the wild type and mutants *ptsNHA*, *ptsNHE*, suggesting that the regulation exerted by PtsN occurs independently of its phosphorylation state.

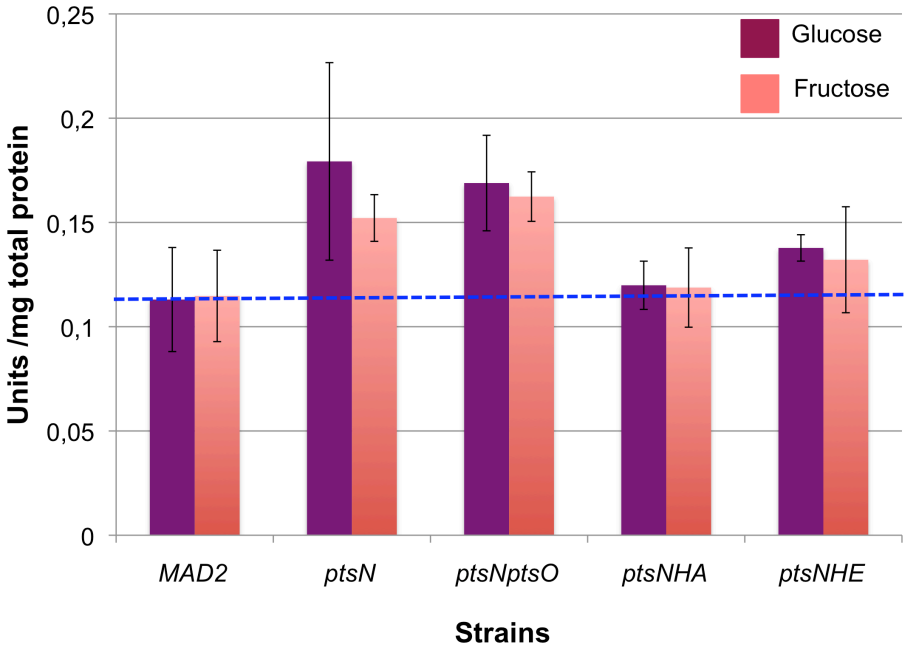

Figure 17. Malic enzyme activity in crude cell extracts of the *P. putida* MAD2 reference strain, *ptsN*, *ptsN/ptsO*, *ptsNHA* and *ptsNHE* mutants. The enzymatic activities were measured on glucose and fructose as carbon source and the data are show in Units per milligram of protein (U/mg protein). Given values represent the mean of three independent experiments and the error bars indicate the standard deviation of these independent experiments.

Thus, PtsN seems to downpregulate the activity of the pyruvate shunt enzymes regardless of its phosphorylation state, in a process that depends only on the presence/absence of the protein. Whether this phenomenon is based on direct interactions between the participating proteins or is a secondary result of carbon flux redistribution cannot be answered with the present data and will be the subject of further investigations.

CHAPTER 2

The Catabolite repressor activator (Cra) regulator from *Pseudomonas putida* and its interplay with the PTS^{Fru} system: *in vitro* studies*

*** This chapter was published as:**

Max Chavarría, César Santiago, Raúl Platero, Tino Krell, José M. Casasnovas & Víctor de Lorenzo. Fructose 1-Phosphate is the preferred effector of the metabolic regulator Cra of *Pseudomonas putida*. *J. Biol. Chem.* (2011) 286, 9351-9359.

---

1. Identification, cloning and purification of the Cra protein of *P. putida*

The genome of *P. putida* bears an ORF for a protein (PP0792) of 331 amino acid residues (coordinates 909206-908211) and 38.4 KDa MW that shares 74% similarity and 48% identity with the *E. coli* Cra protein (Fig. 18). This identity goes up to 70% in the predicted DNA binding domain of the proteins, suggesting that the target genomic sequences ought to be similar (if not identical) as well. All this criteria qualifies PP0792 as a *bona fide* orthologue of the reference enterobacterial counterpart. Yet, unlike *E. coli* and *S. typhimurium*, the $cra_{P.\ putida}$ variant maps adjacent and divergently oriented to the *fruBKA* operon (Figs. 19 and 21).

This gene cluster encodes proteins for phosphorylation and transport of fructose (Velazquez *et al*, 2007) through the phosphoenol pyruvate phosphotransferase carbohydrate system of *P. putida* (Velazquez *et al*, 2007; PTS^{Fru}). Because of this proximity, PP0792 was formerly annotated as FruR, not as Cra (Nelson *et al*, 2002). To ensure the functional assignment, the $cra_{P.\ putida}$ sequence was amplified, added with a metallo-affinity His_6-tag and the protein purified to apparent homogeneity as explained in the Materials and Methods section (Fig. 20).

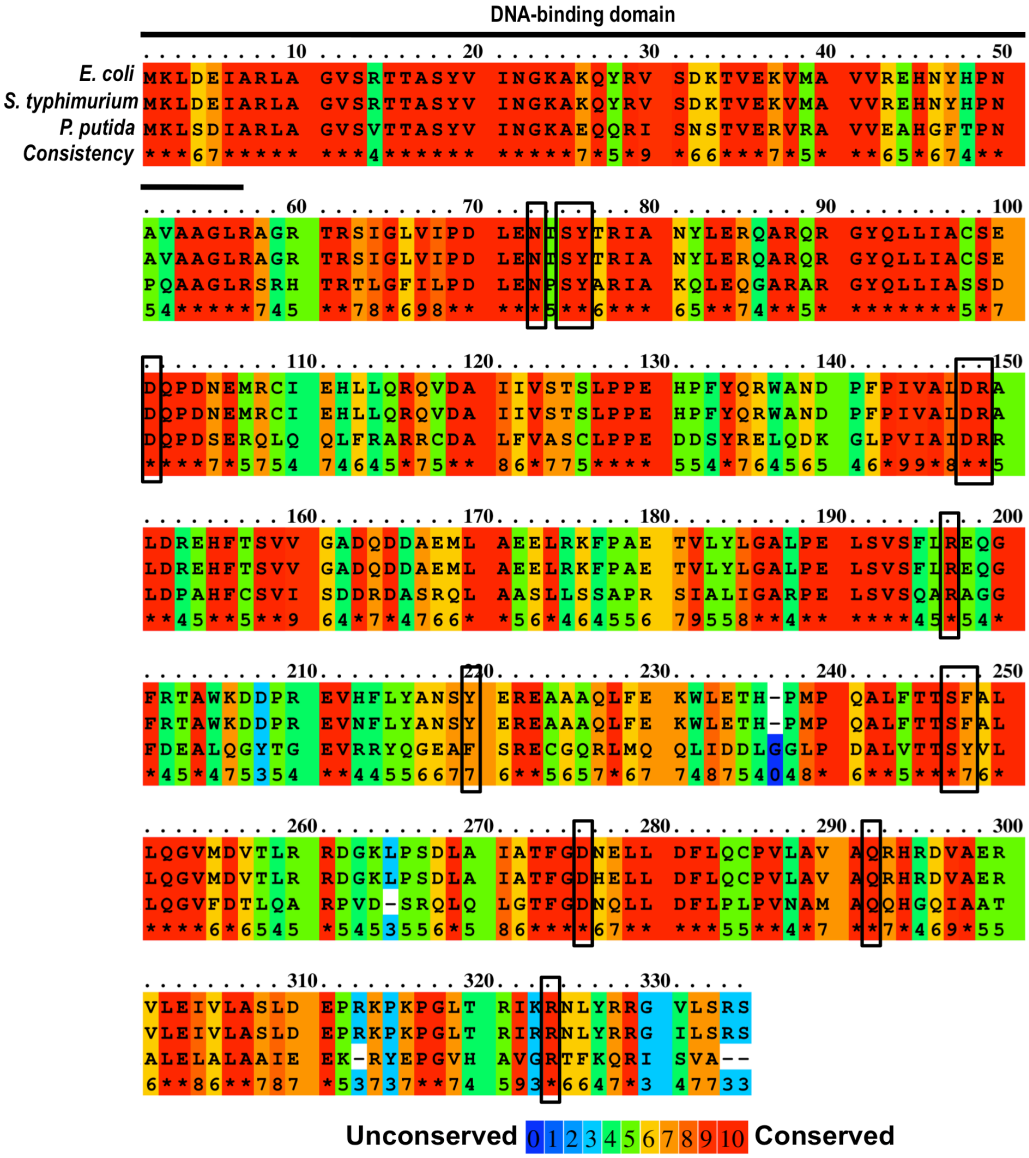

Figure 18. Alignment of Cra proteins from *E. coli, S. typhimurium* and *P. putida* KT2440. The *P. putida* Cra protein has 74% similarity and 48% identity with the *E. coli* counterpart. Identity increases to 70% in the predicted DNA binding domain of the proteins. The DNA binding module is located in the N-terminal side and it is formed by the first 57 aminoacids of the proteins (indicated with a black line). Amino acids that form the effector-binding pocket are marked with black boxes. Note that 85% of the amino acids that form the pocket of the *P. putida* protein are identical, and 100% of them are similar in respect to those of *E. coli* and *S. typhimurium*. The only changes are the Phe220 (Tyr in *E. coli*) and Tyr 248 (Phe in *E. coli*). The alignment and the conservation score were performed with PRALINE software (Simossis and Heringa, 2005). The scoring ranks (consistency values) from 0 for the least conserved alignment position, up to 10 for the most conserved alignment position.

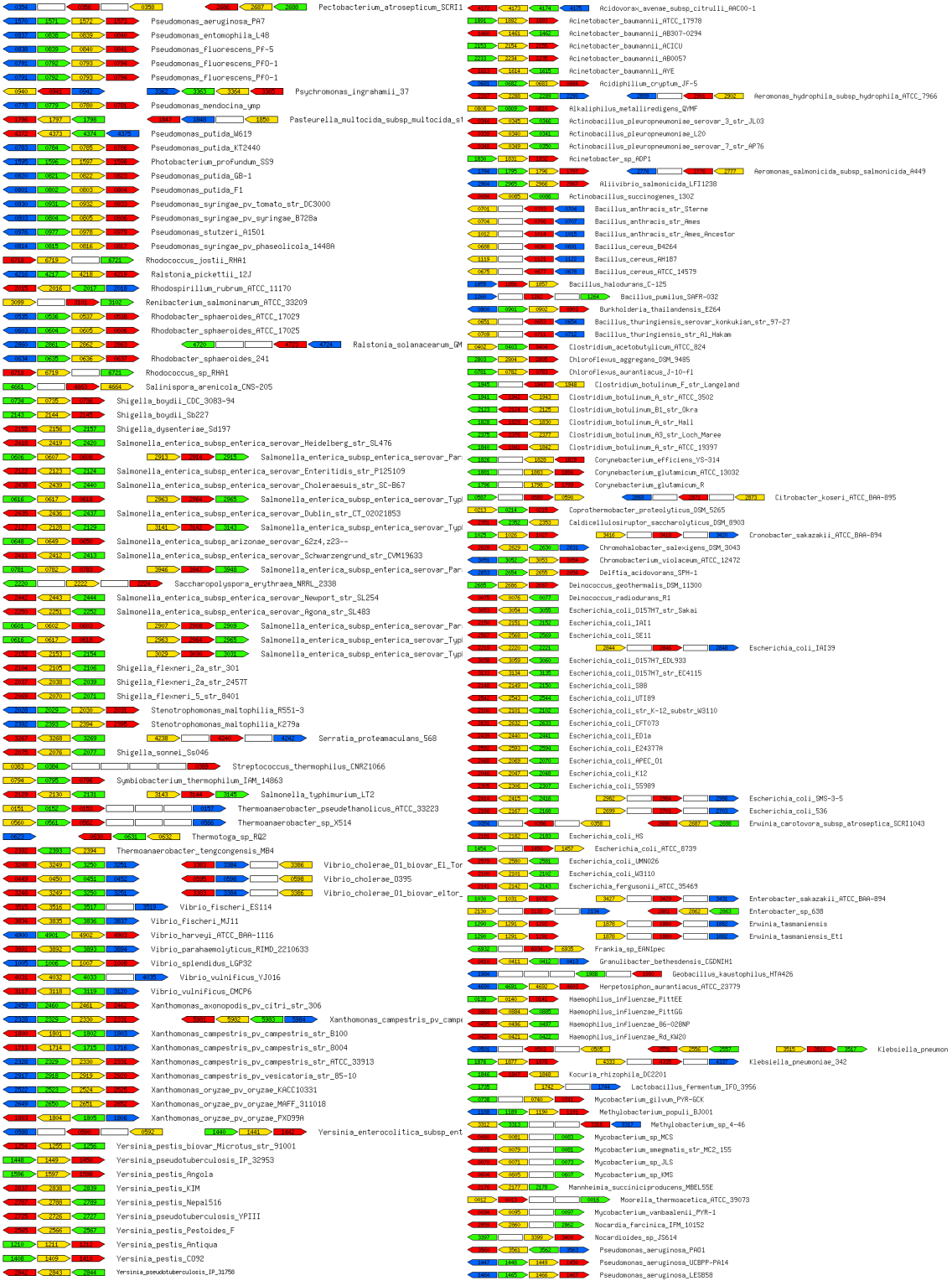

Figure 19. Organization of the fructose operon in bacteria. Comparison of genomic organization of the fructose operon revealed differences between species, e.g. position and orientation of the *fruBKA* operon with respect to the regulator Cra (FruR). Duplicate *fru* genes are not infrequent. Note similarities in the organization of the operon of *E. coli* and *S. typhimurium*, and their difference in respect to *Pseudomonas*. Color code: *fruB* in green, *fruA* in red, *fruK* in yellow and *cra* (*fruR*) in blue. Other genes found in or adjacent to the *fru* operon are shown as empty boxes.

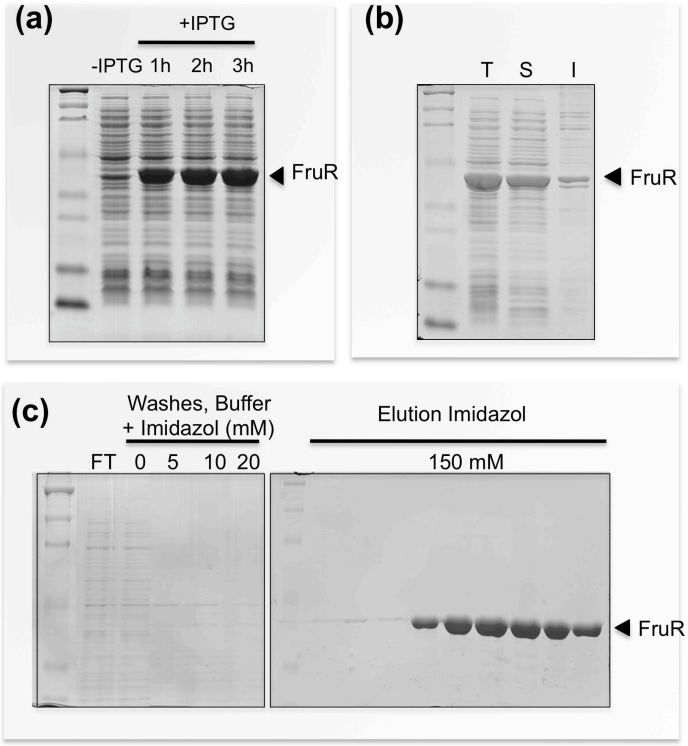

Figure 20. Expression and purification of the Cra protein of *P. putida*. (a) Expression test. A high expression level of Cra (38.4 KDa) from the expression vector was triggered by the addition of 0.5 mM of isopropyl-β-D-thiogalactoside (IPTG) followed by induction for a further 3 h. **(b) Solubility test.** Cell pellets were resuspended in 50 mM sodium phosphate buffer pH 7.0, 200 mM and mechanically lysed using a French press. Then, cell debris were removed by centrifugation. Note that the majority of Cra protein remains in the soluble phase. **T** = total proteins (before lysis); **S** = soluble phase; **I** = insoluble phase (cell debris). **(c) Protein purification**. The native His_6-Cra protein isolated from the lysis supernatant was purified using a TALON Metal Affinity Resin (Clontech). The pure protein elution was done with equilibration buffer 1X plus 150 mM of Imidazol as was described in materials and methods section. **FT** = Flow through.

2. Analysis of the regulatory region of fructose operon of *P. putida*

Analysis of the intergenic region (Fig. 21b) revealed the presence of a motif (5'-TTAAACGTTTCA-3') with a high score to the consensus binding site for the Cra regulator of *E. coli* and *S. typhimurium* (Fig. 21a; Negre *et al*, 1996; Ramseier *et al*, 1993; Shimada *et al*, 2005). To examine whether such a sequence was in fact the operator of $Cra_{P.\ putida}$, a 22 bp double-stranded DNA fragment containing the candidate target was synthesized and employed in the mobility shift assay shown in Figure 22.

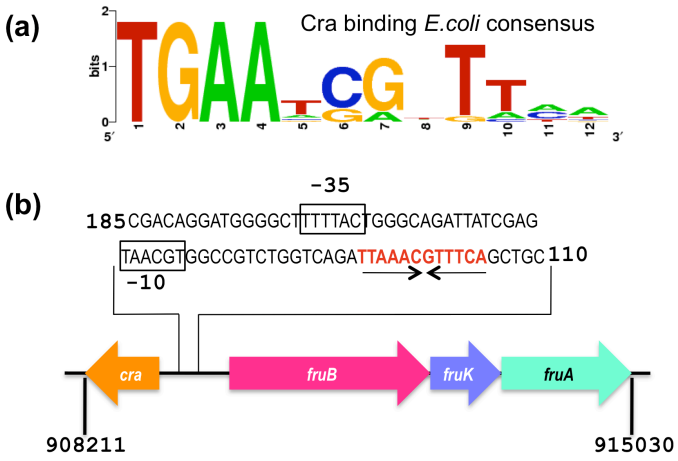

Figure 21. *E. coli* Cra binding consensus sequence and regulatory region of the fructose operon of *P. putida*. **(a)** The *E. coli* consensus sequence for Cra binding site was retrieved from the PRODORIC database (Munch *et al*, 2003). This sequence forms an incomplete palindrome in which the left half-site is considerably better conserved than the right half-site. **(b)** The regulatory region of the *fruBKA* operon in *P. putida* was analyzed and one single operator was identified as shown. The sequence TTAAACGTTTCA (in red) corresponds to the palindromic Cra-binding motif, whereas the black boxes show the putative -35/-10 promoter region upstream of the *fruBKA* operon.

The results indicated the formation of one specific complex between the DNA and the Cra$_{P.\ putida}$, the abundance of which increased with Cra concentration (Fig. 22a). The molar ratio at which the DNA band disappeared entirely from the gel grossly corresponded to DNA:Cra 1:2. These results verified the interaction of the protein with its predicted binding site within the *cra/fruBKA* promoter region and laid the basis for determination of key parameters as explained below.

3. The Cra regulator of *P. putida* is a dimeric protein

The oligomerization state of the purified Cra$_{P.\ putida}$ was determined by means of analytical ultracentrifugation experiments. The sedimentation profile (Fig. 23a) showed the occurrence of one main species to 3.9S with $S_{20,W}$ of 4.8 ± 0.1 (frictional ratio f/f_0 = 1.35), which accounted for 88-94% of the observed molecules and which was compatible with a dimeric form of the protein. The sedimentation equilibrium results (data not shown) predicted a mass value of 72.4 ± 6.0 KDa, which was slightly lower than the theoretical mass for the dimeric form of the protein. But taken together, the velocity and equilibrium sedimentation results indicated that Cra existed mainly as a dimer in solution at the concentrations used. The protein oligomerization state was

confirmed by size-exclusion chromatography (Fig. 23b), in which one main peak of approximately 60-80 KDa (*i.e.* a dimer) was followed by much less abundant species, tailing between the 21-50 KDa markers (*i.e.*, a monomer).

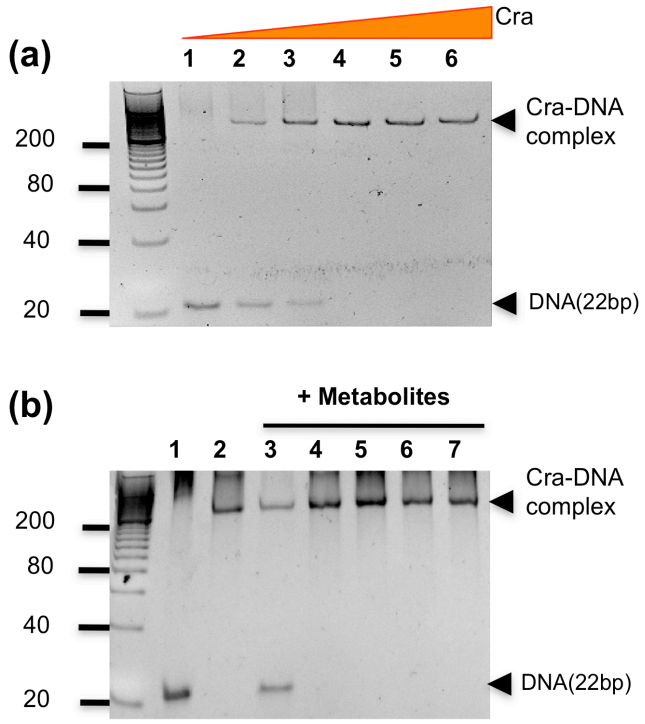

Figure 22. Non-radioactive electrophoretic mobility shift assays (EMSA) of Cra and its binding site in the intergenic *cra/fruBKA* region of *P. putida*. **(a)** EMSA experiment with increasing concentrations of pure Cra protein. Molar ratios DNA:Cra were 1:0 (lane 1), 1:0.5 (lane 2); 1:1 (lane 3), 1:2 (lane 4), 1:4 (lane 5) and 1:8 (lane 6). **(b)** Cra effector identification. DNA (0.75 μM) was incubated with pure protein (1.5 μM) in the presence of 1 mM of different metabolites: F1P (lane 3), FBP (lane 4), F6P (lane 5), G6P (lane 6) and fructose (lane 7). Lanes 1 and 2 correspond to DNA in the absence and presence of Cra respectively, without any added metabolite. Note that only F1P prevents the binding of the protein to DNA.

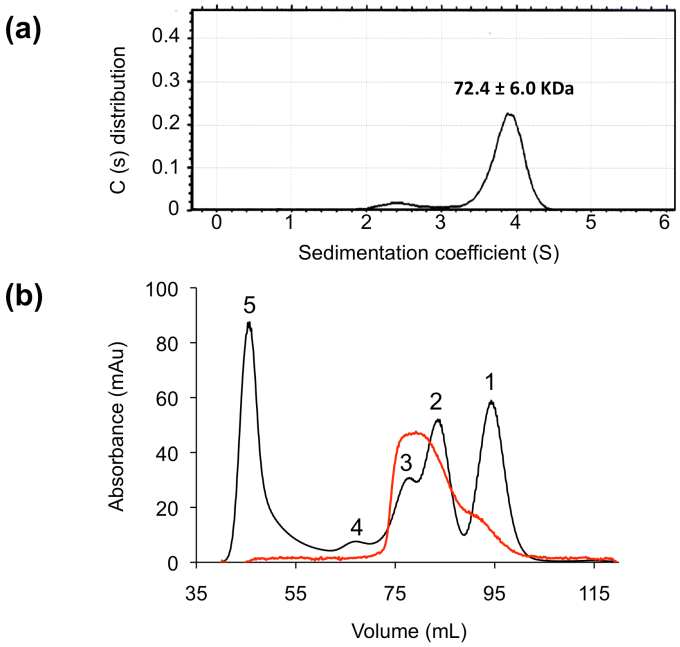

Figure 23. Oligomerization state of the Cra protein of *P. putida*. **(a)** Distribution of sedimentation coefficient population c(s) against s, obtained by sedimentation velocity experiments. The experiments were performed with 0.5, 1 and 1.3 mg/ml of pure Cra protein. The sedimentation profile was dominated by a species of 3.9S, accounting for 88-94% of the observed molecules, followed by a small peak at 2.4S (2.3-8.9%). The predominant species with sedimentation coefficient of 3.9S, was corrected to $S_{20,w}$, using the viscosity value of the solution (measured in a viscometer Anton Paar AMVn). The corrected sedimentation coefficient was 4.8S which is compatible with a globular dimer of the protein. Equilibrium sedimentation experiments predicted that the dominant peak has a molecular mass of 72.4 ± 6.0 KDa. **(b)** Gel filtration. The oligomerization form of *P. putida* Cra was confirmed by size-exclusion chromatography as shown. The main peak of 60-80 KDa is consistent with a dimeric species, while the minor tail of 21-50 KDa surely corresponds to residual monomeric species. The chromatogram shows the superposition of two differents runs: Cra alone (red line) and standard proteins used as weight marker (black line). The proteins in the elution fractions were monitored by SDS-PAGE (not shown). Molecular weight markers were run under the same conditions. 1: chymotrypsin (21 KDa), 2: albumin (50 KDa), 3: BSA (70 KDa), 4: Ab (170 KDa), 5: Dextran.

4. Cra strongly binds its single operator in the *cra/fruBKA* region of *P. putida*

The interaction parameters of the $Cra_{P.\ putida}$ protein with the operator DNA found within the *fruBKA* promoter segment (Fig. 21b) were examined by means of isothermal titration microcalorimetry. The corresponding results are shown in Fig. 24a.

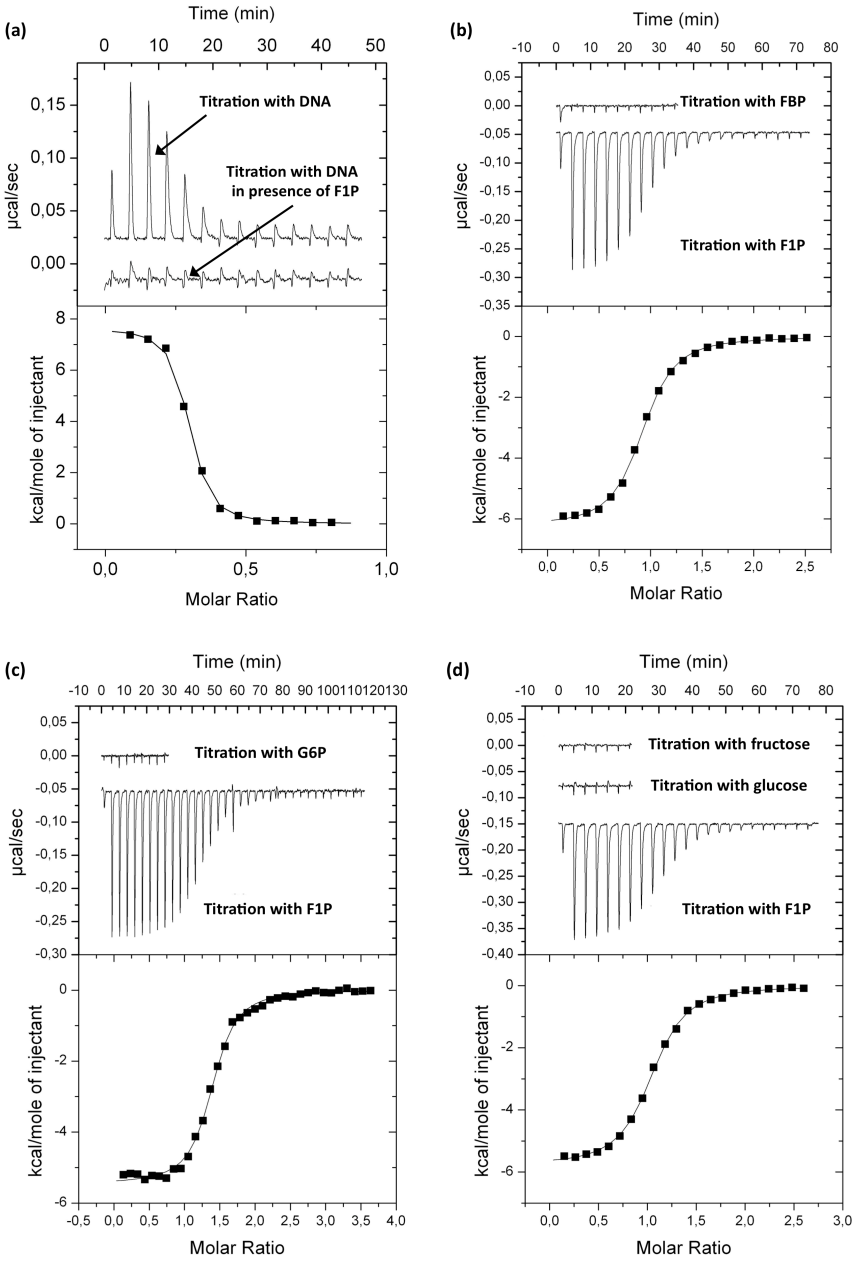

Figure 24. ITC assays with Cra, effectors and DNA. The upper panels plot raw data from representative ITC experiments, while the lower panels show the fitted curves of the same results, but integrated and corrected for dilution. **(a)** Titration of Cra protein with DNA in absence and presence of F1P. Positive peaks represent an endothermic event. Note that no interaction between Cra and the DNA is detected in the presence of F1P. **(b-d)** Titration of Cra protein with FBP, G6P, fructose, glucose and F1P. Note that only the titration with F1P produces a heat change in the experiment. In all the cases, F1P was added after each titration as positive control. Negative peaks are indicative of an exothermic event. The sigmoidal shape of the binding curve allows determination of the protein-effector stoichiometry, which corresponds to the molar ratio (x-axis in lower panel) at the point of inflexion of the curve. In this case, such molar ratio was 1:1; indicating that one molecule (calculated: 1.06 ± 0.06 molecules) of F1P interacts with one molecule of Cra monomer.

Note that in the upper panel peaks go upwards, which indicates that the binding of Cra to DNA is an endothermic process *(*ΔH = 7.66 ± 0.09 kcal/mol). Since enthalpy changes are unfavorable, binding ought to be entirely entropy-driven ($T\Delta S$ = 17.68 ± 0.15 kcal/mol, ΔG = -10.02 ± 0.10 kcal/mol). This situation is not infrequent, as the binding of proteins to DNA is often endothermic but also fostered by the positive entropic effect of the displacement of DNA-bound water molecules (Krell *et al*, 2007). Subsequent calculations allowed us to determine a protein-DNA dissociation constant (K_D) of 26.3 ± 3.1 nM that reflects a very strong interaction and which likely enables Cra$_{P.\ putida}$ to exert a considerable repression on expression of the *fruBKA* genes.

5. Surveying metabolic intermediates as Cra$_{P.\ putida}$ effector candidates

In order to shed light on the nature of Cra effector(s), DNA samples were incubated with pure Cra protein in the presence of different metabolites and submitted to EMSA experiments as before -except for the addition of candidate molecules to the binding mixtures prior to loading the gel. The chemical species that were listed as possible Cra inducers able to release its strong binding to DNA included fructose, F1P, FBP, F6P, and G6P. The EMSA experiments shown in Fig. 22b (lanes 3-7) indicated that only F1P was able to prevent binding of the repressor to the *fruBKA* regulatory region (Fig. 21b) confirming this metabolite as the effector of Cra. These experiments, however, did not altogether rule out that other small molecules could interact with the target protein with a weaker strength unable to withstand the conditions of the EMSA test. Furthermore, the gel of Fig. 22b revealed the persistence of a fraction of the Cra-DNA complex that did form even in the presence of F1P (Fig. 22b, lane 3). To clarify these ambiguities, we again resorted to the ITC technology described before. First, we ran isothermal titration experiments with purified Cra and the various candidate effectors as the interaction partners (Figs. 24b-d). The results shown in Fig. 23b indicated that binding of F1P to Cra was both enthalpy-driven (ΔH = -5.94 ± 0.39 kcal/mol) and entropy-driven ($T\Delta S$ = 3.16 ± 0.4 kcal/mol), producing a total free energy change (ΔG) of -9.10 ± 0.06 kcal/mol. Favourable (negative) enthalpy changes can be attributed to bond formation between F1P and amino acids in the cognate binding site, whereas favorable (positive) entropy changes are generally caused by the ligand-induced release into the medium of otherwise bound water, thereby increasing the disorder (entropy) of the system. Further calculations revealed not only an apparent stoichiometry of 1.06 ± 0.06 molecules of F1P per Cra monomer, but also demonstrated a high protein-effector affinity (K_D = 209

± 20 nM). It is noteworthy that this affinity value is significantly higher than the corresponding figures for other transcriptional regulators of the GalR-LacI family. For instance, the K_D of IPTG binding to LacI is 2.8 μM (Wilson *et al*, 2005), that of 2-ketogluconate to PtxS, 15 μM (Daddaoua *et al*, 2010), and so on. ITC experiments also demonstrated without a doubt that Cra had no affinity, even residual for other metabolites. Specifically, the test run with FBP as a Cra effector-to-be (Fig. 24b) did not produce the slightest indication of interaction. The same was true for other candidate effectors *e.g.* G6P, glucose and fructose (Figs. 24c and 24d), indicating that the repressor is highly selective for F1P. Finally, to clarify whether some residual Cra-DNA complex could still be formed in the presence of F1P, a mixture of Cra and F1P was incubated with the same target DNA employed above for the repressor-operator binding experiments. The resulting ITC curves (Fig. 24a) confirmed that the Cra-F1P complex was altogether unable to bind DNA. This set of data rules out that high concentrations of FBP formed intracellularly during certain physiological conditions could act as a physiological effector of Cra. Instead, the effects of FBP as an inducer of this repressor reported in the literature (Bledig *et al*, 1996; Kotte *et al*, 2010) could be the result of its chemical or enzymatic conversion into F1P.

6. Cra crystallization and structure resolution

While the results above confirmed the nature of F1P as Cra effector, they did not discount that the effector-binding site of the repressor could accommodate other thus far unidentified metabolites. To shed light on this possibility, we set out to determine the tridimensional structure of such a pocket in both the effector-less and the effector-bound Cra structure by X-ray crystallography. The protein was crystallized as described in Materials and methods. SDS-PAGE of extensively washed crystals showed a single, sharp band of ~30 kDa for the crystallized sample, smaller than the theoretical size of 38 kDa. This suggested precise excision of an ~8 kDa fragment from the main protein body during the crystallization process (see below). MALDI-TOFF analysis of the truncated protein produced a predominant peak of 30.4 kDa, confirming the previous data (Fig. 25).

Proteolytic removal of non structured or unstable polypeptides often help the crystallization of the rest of the protein core (Wernimont and Edwards, 2009). This appeared to be our case, because the occurrence of such a cleavage during the

concentration and crystallization of Cra was ultimately beneficial: crystals were obtained that belonged to the $P2_1$ space group, contained two Cra molecules in the asymmetric unit and did diffract to a resolution of 2 Å (see Table 6).

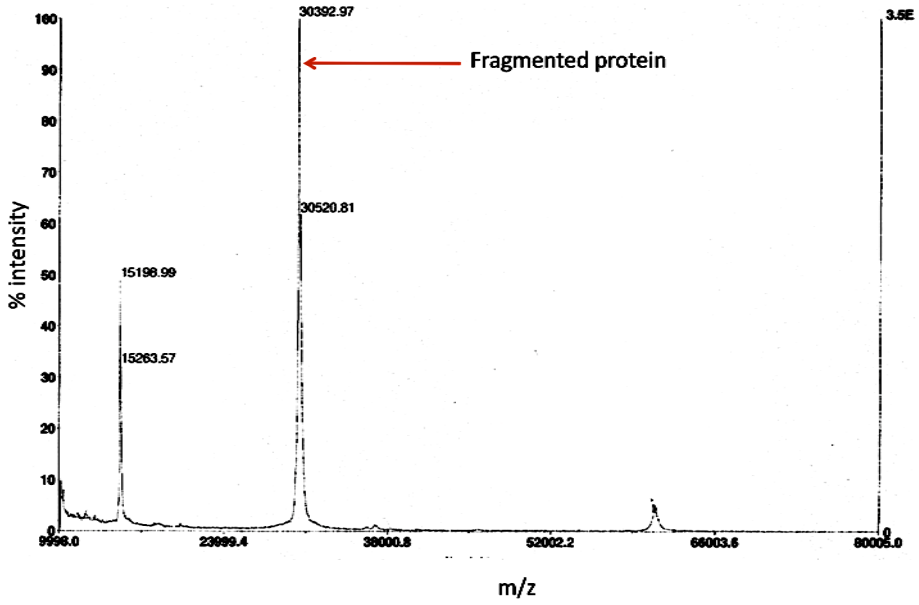

Figure 25. MALDI-TOFF analysis of Cra crystals. Mass spectrometry analysis of the truncated protein produced a predominant peak of 30.4 kDa. This suggested precise excision of an ~8 kDa fragment from the main protein body during the crystallization process.

The structure of the Cra protein was determined for both the effector-free and the F1P-bound forms, in which last case crystals were soaked in a solution containing 1 mM concentration of the metabolite (see Materials and Methods). The corresponding 3D architectures are shown in Fig. 26a. Note that the dimers of the effector-less Cra and its F1P-bound counterpart were very similar, with a root mean square deviation (rmsd) of 0.48 Å for 270 residues. Note also that expectedly the crystal structure lacks the leading N-terminal 59 amino acid residues. As mentioned above, this deletion is irrelevant (if not beneficial) for our purpose, because the missing segment includes the DNA-binding domain and a short linker, but leaves intact the effector-binding site of the protein.

Table 6. Data Collection and Refinement Statistics of Se-Met derivatized protein and Cra with its effector.

Data collection	**Se/Met Cra**	**Cra/F1P**
Space group	$P2_1$	$P2_1$
Wavelength	0.97925 (peak)	0.933
Cell dimensions		
a, b, c (Å)	37.3, 118.5, 61.8	37.7, 120.2, 61.8
a, b, g (°)	90, 107.1, 90	90, 107.4, 90
Resolution (Å)	59-2.0	60-2.3
Highest resolution bin	2.1-2.0	2.42-2.3
No. of unique reflections	34595 (5011)	23340 (3381)
Multiplicity	7.4 (7.4)	3.4 (3.4)
Completeness (%)	99.8 (99.8)	99.8 (100)
R_{sym} or R_{merge}	8.3 (40)	5.0 (35.8)
I / s(I)	5.6 (1.7)	12.6 (2.2)
B-factor Wilson (Å^2)	28	42
Refinement statistics		
Resolution (Å)	15.0-2.0	15.0-2.3
R_{work} / R_{free}	18.4/21.8	18.4/22.1
Reflections (R_{free})	66122 (3320)	22057 (1130)
No. of atoms		
Protein	4193	4186
Ligand	12	32
Water	175	107
B-factors		
Protein A/B	41/40	50/51
Ligand C/D	37/58	30/34
Water	41	41
R.m.s deviations		
Bond lengths (Å)	0.003	0.003
Bond angles (°)	0.71	0.843
Ramachandran plot[a]	91.7/7.9/0/0.4	87.9/11.5/0.2/0.4

*Highest-resolution shell is shown in parentheses. [a]Percentage of residues in most favored regions, allowed regions, generously allowed regions and disfavored regions, respectively.

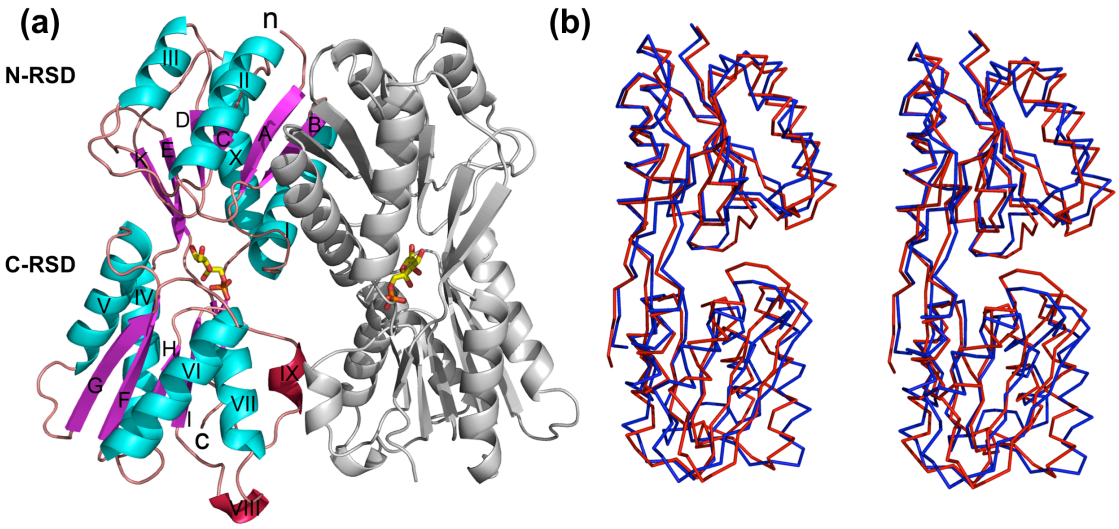

Figure 26. Crystal structure of Cra in complex with F1P. **(a)** Ribbon representation of the crystal structure of the regulatory subdomain of Cra in complex with its ligand F1P. β-strands are colored in magenta, helixes in cyan, 3_{10} helixes in red and loops in orange. F1P is shown with sticks representation and the carbons in yellow, phosphorus in orange and oxygens in red. The N and C terminus are marked with lower case letters and the secondary structure elements with upper case. The N-regulatory subdomain consists of strand A (63 to 68), helix I (74 to 89), strand B (93 to 98), helix II (103 to 115), strand C (120-123), helix III (133 to 139), strand D (144 to 147), strand E (157 to 164), helix X (293 to 310), and strand K (316 to 320). The C-regulatory subdomain is composed of helix IV (163 to 175), strand F (181to 187), helix V (192 to 204), strand G (211 to 217), helix VI (222 to 236), strand H (242 to 245), helix VII (239 to 248), helix VIII (263 to 265), strand I (269 to 273), helix IX (277 to 280), strand J (286 to 290) and strand L (323 to 325). **(b)** Stereo view of the superimposed regulatory domains of Cra from *P. putida* colored in red and from *E. coli* (PDB accession code: 2IKS) in blue. A lateral view of a Cα representation of the structures is shown.

As shown in Figure 26a, both Cra monomers are related by a pseudo two-fold axis and share an interface surface of 1700 Å^2 per monomer. The N-terminal regulatory subdomain (N-RSD) comprising residues from Thr63 to Ser161 and from His293 to Val320, specifically α helices I and II and β strand B (Fig. 26a), contributes most of the interactions to form the dimer: residues from this region are implicated in 12 salt bridges and 80% of the hydrogen bonds between domains. In contrast, the C-terminal regulatory subdomain (C-RSD; residues Asp163-Ala290 and Tre323-Lys325) contributes only with 6 hydrogen bonds to the interaction through helices VII and IX (Fig. 26a). Structural comparisons using the DALI server (Holm and Rosenstrom, 2010) gave a top solution with a Z score of 33 and a sequence identity of 44% with the fructose repressor (Cra/FruR) of *E. coli* deposited in the RCSB database (PDB

accession code: 2IKS), but not yet published. Structural comparison is shown in Fig. 26b. The folds observed in both proteins were close to the domain organization of other members of the family such as LacI (Lewis *et al*, 1996) and PurR (Schumacher *et al*, 1994). These were defined by a central parallel β-sheet formed by six β strands (A-E and K) surrounded by four α helices (I-III and X) for N-RSD, and a parallel β sheet composed of four β strands (G-I), an antiparallel β sheet with two β strands (J and L) with four α helices (IV-VII) and two 3^{10} helices (VIII and IX) for C-RSD.

7. Geometry of the Cra inducer-binding pocket

The F1P molecule could be coherently fitted in the electronic density maps obtained after refinement of the structures determined for the crystal soaked in F1P (Fig. 27). Yet, an attempt was made to generate an additional complex between FBP (instead of F1P) and Cra by soaking effector-less protein crystals in a 1 mM solution of this metabolite as above. The structures obtained from crystals exposed to F1P and FBP were virtually identical, with a rmsd for their superposition in the range of 0.45 Å. But once the structure of the putative FBP-Cra complex was inspected, it was found that the molecule occupying the effector site was no other than F1P. These results suggested that it was the residual F1P present in the nominally 98% pure FBP preparation (see Materials and Methods) what the protein recognized as sole interaction partner. That such selective binding to F1P happens even in the presence of large excess of FBP confirms the very high affinity for the first, consistently detected with the other procedures described above.

The cavity where F1P molecules bind Cra is formed by portions of the N-RSD and C-RSD subdomains (Fig. 26a), at the inter-module cleft. Incubation of Cra native crystals with 1 mM F1P for one hour was enough to obtain an equimolecular 1:1 association of the ligand to each domain present in the asymmetric unit of the crystals. The F1P molecule fitted to perfection the electron density map of the cognate protein cavity determined in the absence of the effector (Fig. 27b). The F1P molecule has a solvent accessible area of 372 $Å^2$, which is completely buried by contacts with the interacting protein residues and solvent molecules.

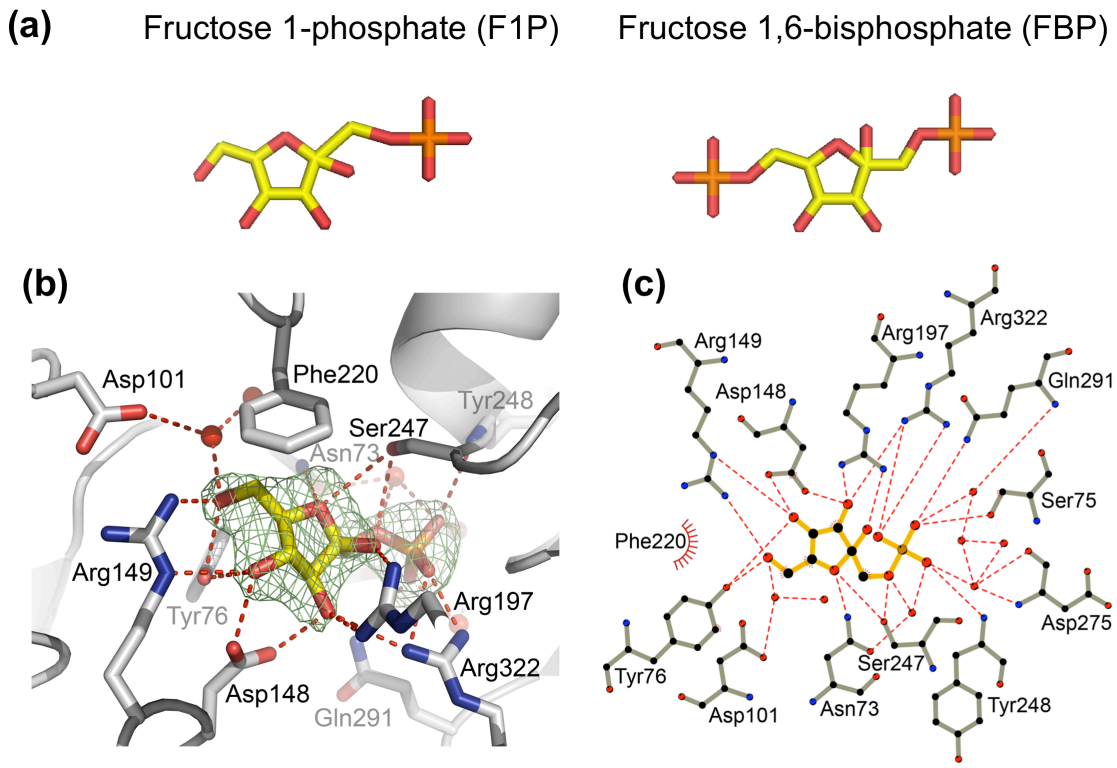

Fig. 27. Detail of the interaction between Cra and F1P. **(a)** Stick representation of F1P and FBP with the same code color as in Fig. 26a. **(b)** Drawing of the Cra effector binding with a bound F1P molecule coordinated to residues of the binding pocket. The electron density map (Fo-Fc) determined in the absence of the F1P molecule is represented as a green mesh at a 3.5 σ contour level. Protein residues are shown with carbons in grey, oxygens in red and nitrogens in blue. Hydrogen bonds are represented as dashed red lines and water molecules are shown as red spheres. **(c)** Ligplot scheme of the F1P interaction with Cra (Wallace *et al*, 1995). The color code is as in panel b. Carbon atoms are colored in black and atoms involved in hydrophobic interactions are represented by red arcs with spokes radiating towards the interacting atom.

Interactions occur with polar and aromatic residues in that cavity through direct hydrogen bonds with residues Tyr76, Ser75, Asn73 and Asp148 of the N-terminal regulatory subdomain (N-RSD), as well as Arg149, Arg197, Ser247 and Tyr248 of the C-terminal regulatory subdomain (C-RSD; Figs. 27b and 27c). Moreover, two residues (Gln291 and Gln322) of the hinge regions connecting both domains contribute with two extra direct hydrogen bonds to the interactions. In addition, water-mediated hydrogen bonds connect F1P with Asn73 and Asp101 of N-RSD and Asp275 and Gln291 of C-RSD. Hydrophobic interactions also play a role in the strong affinity and specificity of Cra for F1P. These involve the furanose ring of the effector, which sits between the side chains of Tyr76 (part of Ser75 and Asp148) and Phe220. These amino acids provide not

less than 5 interactions that trap the sugar ring between two hydrophobic surfaces. The dense constellation of interactions between F1P and Cra shown in Fig. 27 creates a degree of specificity that is unlikely to be matched with any other known metabolite of either *E. coli* or *P. putida*. Moreover, modeling of the FBP molecule (Fig. 28) based on the bound F1P ligand showed that the addition of one phosphate at the Fru C6 would locate this chemical group at ~3.5 and 2.0 Å of Asp70 and Asp101 respectively, and quite close (< 3 Å) to Pro69, *i.e* a non-favorable environment for the second phosphate group. This features may explain the lack of FBP binding. The Asp and Pro residues are conserved in *E. coli* Cra protein suggesting the same architecture for the inducer-binding pocket. The lack of diffraction observed with crystal soaked with other ligands may indicate extensive unspecific interactions with the protein, which can alter the molecule packing in the crystals, thereby impeding crystal diffraction.

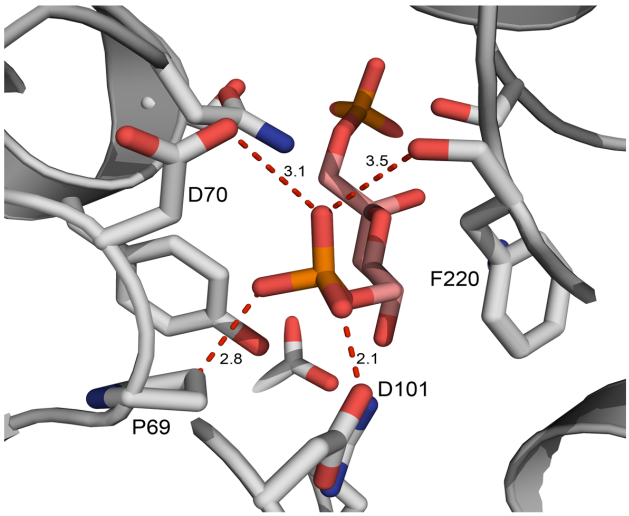

Fig. 28. Modeling of binding of FBP to Cra inducer-binding pocket. The model based on F1P binding showed that residues near to the binding pocket would produce a non-favorable environment for the second phosphate Group at the Fru C6.

In conclusion, we showed that Cra binds to the regulatory region of the fructose operon in *P. putida*. Moreover, we have also extensively characterized the regulator and its effector. In the next Chapter we will show the regulation exerted by Cra on PTS^{Fru} by means of *in vivo* experiments and we examine whether the regulatory effects can be extended to the PTS^{Ntr} through the cross talk between both systems.

CHAPTER 3

Regulation of the catabolite repressor activator (Cra) protein on PTS systems of *Pseudomonas putida*: *in vivo* studies*

***Manuscript in preparation**

Max Chavarría, Tobias Fuhrer, Uwe Sauer, Katharina Pfluger-Grau and Víctor de Lorenzo. (2011). Regulation of Cra on the PTS systems and the central carbon metabolism from *Pseudomonas putida*.

---

1. Cra expression in *P. putida*

In order to examine whether the carbon source affects the expression of the regulator, we started by measuring the activity of the Cra promoter. In first instance, expression of *cra* promoter was evaluated using the classical β-galactosidase protocol (Miller, 1972), however, values less than 50 U Miller were obtained (not shown). This result is coherent since it is known that the expression of many transcriptional factors is generally very low. Therefore, to properly measure the activity of Cra promoter, we resorted to the highly sensitive β-Galacto-Light Plus™ system (Applied Biosystems). Analysis of Cra promoter activity in mid-exponential phase revealed that the regulator is expressed in all the tested conditions (fructose, glucose and succinate), expression on fructose being slightly lower (Fig. 29). That less Cra protein is produced on fructose it is coherent, since the effector of the regulator (F1P) is produced *via* PTS^{Fru} system in this condition, so in the presence of this metabolite most of Cra molecules are unattached to the DNA (catabolic derepression). Therefore, regulatory functions of the protein are deactivated in this condition and additional synthesis of the regulator is not required.

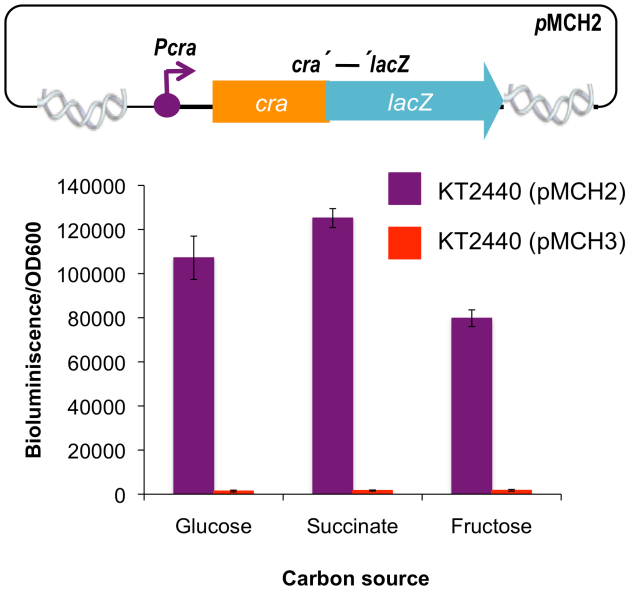

Figure 29. Activity of *cra* promoter in *P. putida* KT2440 as measured by translational fusions to *lacZ* gene in plasmid pMCH2. Cra promoter activity measurements in wild type strain (purple) revealed that the regulator is expressed similarly at low levels in glycolitic and gluconeogenic conditions. The regulador seems to be produced in lower amounts on fructose than glucose and succinate. A schematic diagram is shown of the *cra´-´lacZ* gene fusion fragment in plasmid pMCH2. The negative control corresponds to *P. putida* KT2440 electroporated with pMCH3 (empty vector, red).

2. Expression and activity of the fructose operon in *P. putida*

2.1. Expression levels of fructose operon in different conditions

Expression of the fructose operon in *P. putida* KT2440 was measured with a *fruB´-´lacZ* translational fusion in plasmid pMCH1 using the classical β-galactosidase protocol in different conditions (fructose, glucose and succinate, Fig. 30). As expected the highest levels of expression were obtained on fructose as carbon source. Surprisingly, on glucose the activity level albert low was 10 times higher than on succinate (23 ± 8 vs 2 ± 1 U Miller). This interesting observation will be studied in depth in the next section. It should be noted that *in vivo* metabolic measurements of FBP and F1P (Fig. 31) were consistent with our gene expression data since the highest levels of both metabolites were obtained on fructose as carbon source (Fructose→F1P→FBP *via fruBKA*). As was mentioned in Chapter 1 the presence of significant FBP levels on glucose and succinate can be explained by the presence of the discussed cyclic ED pathway. On the other hand, presence of low amounts of F1P on glucose and succinate (see Fig. 31) is intriguing since to the best of our knowledge, there are not known enzymes for producing F1P during growth on other carbon source than fructose.

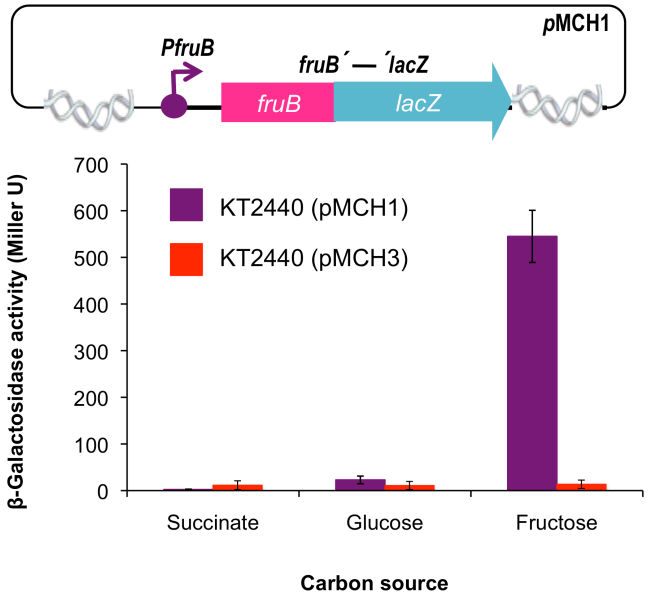

Figure 30. *fruBKA* promoter activity in *P. putida* as measured by translational fusions to *lacZ* gene in plasmid pMCH1. As expected the highest PTS^{Fru} activity levels were measured on fructose as carbon source (545 ± 56 U Miller). On the other hand, PTS^{Fru} system expression was very low on glucose (23 ± 8 U Miller) and succinate (2 ± 1 U Miller). A schematic diagram is shown of the *fruB´-´lacZ* gene fusion fragment in plasmid pMCH1. The negative control corresponds to *P. putida* KT2440 electroporated with pMCH3 (empty vector, red).

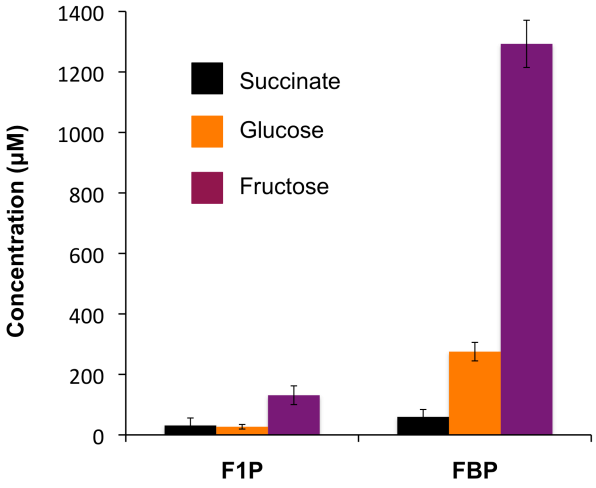

Figure 31. *In vivo* concentrations of F1P and FBP in *P. putida*. F1P and FBP were measured in *P. putida* by HPLC-MS on succinate (black), glucose (orange) and fructose (purple). Highest levels of F1P and FBP were detected on fructose where PTS^{Fru} is active. Fructose intake is performed by FruAB to produce F1P and then this compound is transformed to FBP by FruK.

But, for the most part, the results of gene expression and metabolic data allow us to conclude that the PTS^{Fru} system is expressed only on fructose where the extracellular sugar is phosphorylated to F1P and subsequently phosphorylated again to generate FBP.

2.2. Activity of PTS^{Fru} system on glucose as carbon source is due to inherent fructose contamination on glucose preparations

From β-galactosidase activity measurements a higher activity of the fructose operon promoter on glucose (23 ± 8 U Miller) was noticeable with respect to succinate (2 ± 1 U miller). This observation was reproducible not only with the Miller protocol (Fig. 30) but also with the protocol based on chemiobioluminescence (Fig. 32b). This higher activity of fructose operon could explain previous observations made in our laboratory suggesting that FruB is active during growth on glucose and is able to phosphorylate PtsN in this condition (for details see section 4 in this Chapter). The notion that FruB can phosphorylate to PtsN on glucose is quite surprising and not trivial. We hypothesize two possible explanations for this phenomenon: [i] that glucose preparations could be contaminated with small amounts of fructose that can activate the system or [ii] that that the glycolitic activity in *P. putida* may be enough to derepress *fruB* expression, *i.e.*, that FBP or other glycolytic metabolite could be transformed to F1P by an unknown enzyme. To adress these possibilities, first we constructed a *fruB* mutant, which is unable to transport fructose as carbon source (Fig. 32a). If fructose is present in the medium as a contaminant the sugar is unable to enter the cell in this mutant. We measured the expression of the operon in *fruB* strain as well in wild type strain with the β-Galacto-Light Plus™ system (Fig. 32b) which is more reliable for measuring low amounts of β-galactosidase.

As can be observed in Figure 32b, promoter activity decreased in the Δ*fruB* strain to same levels on glucose as the wild strain on succinate, suggesting that the higher activity of the *fruBKA* operon on glucose with respect to succinate is due to the contamination of this sugar with fructose. However, it is still surprising that small amounts of fructose in presence of a preferential carbon source such as glucose may increase ten times the promoter activity in respect to the baseline. To clarify this observation we measured the promoter activity on glucose (10 mM, 99.5% purity, SIGMA) with increasing concentrations of fructose in the culture medium (0, 10 μM and 100 μM). These very low concentrations of fructose are equivalent to mixtures of glucose:fructose of 99.9:0.1 and 99:1 respectively.

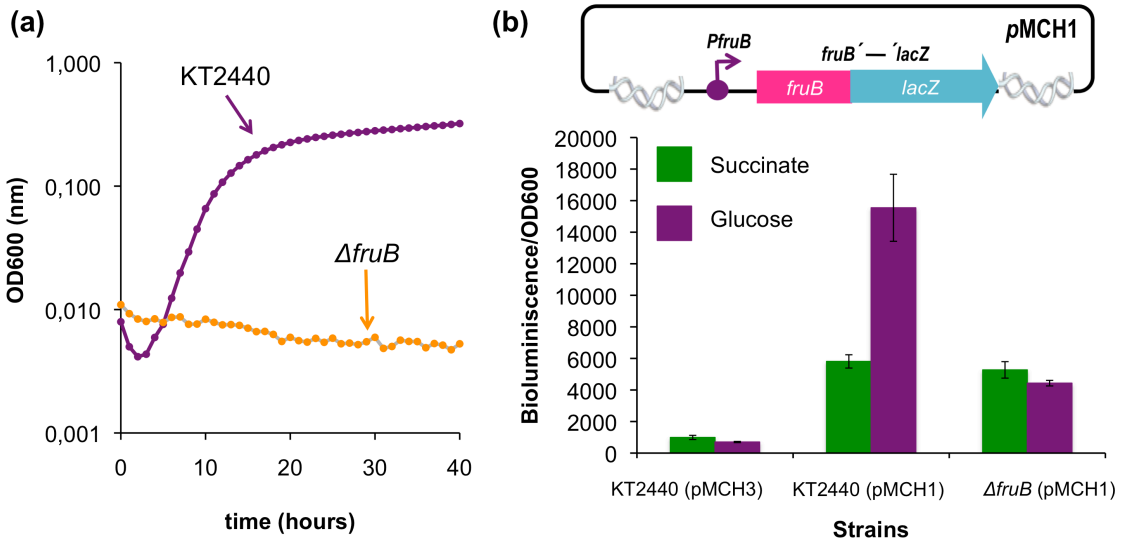

Figure 32. Growth and fructose operon promoter activity of *P. putida fruB* mutant. **(a)** Growth of *P. putida* KT2440 (purple) and *ΔfruB* mutante (orange) in minimum medium with fructose as the only carbon source. **(b)** Expression of fructose operon in wild type strain and *ΔfruB* mutant on succinate (green) and glucose (purple) as carbon sources. Experiments were performed with β-Galacto-Light Plus™ system. A schematic diagram is shown of the *fruB´-´lacZ* gene fusion fragment in plasmid pMCH1. The negative control corresponds to *P. putida* KT2440 electroporated with pMCH3 plasmid (empty vector).

Results (Fig. 33) showed clearly that very low concentrations of fructose in the medium are enough to activate the expression of the fructose operon. Therefore, the small quantities of F1P that are produced due to fructose contamination are recognized by Cra, leading to slight derepression of the system. This observation is consistent with our *in vitro* studies of Chapter 2 in which we demonstrated the high affinity of the regulator by F1P. In contrast, the activity of the fructose operon promoter in *fruB* strain remains unchanged, due to the inability of the strain to internalize fructose and increase the intracellular concentrations of F1P.

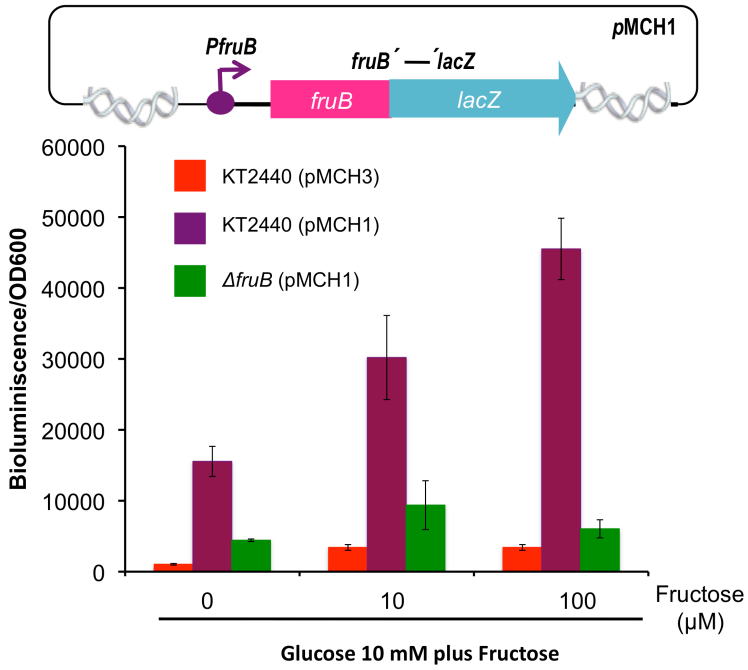

Figure 33. Activity of fructose operon promoter in *P. putida* KT2440 (purple) and *fruB* mutant (green) on glucose 10 mM (0.2%) with increasing concentrations of fructose. Experiments were performed with the β-Galacto-Light Plus™ system. Note that the activity of the fructose operon in Δ*fruB* strain is not significantly altered by the addition of fructose in the medium. A schematic diagram is shown of the *fruB´-´lacZ* gene fusion fragment in plasmid pMCH1. The negative control corresponds to *P. putida* KT2440 electroporated with pMCH3 plasmid (empty vector, red).

3. *In vivo* regulation of fructose operon by Cra protein

In a next step for understanding in depth the regulation of the PTS^{Fru} system in *P. putida* we monitored the *fruBKA* promoter activity in several conditions in a strain in which the regulator Cra has been deleted (Δ*cra*). The results are shown in the Figure 34, where it can be observed that in all the carbon sources the activity of the fructose operon in the mutant was higher that in the wild type strain. It is even possible to observe these differences in solid medium (Fig. 34b). These observations verified that Cra is a repressor of the fructose operon in *P. putida*. The promoter activity data revealed that the derepression on succinate is very strong: *lacZ* activity increased two hundred times in the *cra* mutant with respect to wild type strain, while on glucose the promoter activity in the *cra* mutant was increased only 6 times. It is plausible that when *P. putida* grows on glucose as the sole carbon source the PTS^{Fru} system is repressed by another thus far unknown factor that is expressed mainly in glycolytic conditions. On the other hand, on

fructose, the activity of the promoter in the mutant was only 1.4 times higher with respect to the wild type strain. This is an expected result since F1P is generated in this carbon source (see Figure 31). Therefore, in this conditions most (but not all) molecules of Cra are linked to the effector thereby making the PTS^{Fru} system to be derepressed in the wild type strain since the regulator is unable to bind to the operator.

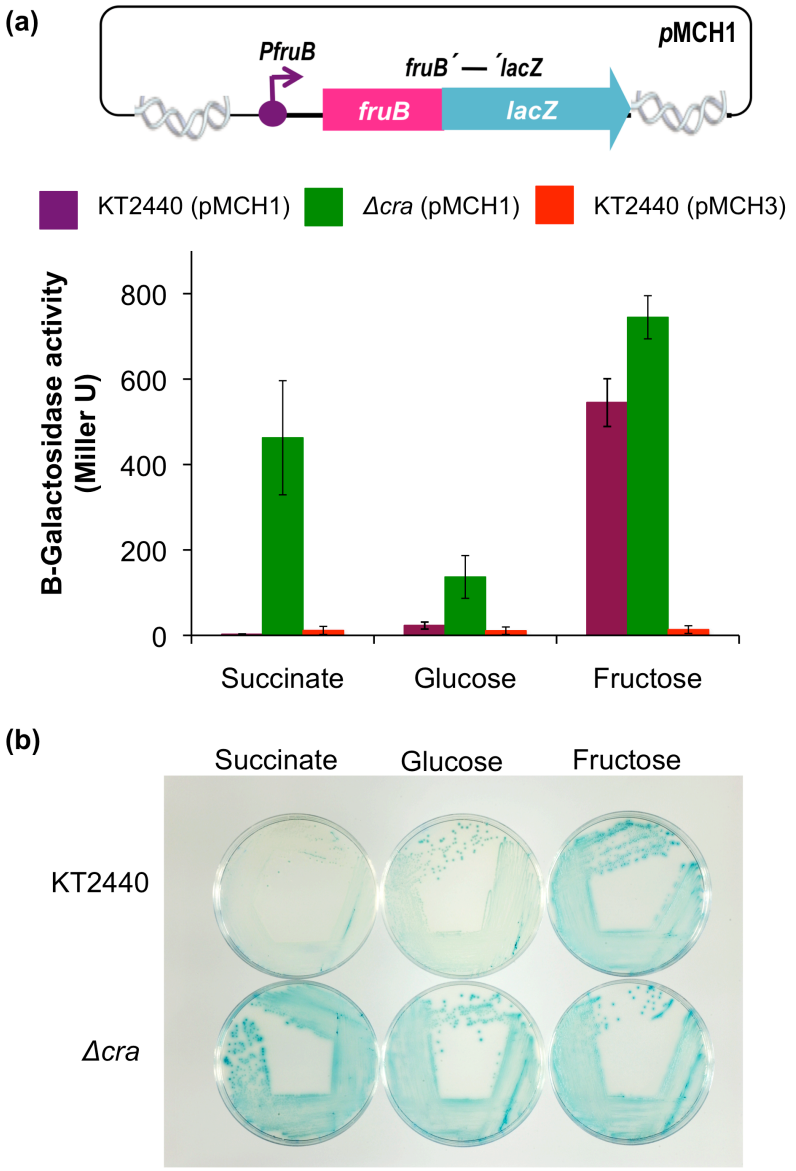

Figure 34. Activity of fructose operon promoter in *P. putida* KT2440 (purple) and *cra* mutant (green). (**a**) Experiments in liquid medium showed that deletion of the transcriptional regulator Cra derepress the activity of fructose operon in all the tested conditions. A schematic diagram is shown of the *fruB´-´lacZ* gene fusion fragment in plasmid pMCH1. The negative control corresponds to *P. putida* KT2440 electroporated with pMCH3 plasmid (empty vector, red). **(b)** Experiments in solid medium with the carbon sources indicated and Xgal displayed the same behavior that liquid experiments.

4. Cra regulates indirectly the phosphorylation state of PtsN

Under certain metabolic conditions an *in vivo* cross talk between the two PTS systems found in *P. putida* can be observed (Pfluger and de Lorenzo, 2008), so that the FruB protein can transfer the phosphoryl group to proteins PtsO or PtsN. With these previous observations, we wondered whether the nitrogen PTS system can be regulated indirectly *via* the PTS^{Fru} system by Cra. To address this question we monitored the phosphorylation state of the protein PtsN in the wild type strain, and the mutants *Δcra*, *ΔptsP* and *ΔcraΔptsP* using the protocol developed in our laboratory previously (Pfluger and de Lorenzo, 2007) and described in Materials and Methods. *ΔptsP* and *ΔcraΔptsP* strains were used since the phosphorylation cascade of the nitrogen PTS system is interrupted in these mutants, this allows us to monitor the ratio PtsN/PtsN~P under conditions where the phosphate would be transferred to the PtsN protein only by FruB (see Figure 35).

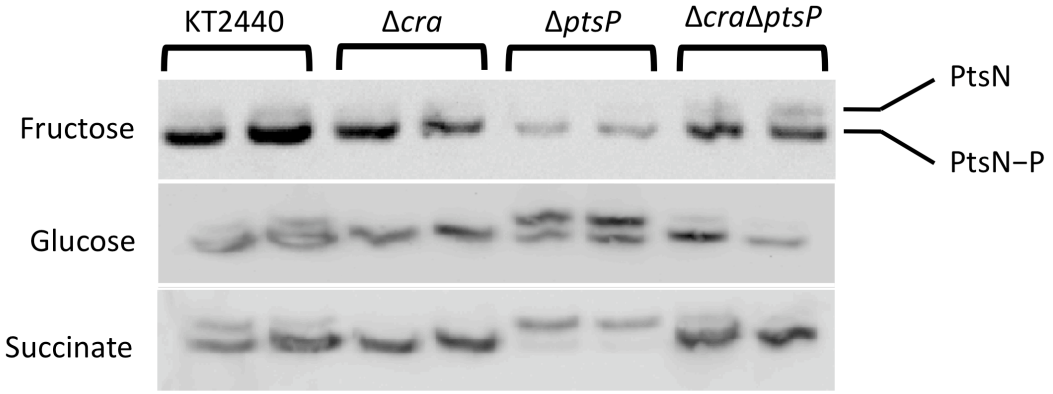

Figure. 35. Monitoring non-phosphorylated *vs*. phosphorylated PtsN share in *P. putida* cells grown in different carbon sources. Cells were grown at 30 ºC in mineral M9 medium amended with 0.2% (w/v) of fructose, glucose or succinate and analyzed in a native PAGE system. Results from duplicate experiments are shown for each of the mutants indicated transformed with pVLT*ptsN*_Etag. The position of each of the PtsN protein species is marked to the right side.

Our results (Fig. 35) showed that the PtsN/PtsN~P ratio in wild type strain and *Δcra* mutant was identical in all the tested conditions. We concluded, that the regulatory effect of Cra on PtsN *via* FruB can not be determined properly (at least with this method) in these strains because most of the phosphate of PtsN comes from PtsP/PtsO. In contrast, the phosphorylation state of PtsN in strains which have blocked the

phosphorylation cascade in PTS^{Ntr} system (*ΔptsP* and *ΔcraΔptsP)* accredit the regulation of Cra on the *fruB* expression, whose encoged products transfer phosphate to PtsN. As can be seen in the Figure 35, differences in the phosphorylation of PtsN on fructose were not observed between the single and double mutants (lines 5, 6 vs 7, 8), since the amount of FruB is enough in both strains in this condition to phosphorylate PtsN. This observation is in agreement with our results of gene expression (Fig. 34). On the other hand, on glucose (Figure 35) was observed in the *ΔptsP* mutant (lines 5, 6) a distribution ~50:50 of phosphorylated/dephosphorylated protein, while in the *ΔcraΔptsP* mutant (lines 7, 8) was observed that virtually all protein is found in phosphorylated form. The 50% of PtsN~P in Δ*ptsP* is in agreement with the conclusions of the section 2.2 of this Chapter *re.*, *fruB* expression on glucose due to the contamination of the carbon source with fructose. Thus, the amount of FruB expressed on glucose was sufficient to phosphorylate partially to PtsN. As expected, when the PTS^{Fru} system was derepressed (*ΔcraΔptsP,* lines 7, 8) the amount of FruB increases and therefore PtsN appears only in phosphorylate form. Similar conclusions about the regulation of Cra and its effect on PtsN could be achieved on succinate. In this carbon source, changes in the phosphorylation state are more dramatic because, as shown in the Figure 35, the whole protein remains in the dephosphorylated form in the *ptsP* mutant (lines 5, 6) while deletion of the regulator (*ΔcraΔptsP)* derepressed the system and the whole protein is found in the phosphorylated form. According to data on phosphorylation levels, we conclude that Cra modulates the phosphorylation state of PtsN and thus, Cra would be considered as a fine tuning regulator of PTS^{Ntr} system in *P. putida*.

V. DISCUSSION

1. Analysis of glucose and fructose catabolism in *P. putida*

The measured distribution of catabolic fluxes for glucose and fructose fits well with qualitative observations made in various Laboratories since the late 1970s, on glucose, fructose, and gluconate metabolism in *P. putida* (del Castillo *et al*, 2007; Lessie and Phibbs, 1984; Sawyer *et al*, 1977; Vicente and Canovas, 1973a, b). Glucose is almost exclusively metabolized through the ED pathway, and only a very small fraction of about 4% enters into the PP pathway. In the ED pathway, glucose gets phosphorylated to glucose-6-phosphate, which is then converted into 6-phosphogluconate and eventually into 2-dehydro-3-deoxygluconate phosphate. This intermediate is then split into pyruvate and glyceraldehyde-3-phosphate, which next is either transformed to other C_3 metabolites or feedbacks to C_6 compounds through the cyclic mode of ED pathway. Glucose can also join the ED route by its direct conversion into gluconate and subsequent phosphorylation to 6-phosphogluconate (del Castillo *et al*, 2007; Lessie *et al*, 1984). In *P. putida*, it has been reported that glucose is metabolized through three initial pathways that converge at the level of 6-phosphogluconate and that its simultaneous operation is necessary to achieve maximal growth rates (del Castillo *et al*, 2007). Using our fluxomic data no prediction can be made about the early steps of glucose metabolism, as in the metabolic model, which laid the basis for the whole analysis, does not differentiate between these initial steps of glucose consumption.

Our data on glucose showed that this substrate necessarily employed almost exclusively *via* the ED pathway because 6-phosphofructokinase is missing in this bacterium (Velazquez *et al*, 2004). Fructose, in contrast, is degraded to about ~34% *via* the EMP pathway and ~52% *via* the ED pathway (Fig. 6). These data correlate well with the prediction of radiolabelling experiments with [1-^{14}C]-fructose (Sawyer *et al*, 1977). Fructose is taken up and phosphorylated by the activity of the components of the PTS^{Fru} to fructose-1-phosphate with the concomitant conversion of PEP to pyruvate. F1P is eventually converted to fructose-1,6-bisphosphate, which now either enters the ED pathway through the activity of the Fbp or follows the thermodynamically more favourable EMP pathway. In the EMP pathway, FBP is cleaved to produce glyceraldehyde-3-phosphate and dihydroxyacetone phosphate, which are then channelled *via* PEP to produce pyruvate and acetyl-CoA, that end in the TCA cycle (Fig. 1). A small fraction of ~11% of the fructose initially taken up is metabolized through the PP pathway. Thermodynamically, the preference of *P. putida* by the ED

pathway over EMP pathway for degrading fructose is not obvious. We think, that utilization of the ED pathway could provide physiological advantages to *P. putida* to withstand oxidative stress, since more equivalents of NADPH per molecule of sugar degraded are produced through this step with respect to the classical EMP pathway. This idea is not without experimental evidence since in *E. coli*, the ED pathway has been related with other functions apart from sugar catabolism such as participation in SOS response and resistance to UV radiation (Peekhaus and Conway, 1998).

From an evolutionary standpoint, the ED pathway is the oldest (Conway, 1992; Peekhaus *et al*, 1998) and most conserved metabolic route. Based on the usual niche of *P. putida*, it would be reasonable to consider that this bacterium has kept the ED pathway as its main device for carbohydrate degradation because [i] it provides additional resistance to environmental stress and [ii] in aerobic conditions (the usual *P. putida* niche), the utilization of EMP pathway does not endow any advantage, since the necessary ATP for carrying out the biological functions can be produced abundantly through oxidative phosphorylation in the TCA cycle.

Apart from differences in the fluxes of the upper pathway between glucose and fructose consumption, changes in the fluxes around the PEP-Pyr-OAA node could also be observed. On fructose, fluxes from PEP to pyruvate, fluxes of the pyruvate shunt formed by malic enzyme and pyruvate carboxylase (pyruvate from malate and oxaloacetate from pyruvate), and gluconeogenesis (PEP from OAA) were higher than in glucose. On glucose, ~83% of the carbon flux from the TCA cycle proceeds *via* the malate dehydrogenase, and only ~17% is channelled through the malic enzyme. On fructose, ~42% of the carbon flux is directed *via* the malic enzyme, bypassing the malate dehydrogenase (see Fig. 13, 14). Thus, our data suggest that the activity of the pyruvate shunt is higher in cells grown on fructose than on glucose. In bacteria, this shunt has to be seen in the overall context of the PEP-Pyr-OAA node as a switch point for carbon flux distribution of the central metabolism. The node is essential but flexible, in order to adjust the carbon flow to the energetic and anabolic demands in given conditions. Its enzymes are allosterically controlled, *i.e.* positively and/or negatively regulated by a variety of metabolites of the central metabolism and may be subjected to substrate inhibition (Sauer and Eikmanns, 2005). It has been proposed that the pyruvate shunt (see Fig. 1 malate→pyruvate→OAA) can be used to supply oxaloacetate for gluconeogenesis and production of amino acids (Diesterhaft and Freese, 1973). In this

shunt, one ATP is used and thus more energy is required than in the direct conversion of malate to oxalacetate *via* malate dehydrogenase. For this reason, it is believed that the pyruvate shunt is used mainly for the production of oxaloacetate, while malate dehydrogenase functions primarily to provide energy *via* the citric acid cycle (Diesterhaft *et al*, 1973). Moreover, the pyruvate shunt may be a mechanism to remove excess carbon in *P. putida* (del Castillo *et al*, 2007). Taking together this information and our data, we entertain that the cell adjusts the extension of the pyruvate shunt depending of the carbon source (glucose *vs* fructose) so it can meet the energetic and anabolic demands in each growth condition.

Other differences in the metabolic fluxes of *P. putida* observed with glucose *vs*. fructose as a sole carbon source can be explained by the activity of the PTS^{Fru} system, which is responsible for additional conversion of PEP to pyruvate in the process of fructose uptake, increasing this flux, and for fructose degradation *via* the EMP pathway. As was mentioned, degradation of fructose *via* the EMP pathway is thermodynamically more favourable than degradation *via* the ED pathway. It is estimated that one molecule ATP is gained per molecule fructose degraded through the EMP pathway compared to degradation following the ED pathway (Van Dijken and Quayle, 1977). This might contribute to the higher biomass yield per molecule of fructose observed in *P. putida* (see Tables 4 and 5). Furthermore, as only one molecule of PEP is produced per molecule of hexose *via* the ED pathway, the PEP supply is emptied during catabolism of hexoses to pyruvate in the presence of a functional PTS for sugar uptake (Van Dijken *et al*, 1977). Therefore, degradation of fructose through the EMP pathway is not only energetically more favourable in terms of ATP yield, but also leads to the generation of two molecules of PEP per molecule of fructose, refilling the PEP pool. The approximately two-fold higher flux from OAA to PEP on fructose might also be a consequence of the need to refill the PEP pool for the biosynthetic purposes such as synthesis of aromatic amino acids, or cell wall polymers. In conclusion, the metabolic flux analysis demonstrates that differences in the catabolism of glucose and fructose in *P. putida* are not just limited to the upper metabolism (ED vs EMP pathways), but also to the lower metabolism (pyruvate shunt, TCA cycle). On the other hand, our results clearly show that the PTS^{Ntr} proteins do not have any modulating effect on the three main degradation pathways for hexoses (ED, EMP, PP pathways).

2. Central metabolism in *P. putida* is run through an atypical version of the ED pathway

ED metabolism is far more widely distributed in Nature than has been recognized, and the enzymes of this pathway are highly conserved (Conway, 1992; Peekhaus *et al*, 1998). Previously, it has been accepted that the ED pathway operates in several different modes. However, for many organisms the operational mode is not known because there is insufficient biochemical and regulatory data available. Nevertheless, an examination of the literature reveals predictable patterns of association of certain microbial lifestyles with specific modes of ED metabolism (Conway, 1992). In several bacterial genera, (including enterobacteria) the ED pathway operates in a linear fashion (Conway, 1992). Microorganisms as *Rhodobacter capsulata* and *E. coli* are examples of species that work with a linear ED pathway, which, in some cases, is only induced for growing on particular carbon sources. On the other hand, the operation of a cyclic ED pathway has been previously suggested for several Pseudomonads species (Conway, 1992) although most of the studies (if not all) have been focused on *P. aeruginosa*. While some reviews (Conway, 1992; Portais and Delort, 2002) mentione *that there is substantial evidence* of the operation of a cyclic ED pathway, a closer examination of the literature reveals that the hypothesis of the existence of the cycle in *Pseudomonas* has been based only on growth experiments with mutants deficient in enzymes of the upper central metabolism.

Our results shown in Chapter 1 demonstrate that the ED pathway operates in a cyclic mode in *P. putida* (see Fig. 36), which provides a new vision of the central metabolism of this bacterium. Given the limited number of articles that have been published about it, the occurrence of the cyclic ED pathway has not been taken into consideration in most studies of central metabolism in *P. putida,* including the two existing metabolic models that were developed recently (Nogales *et al*, 2008; Puchalka *et al*, 2008). Thus, our work clarifies the flow of carbon into the central metabolism of this bacterium and we advocate to consider these new features in future *P. putida* models/studies. In this cyclic version of the ED pathway, the triose phosphates are recycled to DHAP/FBP/F6P/G6P *via* the gluconeogenic enzymes TpiA, Fda, Fbp and Pgi. Moreover, our data indicate that the cyclic ED is carried out in both glycolytic and gluconeogenic conditions, suggesting that this cycle is constitutive in this bacterium and not only inducible by certain carbon sources. The ocurrence of a cyclic version of the ED pathway is compatible with the results obtained by flux analysis and discussed

above, as the biochemical network used is only able to differentiate between the degradation routes (ED, EMP or PP pathways) but can not distinguish the mode in which each works (cyclic, linear, etc).

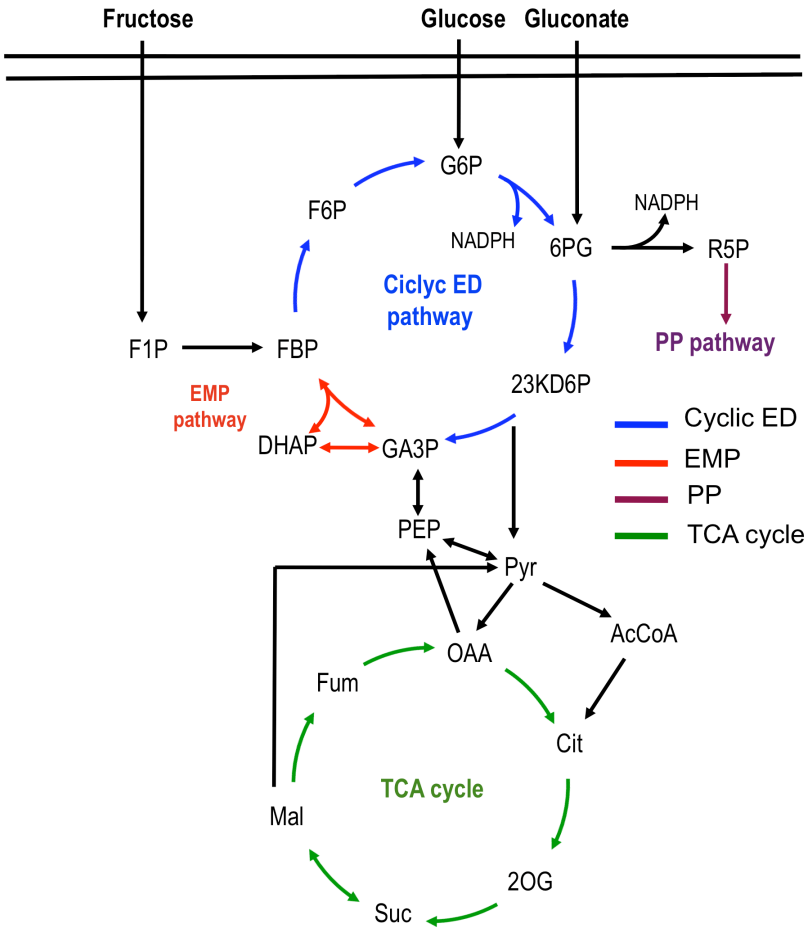

Figure 36. Proposed layout of central carbon metabolism in *P. putida*. In this picture we indicate the occurrence of a cyclic version of the ED pathway, where GA3P can be recycled to FBP or degraded for energy production to the TCA cycle. Color codes: cyclic ED pathway in blue, EMP pathway in red, PP pathway in purple, TCA cycle in green.

The occurrence of the cyclic ED pathway in fructose is difficult to explain because according to the flux analysis, 34% of this substrate is degraded through EMP pathway. We have two possible hypotheses about it:

[i] The Fda enzyme could operate in both directions simultaneously, contributing partially to the cyclic ED (DHAP + GA3P → FBP) and the degradation of the substrate through glycolysis (FBP → DHAP + GA3P). A simultaneous double functionality for Fda has been reported *in vivo* for *S. cerevisiae* (Navas *et al*, 1993), *E. coli* (Shulman *et al*, 1979), *Corynebacterium melasssecola* (Rollin *et al*, 1995) and *Lactococcus lactis* (Neves *et al*,

1999). The occurrence of *metabolite cycling*, where opposite processes operate simultaneously, may seem disconcerting, mainly given the tight regulation of metabolism usually assumed to provide coherent partitioning of resources over the various energetic and biosynthetic requirements. However, there are evidences that these phenomena could take place in the cell (Portais *et al*, 2002). Evidently, its presence may significantly affect the carbon, energetic and redox status of the cell, therefore, the double direction in the performance of an enzyme may itself play regulatory funtions (Portais *et al*, 2002).

[ii] The Fda enzyme may operate in a stochastic regime. It might be reasonable to think that at any given time, some cells can grown under a mode (cyclic ED) and others at a different regimen (EMP pathway).

Our data cannot discern whether this is a stochastic phenomenon or reflects double functionality of the Fda enzyme.

The existence of the cyclic ED pathway explains also the poor growth in glycolytic and gluconeogenic carbon sources when the PfkA was expressed in a wild type strain. This is because the enzyme catalyzes a reaction that opposes the innate carbon flux in this bacterium. Thus, expression of PfkA in this species produces a futile cycle in the central metabolism that wastes the ATP needed for other biological functions such as biomass formation. In past years, Steinbuchel *et al.* (1986) demonstrated that it is possible to convert *Alcaligenes eutrophus* (a naturally 6-phosphofructokinase deficient organism with ED pathway in cyclic mode) to EMP metabolism by expression of PfkA. We do not have an easy explanation for their results. Perhaps expression and regulation of Fbp/Fda is different between organisms, and maybe in the case of *A. eutrophus* the futile cycle is not established. Therefore, it seems that the central metabolism in *P. putida* cannot redirected entirely to EMP pathway by PfkA knock-in such as in the case of A. *eutrophus* even in the case where the cyclic ED pathway is inactivated. New strategies are currently being developed in our laboratory to engineer *P. putida* into a bacterium that uses only the EMP pathway to break down sugars. This will allow us to better understand the importance of the ED pathway in *P. putida*.

Growth experiments with mutants of different enzymes of the cyclic ED pathway indicate that the recycling of triose phosphates to hexoses on glucose and succinate is

essential for the cell. These results indicate that the importance of the *upper* metabolism lies in the ability to generate certain metabolites that form the cycle, specifically DHAP, FBP, F6P and G6P. On the other hand, the production of some of these metabolites on fructose is partially supplied by EMP pathway and sufficient for bacterial growth, as can be deduced from the behavior of the *edd* strain. Taken together all the experiments on fructose (growth, PfkA expression, metabolome) suggest that the cyclic ED pathway really occurs in cells growing in this sugar, but seems not to be essential.

Why the ED pathway works in *P. putida* in a cyclical fashion? In *P. aeruginosa* the cyclic ED pathway seems to support the formation of the polysaccharide precursor F6P in several metabolic conditions (Conway, 1992). However, we think that the function of the cycle is not only to supply DHAP, FBP, F6P and G6P for macromolecular biosynthesis, but also to play a role in the optimization of NADPH synthesis for sustaining anabolic demands and resistance to oxidative stress. As was mentioned above, in the linear ED pathway, one NADPH molecule is generated per molecule of glucose-6-phosphate entering the process. In the cyclic version, the yield of NADPH can increase up to 2-fold depending on the extent of recycling (Portais *et al*, 2002). Therefore, its presence could be particularly relevant in organisms where PP pathway activity is low as is the case of *P. putida* (see Figs. 6 and 9). A high number of antioxidant enzymes are coupled to NADPH as a redox cofactor. Therefore functional defense mechanisms against oxidative stress depends upon the availability of NADPH. We hypothesized that the cyclic ED pathway might protect against oxidative stress to *P. putida* due to the enhanced cellular production of this molecule. As a sidelight, our results show how different the central metabolism between bacterial species can be. Model species such as *E. coli* or *B. subtilis* are not entirely representative of global microbial metabolism and their generalization can lead to significant errors.

3. PtsN is a fine tuning regulator of carbon central metabolism

In this Thesis, we analyzed the metabolic fluxes in the central carbon metabolism of isogenic PTS mutant strains of *P. putida* (Chapter 1) growing on a PTS sugar (fructose) or on a non-PTS sugar (glucose). Two main conclusions regarding the influence of PTS proteins could be drawn from those data: [i] that the PTS mutants did not affect the carbon flux distribution of the pathways implicated in the upper metabolism (EDP, EMP and PPP) with the exception of *fruB* mutants which are unable to transport

fructose in the cell, and [ii] that PtsN is involved in the regulation of the pyruvate shunt in the central metabolism, irrespective of the carbon source used and of its phosphorylation state.

The regulation of PtsN on pyruvate shunt was observed on first instance through flux analysis (see Figs. 13 and 14), and then confirmed with enzymatic assays (Fig. 16). In both approaches, a higher activity of the malic enzyme and pyruvate carboxylase were observed in the *ptsN* mutant, as well as in the *ptsN/ptsO* mutant with respect to the wild type strain suggesting a repressor role of PtsN on the pyruvate shunt. Moreover, our results suggest that the regulatory influence is not dependent of the phosphorylation status of the protein, as:

[i] No effects on the metabolic fluxes were observed in a *ptsP/fruB* mutant (see Fig. 12). This strain lacks both EI components of the PTS and therefore does not support phosphorylation of PtsN, thus $EIIA^{Ntr}$ would not be phosphorylated under any condition (Pfluger and de Lorenzo, 2008), and

[ii] No changes in malic enzyme activity were observed in *ptsNHA* and *ptsNHE* mutants (see Fig. 17). These strains contain a *ptsN* allele with changes in the triplet corresponding to the phosphorylable position H68 of PtsN (*ptsNHA* HisxAla and *ptsNHE* HisxGlu). These genetic modifications generate that *ptsNHA* strain has in any time the PtsN protein in dephosphorylated form whereas *ptsNHE* strain has this protein in a state that resembles to the phosphorylated species. The fact that no changes were observed in malic enzyme activity in a scenario where the PtsN is fully phosphorylated or dephosphorylated suggest that the observed effect of PtsN can be traced down to the sole presence/absence of the protein irrespective of its phosphorylation state.

While most studies suggest that the dephosphorylated form of PtsN is responsible for its regulatory functions (Begley and Jacobson, 1994; Lee *et al*, 2005; Luttmann *et al*, 2009; Pfluger-Grau *et al*, 2011; Segura and Espin, 1998), the fact that the PtsN protein regulates the activity of an enzyme independently of their state of phosphorylation is not new. Recently Choi *et al.* (2010) reported in *Salmonella* a direct protein-protein interaction between $EIIA^{Ntr}$ and the response regulator SsrB, a component required for *Salmonella* virulence. This work showed with *in vivo* and *in vitro* experiments that $EIIA^{Ntr}$ interact with SsrB and it performs its regulatory function in a fashion entirely

independent of the phosphorylation state. On the other hand, other studies have reported regulatory functions of PtsN that depends on the phosphorylated form (Cases *et al*, 1999; Hayden and Ades, 2008). With these premises, the simplest interpretation is that the state of phosphorylation is one of the features that PtsN uses to carry out its multiple regulatory functions. Therefore, we believe that the various phenotypes observed in PtsN mutants may be due to any of the following: [i] the phosphorylation state, [ii] the amount of protein expressed and, [iii] the ability of PtsN to interact with other macromolecules to form protein complexes.

Perhaps, the two forms of $EIIA^{Ntr}$ (phosphorylated and nonphosphorylated) have specialized in controling different sets of proteins, so the regulatory functions are carried out through several/different mechanisms. According to the literature (Lee *et al*, 2007; Choi *et al*, 2010; Pfluger-Grau *et al*, 2011) it seems clear that one of these mechanisms is through direct protein-protein interaction suggesting that PtsN may have a role in scaffolding multiprotein complexes.

Our experiments do not allow to deduce whether this regulation is due to direct protein-protein interaction of PtsN with the pyruvate shunt enzymes or by a secondary effect due to altered intracellular metabolite composition. For instance, it is known that in *Bacillus subtilis* acetyl-CoA has an inducing effect on the activity of the pyruvate carboxylase (Diesterhaft *et al*, 1973). However, in other bacteria, as *e.g.* in *Pseudomonas citronellosis*, *Methanobacterium thermautotrophicum*, and *Clostridium glutamicum,* no dependence on the presence of acetyl-CoA has been observed on Pyruvate carboxylase (Attwood, 1995; Jitrapakdee and Wallace, 1999). Recently, it was shown that the non-phosphorylated form of PtsN binds to the AceE component of PDH *in vitro*, downregulating its activity (Pfluger-Grau *et al,* 2011). Therefore, a *ptsN* mutant should have higher fluxes towards acetyl-CoA, if not even higher amounts of this metabolite. Analyzing the metabolic net fluxes only a slight increase is predicted for the reaction catalyzed by the PDH complex in the *ptsN* mutants (see Figs. 13, 14). However, measurements of the PDH activity in cell free extracts of *P. putida* wild type and *ptsN* mutant showed ~2-fold higher activity of the enzyme complex in the absence of PtsN (Pfluger-Grau *et al,* 2011). Thus, we cannot exclude that the higher activity of the pyruvate carboxylase is at least to some extend an effect of its induction by acetyl-CoA.

Even when we cannot provide a detailed functional mechanism, we have evidence that

the pyruvate shunt is induced in the absence of PtsN. As mentioned above, the pyruvate shunt has been related with the production of additional amounts of OAA for gluconeogenesis, amino acids biosynthesis (aspartate, isoleucine, threonine), and energy production *via* the citric acid cycle (Diesterhaft *et al*, 1973). The fact that PtsN repress the pyruvate shunt (and therefore modulates the pool of oxaloaceate) indicates that PtsN would indirectly regulate the biosynthesis of amino acids.

Although the observed differences in *ptsN*$^{+}$/*ptsN*$^{-}$ strains in the fluxes and enzymatic assays are somewhat low, small changes in central metabolic reactions can lead to significant changes in other regulatory processes. Therefore, considering the robustness of the central metabolism it is very remarkable that PtsN can regulate its activity. We are just at the beginning of understanding some of the signals and regulatory devices orchestrating the metabolic flux distribution through the pyruvate shunt node and thereby guiding the carbon flow to the different metabolic modules.

In summary, we produced evidence that PtsN is one player in the complex machinery that is responsible for carbon flux distribution in the central metabolism of *P. putida*. Our data suggest a role of PtsN in the fine-tuning of the central carbon metabolism helping to adjust the metabolic fluxes to satisfy the anabolic and energetic demands of overall cell physiology.

4. F1P is the one and only effector of the transcriptional regulator Cra from bacteria

The catabolite repressor/activator (Cra) protein is a global sensor and regulator of carbon fluxes through the central metabolic pathways of Gram-negative bacteria, but the actual effector (or effectors) that signal such fluxes to the protein has never been unambiguously determined. This bit of information is decisive for setting reliable connections between the central fluxes for catabolism/anabolism of carbohydrates (which are reported by FBP levels; Ramseier *et al*, 1993), and the metabolic and non-metabolic transcriptome (Kotte *et al*, 2010). In this Thesis, the Cra protein of *P. putida* was purified and characterized, and its tridimensional structure determined.

Analytical ultracentrifugation, gel filtration and mobility shift assays showed that the effector-free Cra is a dimer which binds an operator DNA sequence in the promoter

region of the *fruBKA* cluster. The observation that Cra protein of *P. putida* occurs predominantly in a dimeric form is a feature that differs from the same regulator of *E. coli*, known to be a tetramer (Alberti *et al*, 1993; Chakerian *et al*, 1991; Chen and Matthews, 1992). However, this divergence is understandable, because the leucine mini-zipper that causes tetramerization of proteins of the LacI family through their the carboxyl-terminal regions is conserved in *E. coli* Cra (Cortay *et al*, 1994) but not in the *P. putida* counterpart (Fig. 37).

On the other hand, the Cra binding site in the *fruBKA* promoter region of *E. coli* contains two nearby operators O_1 (TGAAAC|GTTTCA) and O_2 (TGAATC|GTTTCA), which could accommodate the cognate repressor tetramer (Ramseier *et al*, 1993). In contrast, the same region of the *P. putida* genome has only one Cra site (Fig. 21b). A plausible consequence of this is that the affinity of the Cra dimer for the single site in the *fruBKA* promoter region of *P. putida* ought to be high to compensate the more extended range of interactions of the tetramer/two-operator scenario of the same regulatory device in *E. coli*.

Cra *E. coli (AA 305-334)*	ASLDEPRKPKPGLTRIKRNLYRRGVLSRS-**COOH**
LacI *E. coli (AA 331-360)*	PNTQTASPRALADSLMQLARQVSRLESGQ-**COOH**
Cra *P. putida (AA 302-331)*	LALAAIEEKRYEPGVHAVGRTFKQRISVA-**COOH**

Figure 37. Alignment of the C-terminal amino acid sequence of regulators Cra (*E. coli*), LacI (*E. coli*) and Cra (*P. putida*). Note that the *E. coli* tetrameric regulators Cra and LacI contain a leucine mini-zipper, which seems to be required to tetramerization. This mini-zipper is absent in the *P. putida* Cra protein.

One of our main results is that F1P (but not FBP) is the only metabolic effector of the bacterial regulator Cra. Thermodynamic parameters of the F1P-Cra-DNA interaction calculated by isothermal titration calorimetry revealed that the factor associates tightly to the DNA sequence 5'-TTAAACGTTTCA-3' (K_D = 26.3 ± 3.1 nM) and that F1P binds the protein with an apparent stoichiometry of 1.06 ± 0.06 molecules per Cra monomer and a K_D of 209 ± 20 nM. Other effectors like FBP, believed so far to be one metabolic partner of Cra, did not display any affinity for the regulator. Moreover, the structure of Cra and its co-crystal with F1P at 2Å resolution implies that any small molecule other than F1P can hardly match the geometry of the effector pocket. The extensive contacts of F1P with Cra lead to a high affinity binding interaction (K_D ~ 200

nM). Since the residues that hold the 13 molecular interactions shaping the pocket for F1P binding are faithfully preserved in the same protein of *E. coli* and *S. typhimurium* (Figs. 18, and 27), we can assume that the same conclusion holds true for the enterobacterial Cra protein as well. Superimposition of protein structures reveal the tightening of the effector binding site of Cra from *P. putida* in respect to the *E. coli* counterpart due to the presence of glycerol (introduced in the crystallization process) in the corresponding pocket. But otherwise the architecture of the sites is identical. The extensive similarity between the proteins of *P. putida* and *E. coli* suggest that they could also share the same structural transmission pathway to regulate its function, which is likely to be identical to that of known members of the family (Schumacher *et al*, 1995; Schumacher *et al*, 1994). Our results thus point to F1P as the one and only metabolic effector of the bacterial regulator Cra.

That F1P could ultimately be the only effector of Cra opens new questions, because current metabolic models entertain F1P appearance only as a result of fructose phoshorylation by the PTS system (Nogales *et al*, 2008; Puchalka *et al*, 2008; Sawyer *et al*, 1977). To the best of our knowledge, there are not known enzymes for producing F1P during growth on glucose or other carbon source other than fructose. But, since Cra controls expression of various glucose catabolism genes (Ow *et al*, 2007) there must be alternative ways of producing F1P as a descriptor of glycolytic/gluoconeogenic activity (Kotte *et al*, 2010). One way or the other, it is likely that the first regulatory duty of Cra was that of a repressor of fructose metabolism which was later co-opted as a global regulator (Saier and Ramseier, 1996).

5. Cra is a transcriptional repressor of PTS^{Fru} system in *P. putida*

In vitro experiments performed with the regulator, the operator, and F1P produced evidence that Cra$_{P.putida}$ represses expression of the fructose-related phosphoenolpyruvate phosphotransferase carbohydrate system of *P. putida* (PTS^{Fru}) in a fashion (predictably) dependent on F1P binding (Fig. 38). This observation was examined in depth through *in vivo* experiments (Chapter 3). First, by measuring the promoter activity and metabolite concentrations we monitored the expression of the fructose operon in a wild type strain in different carbon sources, which revealed (as expected) that fructose operon is expressed only in presence of fructose and maintained low levels on glucose and succinate. Moreover, we demostrated that the higher basal *fruBKA* levels on glucose with

respect to succinate was due to the contamination of glucose preparations. The presence of a small amount of fructose in the glucose could be due to [i] impurities in glucose powder (Sigma, 99.5% purity) and/or [ii] the Lobry de Bruyn-van Ekenstein (1895) rearrangement of glucose into fructose in stock glucose solutions prepared in the laboratory (20% glucose in water, pH = 4). The rearrangement of glucose takes place primarily in alkaline solution, although some rearrangement occurs in the presence of salts and slightly acid conditions. The mechanism which has generally been accepted to account for this reaction involves the assumption of an intermediary enediol. Ohno *et al.* (1961) reported that this isomerization of glucose to fructose could occur at a pH greater than 4.0 which can explain the inevitable presence of a small amount of fructose in glucose solutions regardless of its nominal purity.

Activity of P_{fruBKA} promoter in the *cra* strain, revealed that [i] the regulator is a very strong repressor of PTS^{Fru} system in *P. putida* and [ii] the operon expression is controled enterely by F1P levels as was suggested by *in vitro* experiments. These claims are represented in Fig. 38.

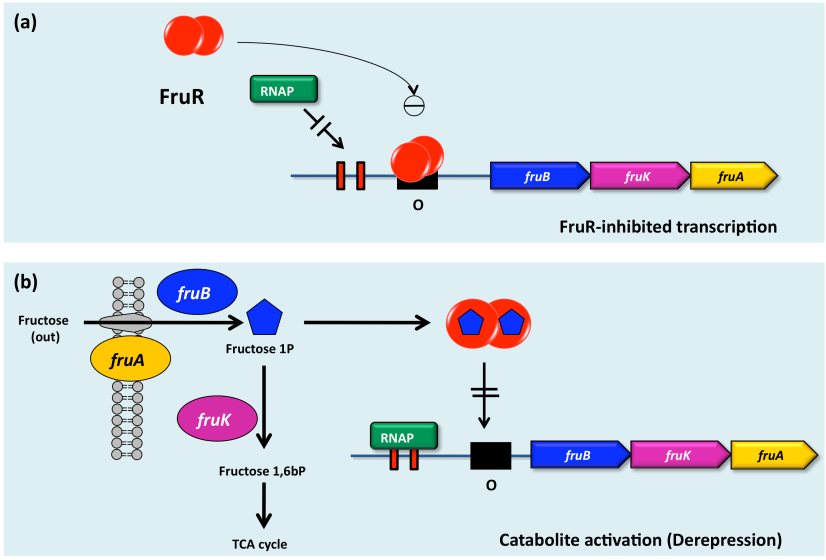

Figure 38. Mechanism of repression/derepression of PTS^{Fru} system by Cra protein in *P. putida*. **(a)** In absence of F1P, the protein binds tightly as a dimer to a single operator in the regulatory region, which inhibits transcription. **(b)** In fructose as carbon source, F1P is produced, which binds with high affinity to the regulator. The binding of the protein with the effector change its conformation causing the release of the protein and the derepression of the fructose operon.

In absence of F1P, the free protein binds tightly as a dimer to the single operator in the regulatory region of fructose operon, which inhibits its transcription. On the other

hand, when fructose is the carbon source, F1P is produced, which binds with high affinity to the regulator. That prevents the binding of Cra to the DNA leading to the derepression of the system.

6. Cra modulates the phosphorylation state of PtsN in *P. putida*

Analysis of the phosphorylation state of $EIIA^{Ntr}$ in *cra* and *ptsP* mutants showed that the regulation exerted by Cra on *fruB* is transferred to the nitrogen PTS system through the cross-talk reported in this bacterium. All our phosphorylation data correlate well with the gene expression results of *fruB*. Changes in phosphorylation of PtsN produced by the deletion of Cra were visualized only under conditions where PtsP was inactivated. This clearly suggests that most of the phosphate of PtsN is obtained *via* PtsP/PtsO (this is based on the observation that *cra* mutant showed similar phosphorylation than the reference strain). Therefore, we hypothetize, that Cra provides a fine tunning regulation on PTS^{Ntr} system, so that it can perform small variations/settings in the ratio of phosphorylated/dephosphorylated PtsN. It has been reported previously, that a large number of phenotypes associated to PtsN depend on its phosphorylation state. Thus, it could be that Cra indirectly modulates other processes including polyhydroxyalkanoate (PHA) accumulation (Velazquez *et al*, 2007), C-source repression of *m*-xylene catabolism (Cases *et al*, 1999), biofilm formation (Pflüger-Grau, data not published) and swimming (Pflüger-Grau, data not published), since some of them depend on the phosphorylation state.

VI. CONCLUSIONS

The work described throughout this Thesis has given rise to the following conclusions:

1. *Carbon central metabolism in P. putida is carried out through an cyclic version of the Entner-Doudoroff pathway*. Differences between the metabolism of *P. putida* and other species such as *E. coli*, indicate a clear specialization of central metabolism as a result of habitat and nutritional requirements of each species.

2. *PTS^{Ntr} system plays regulatory functions on carbon central metabolism of P. putida.* This regulation can be traced mainly to the protein $EIIA^{Ntr}$ (PtsN), which controls the connection of pyruvate to the TCA cycle by downregulating the pyruvate shunt, that bypasses malate dehydrogenase in the TCA cycle.

3. *F1P is the one and only effector of the transcriptional regulator Cra from bacteria***.** In this work, we have studied the Cra protein of *P. putida*, however, we consider that all our observations about the effector can be generalized to other species as *E. coli* and *S. typhimurium* because of the high similarity in the sequence and three-dimensional structure of the effector binding site. Thus, our results suggest that F1P is the only effector of the bacterial regulator Cra.

4. *Cra is a transcriptional repressor of PTS^{Fru} system in P. putida. In vitro* and *in vivo* experiments demonstrated that Cra is very strong repressor of fructose operon, where the whole process is controlled by the intracellular concentrations of F1P.

5. *Cra is a modulator of the PTS^{Ntr} system in P. putida.* The regulation exerted by Cra on fructose operon modulates the phosphorylation state of PtsN under certain metabolic conditions.

El trabajo descrito a lo largo de esta Tesis ha dado lugar a las siguientes conclusiones:

1. *El metabolismo central en P. putida se lleva a cabo a través de una versión cíclica de la ruta Entner-Doudoroff*. Las diferencias entre el metabolismo central de *P. putida* y otras especies tales como *E. coli*, indican una clara especialización de la maquinaria metabólica como resultado del hábitat y las necesidades nutricionales de cada especie.

2. *El Sistema PTS^{Ntr} desempeña funciones regulatorias sobre el metabolismo central de P. putida.* Esta regulación es llevada a cabo por la proteína EIIA^{Ntr} (PtsN), donde hemos demostrado que esta proteína controla la conexión entre el piruvato y el ciclo de Krebs reprimiendo la actividad del desvío del piruvato (*pyruvate shunt*).

3. *La F1P es el único efector del regulador transcripcional bacteriano Cra.* En este trabajo, hemos estudiado la proteína Cra de *P. putida*, sin embargo, consideramos que todas nuestras observaciones sobre su efector pueden ser generalizadas a otras especies como *E. coli* y *S. typhimurium*, debido a la alta similitud en la secuencia y estructura tridimensional del sitio de unión en las proteínas Cra de estas especies. Por lo tanto, nuestros resultados indican que F1P es el único efector del regulador bacteriano Cra.

4. *Cra es un represor transcripcional del sistema PTS^{Fru} de P. putida*. Experimentos *in vitro* e *in vivo* demostraron que Cra es un represor muy fuerte del operón de la fructosa, donde el proceso de expresión está controlado enteramente por las concentraciones intracelulares de F1P.

5. *Cra es un modulador del sistema PTS^{Ntr} de P. putida*. La regulación ejercida por Cra sobre el operón fructosa modula el estado de fosforilación de la proteína PtsN bajo ciertas condiciones metabólicas.

VII. REFERENCES

Adams PD, Afonine PV, Bunkoczi G, Chen VB, Davis IW, Echols N, Headd JJ, Hung LW, Kapral GJ, Grosse-Kunstleve RW, McCoy AJ, Moriarty NW, Oeffner R, Read RJ, Richardson DC, Richardson JS, Terwilliger TC, Zwart PH PHENIX: a comprehensive Python-based system for macromolecular structure solution. *Acta Crystallogr D Biol Crystallogr* **66:** 213-221.

Alberti S, Oehler S, von Wilcken-Bergmann B, Muller-Hill B (1993) Genetic analysis of the leucine heptad repeats of Lac repressor: evidence for a 4-helical bundle. *EMBO J* **12:** 3227-3236.

Attwood PV (1995) The structure and the mechanism of action of pyruvate carboxylase. *Int J Biochem Cell Biol* **27:** 231-249.

Baart GJ, Langenhof M, van de Waterbeemd B, Hamstra HJ, Zomer B, van der Pol LA, Beuvery EC, Tramper J, Martens DE (2010) Expression of phosphofructokinase in *Neisseria meningitidis*. *Microbiology* **156:** 530-542.

Bachmann BJ (1987) Derivations and genotypes of some mutant derivatives of *Escherichia coli* K-12. In *Escherichia coli and Salmonella typhimurium: cellular and molecular biology*, F. C. Neidhardt JLI, K. B. Low, B. Magasanik, M. Schaechter, and H. E. Umbarger (ed), pp 1190–1219. Washington, D.C: American Society for Microbiology.

Bagnara AS, Finch LR (1972) Quantitative extraction and estimation of intracellular nucleoside triphosphates of *Escherichia coli*. *Anal Biochem* **45:** 24-34.

Banerjee PC (1989) Fructose-bisphosphatase-deficient mutants of mucoid *Pseudomonas aeruginosa*. *Folia Microbiol (Praha)* **34:** 81-86.

Banerjee PC, Vanags RI, Chakrabarty AM, Maitra PK (1985) Fructose 1,6-bisphosphate aldolase activity is essential for synthesis of alginate from glucose by *Pseudomonas aeruginosa*. *J Bacteriol* **161:** 458-460.

Begley GS, Jacobson GR (1994) Overexpression, phosphorylation, and growth effects of ORF162, a *Klebsiella pneumoniae* protein that is encoded by a gene linked to *rpoN*, the gene encoding sigma 54. *FEMS Microbiol Lett* **119:** 389-394.

Bekker M, Alexeeva S, Laan W, Sawers G, Teixeira de Mattos J, Hellingwerf K (2010) The ArcBA two-component system of *Escherichia coli* is regulated by the redox state of both the ubiquinone and the menaquinone pool. *J Bacteriol* **192:** 746-754.

Bledig SA, Ramseier TM, Saier MH, Jr. (1996) FruR mediates catabolite activation of pyruvate kinase (*pykF*) gene expression in *Escherichia coli*. *J Bacteriol* **178:** 280-283.

Blencke HM, Homuth G, Ludwig H, Mader U, Hecker M, Stulke J (2003) Transcriptional profiling of gene expression in response to glucose in *Bacillus subtilis*: regulation of the central metabolic pathways. *Metab Eng* **5:** 133-149.

Borneman AR, Gianoulis TA, Zhang ZD, Yu H, Rozowsky J, Seringhaus MR, Wang LY, Gerstein M, Snyder M (2007) Divergence of transcription factor binding sites across related yeast species. *Science* **317:** 815-819.

Bradford MM (1976) A rapid and sensitive method for the quantitation of microgram quantities of protein utilizing the principle of protein-dye binding. *Anal Biochem* **72:** 248-254.

Browning DF, Busby SJ (2004) The regulation of bacterial transcription initiation. *Nat Rev Microbiol* **2:** 57-65.

Buell CR, Joardar V, Lindeberg M, Selengut J, Paulsen IT, Gwinn ML, Dodson RJ, Deboy RT, Durkin AS, Kolonay JF, Madupu R, Daugherty S, Brinkac L, Beanan MJ, Haft DH, Nelson WC, Davidsen T, Zafar N, Zhou L, Liu J, Yuan Q, Khouri H, Fedorova N, Tran B, Russell D, Berry K, Utterback T, Van Aken SE, Feldblyum TV, D'Ascenzo M, Deng WL, Ramos AR, Alfano JR, Cartinhour S, Chatterjee AK, Delaney TP, Lazarowitz SG, Martin GB, Schneider DJ, Tang X, Bender CL, White O, Fraser CM, Collmer A (2003) The complete genome sequence of the *Arabidopsis* and tomato pathogen *Pseudomonas syringae* pv. tomato DC3000. *Proc Natl Acad Sci U S A* **100:** 10181-10186.

Buescher JM, Moco S, Sauer U, Zamboni N (2010) Ultrahigh performance liquid chromatography-tandem mass spectrometry method for fast and robust quantification of anionic and aromatic metabolites. *Anal Chem* **82:** 4403-4412.

Cases I, Lopez JA, Albar JP, De Lorenzo V (2001a) Evidence of multiple regulatory functions for the PtsN (IIA^{Ntr}) protein of *Pseudomonas putida*. *J Bacteriol* **183:** 1032-1037.

Cases I, Perez-Martin J, de Lorenzo V (1999) The IIA^{Ntr} (PtsN) protein of P*seudomonas putida* mediates the C source inhibition of the sigma54-dependent *Pu* promoter of the TOL plasmid. *J Biol Chem* **274:** 15562-15568.

Cases I, Velazquez F, de Lorenzo V (2001b) Role of ptsO in carbon-mediated inhibition of the *Pu* promoter belonging to the pWW0 *Pseudomonas putida* plasmid. *J Bacteriol* **183:** 5128-5133.

Cases I, Velazquez F, de Lorenzo V (2007) The ancestral role of the phosphoenolpyruvate-carbohydrate phosphotransferase system (PTS) as exposed by comparative genomics. *Res Microbiol* **158:** 666-670.

Chakerian AE, Tesmer VM, Manly SP, Brackett JK, Lynch MJ, Hoh JT, Matthews KS (1991) Evidence for leucine zipper motif in lactose repressor protein. *J Biol Chem* **266:** 1371-1374.

Chen J, Matthews KS (1992) Deletion of lactose repressor carboxyl-terminal domain affects tetramer formation. *J Biol Chem* **267:** 13843-13850.

Choi J, Shin D, Yoon H, Kim J, Lee CR, Kim M, Seok YJ, Ryu S (2010) *Salmonella* pathogenicity island 2 expression negatively controlled by $EIIA^{Ntr}$-SsrB interaction is required for *Salmonella* virulence. *Proc Natl Acad Sci U S A* **107:** 20506-20511.

Choi KH, Kumar A, Schweizer HP (2006) A 10-min method for preparation of highly electrocompetent *Pseudomonas aeruginosa* cells: application for DNA fragment

transfer between chromosomes and plasmid transformation. *J Microbiol Methods* **64:** 391-397.

Clarke PH (1982) The metabolic versatility of pseudomonads. *Antonie Van Leeuwenhoek* **48:** 105-130.

Cole JL (2004) Analysis of heterogeneous interactions. *Methods Enzymol* **384:** 212-232.

Collaborative computational project number 4 (1994) The CCP4 suite: programs for protein crystallography. *Acta Crystallogr D Biol Crystallogr* **50:** 760-763.

Commichau FM, Forchhammer K, Stulke J (2006) Regulatory links between carbon and nitrogen metabolism. *Curr Opin Microbiol* **9:** 167-172.

Conway T (1992) The Entner-Doudoroff pathway: history, physiology and molecular biology. *FEMS Microbiol Rev* **9:** 1-27.

Cortay JC, Negre D, Scarabel M, Ramseier TM, Vartak NB, Reizer J, Saier MH, Jr., Cozzone AJ (1994) *In vitro* asymmetric binding of the pleiotropic regulatory protein, FruR, to the *ace* operator controlling glyoxylate shunt enzyme synthesis. *J Biol Chem* **269:** 14885-14891.

Daddaoua A, Krell T, Alfonso C, Morel B, Ramos JL (2010) Compartmentalised Glucose Metabolism in *Pseudomonas putid*a is Controlled by the PtxS Repressor. *J Bacteriol*. **192**: 4357-4366.

Dauner M, Sauer U (2000) GC-MS analysis of amino acids rapidly provides rich information for isotopomer balancing. *Biotechnol Prog* **16:** 642-649.

de Lorenzo V, Eltis L, Kessler B, Timmis KN (1993) Analysis of *Pseudomonas* gene products using lacIq/Ptrp-lac plasmids and transposons that confer conditional phenotypes. *Gene* **123:** 17-24.

de Lorenzo V, Herrero M, Jakubzik U, Timmis KN (1990) Mini-Tn5 transposon derivatives for insertion mutagenesis, promoter probing, and chromosomal insertion of cloned DNA in gram-negative eubacteria. *J Bacteriol* **172:** 6568-6572.

del Castillo T, Ramos JL, Rodriguez-Herva JJ, Fuhrer T, Sauer U, Duque E (2007) Convergent peripheral pathways catalyze initial glucose catabolism in *Pseudomonas putida*: genomic and flux analysis. *J Bacteriol* **189:** 5142-5152.

Deutscher J, Francke C, Postma PW (2006) How phosphotransferase system-related protein phosphorylation regulates carbohydrate metabolism in bacteria. *Microbiol Mol Biol Rev* **70:** 939-1031.

Diesterhaft MD, Freese E (1973) Role of pyruvate carboxylase, phosphoenolpyruvate carboxykinase, and malic enzyme during growth and sporulation of *Bacillus subtilis*. *J Biol Chem* **248:** 6062-6070.

Doi RH, Igarashi RT (1965) Conservation of Ribosomal and Messenger Ribonucleic Acid Cistrons in *Bacillus* Species. *J Bacteriol* **90:** 384-390.

Downs DM (2006) Understanding microbial metabolism. *Annu Rev Microbiol* **60:** 533-559.

Duque E, Filloux A, Molina-Henares A, Torre J, Molina-Henares M, Castillo T, Lam J, Ramos JL (2007) Towards a Genome-Wide Mutant Library of *Pseudomonas putida* KT2440. In *Pseudomonas*, Ramos JL (ed), Vol. V, pp 227-251. London, United Kingdom.: Kluwer.

Edelstein PH, Edelstein MA, Higa F, Falkow S (1999) Discovery of virulence genes of *Legionella pneumophila* by using signature tagged mutagenesis in a guinea pig pneumonia model. *Proc Natl Acad Sci U S A* **96:** 8190-8195.

Eisenberg RC, Dobrogosz WJ (1967) Gluconate metabolism in *Escherichia coli*. *J Bacteriol* **93:** 941-949.

Emsley P, Lohkamp B, Scott WG, Cowtan K (2010) Features and development of Coot. *Acta Crystallogr D Biol Crystallogr* **66:** 486-501.

Entner N, Doudoroff M (1952) Glucose and gluconic acid oxidation of *Pseudomonas saccharophila*. *J Biol Chem* **196:** 853-862.

Eyzaguirre J, Cornwell E, Borie G, Ramirez B (1973) Two malic enzymes in *Pseudomonas aeruginosa*. *J Bacteriol* **116:** 215-221.

Feil H, Feil WS, Chain P, Larimer F, DiBartolo G, Copeland A, Lykidis A, Trong S, Nolan M, Goltsman E, Thiel J, Malfatti S, Loper JE, Lapidus A, Detter JC, Land M, Richardson PM, Kyrpides NC, Ivanova N, Lindow SE (2005) Comparison of the complete genome sequences of *Pseudomonas syringae* pv. syringae B728a and pv. tomato DC3000. *Proc Natl Acad Sci U S A* **102:** 11064-11069.

Fernandez S, de Lorenzo V, Perez-Martin J (1995) Activation of the transcriptional regulator XylR of *Pseudomonas putida* by release of repression between functional domains. *Mol Microbiol* **16:** 205-213.

Fischer E, Sauer U (2003) Metabolic flux profiling of *Escherichia coli* mutants in central carbon metabolism using GC-MS. *Eur J Biochem* **270:** 880-891.

Frank S, Klockgether J, Hagendorf P, Geffers R, Schock U, Pohl T, Davenport CF, Tummler B (2011) *Pseudomonas putida* KT2440 genome update by cDNA sequencing and microarray transcriptomics. *Environ Microbiol*. In press.

Fuhrer T, Fischer, E. and Sauer U (2005) Experimental Identification and Quantification of Glucose Metabolism in Seven Bacterial Species. *J Bacteriol* **187:** 1581-1590.

Fuhrer T, Sauer U (2009) Different biochemical mechanisms ensure network-wide balancing of reducing equivalents in microbial metabolism. *J Bacteriol* **191:** 2112-2121.

Gasteiger E, Hoogland C, Gattiker A, Duvaud S, Wilkins MR, Appel RD, Bairoch A (2005) Protein Identification and Analysis Tools on the ExPASy Server. In *The Poteomics Protocols Handbook*, Walker JM (ed), pp 571-607: Humana Press.

Geer BW, Krochko D, Williamson JH (1979) Ontogeny, cell distribution, and the physiological role of NADP-malic enzyme in *Drosophila melanogaster*. *Biochem Genet* **17:** 867-879.

Georgellis D, Lynch AS, Lin EC (1997) In vitro phosphorylation study of the *arc* two-component signal transduction system of *Escherichia coli*. *J Bacteriol* **179:** 5429-5435.

Gosset G, Zhang Z, Nayyar S, Cuevas WA, Saier MH, Jr. (2004) Transcriptome analysis of Crp-dependent catabolite control of gene expression in *Escherichia coli*. *J Bacteriol* **186:** 3516-3524.

Govan JR, Deretic V (1996) Microbial pathogenesis in cystic fibrosis: mucoid *Pseudomonas aeruginosa* and *Burkholderia cepacia*. *Microbiol Rev* **60:** 539-574.

Hanahan D (1983) Studies on transformation of *Escherichia coli* with plasmids. *J Mol Biol* **166:** 557-580.

Hayden JD, Ades SE (2008) The extracytoplasmic stress factor, sigmaE, is required to maintain cell envelope integrity in *Escherichia coli*. *PLoS One* **3:** e1573.

Herrero M, de Lorenzo V, Timmis KN (1990) Transposon vectors containing non-antibiotic resistance selection markers for cloning and stable chromosomal insertion of foreign genes in gram-negative bacteria. *J Bacteriol* **172:** 6557-6567.

Holm L, Rosenstrom P Dali server: conservation mapping in 3D. *Nucleic Acids Res* **38 Suppl:** W545-549.

Horton, RM, Hunt HD, Ho SN, Pullen JK and Pease LR (1989) Engineering hybrid genes without the use of restriction enzymes: gene splicing by overlap extension. *Gene* **77:** 61-68.

Jensen LJ, Skovgaard M, Sicheritz-Pontén T, Tue Hansen N, Johansson H, Jorgensenn MK, Kiil K, Hallin PF, Ussery D (2004) Comparative Genomics of four *Pseudomonas* species. In *Pseudomonas: Genomics, Life atyle and Molecular Architecture*, Ramos JL (ed), Vol. 1, pp 139-162. New York: Kluwer Academic/Plenum publishers.

Jimenez JI, Minambres B, Garcia JL, Diaz E (2002) Genomic analysis of the aromatic catabolic pathways from *Pseudomonas putida* KT2440. *Environ Microbiol* **4:** 824-841.

Jin S, Ishimoto K, Lory S (1994) Nucleotide sequence of the rpoN gene and characterization of two downstream open reading frames in *Pseudomonas aeruginosa*. *J Bacteriol* **176:** 1316-1322.

Jitrapakdee S, Wallace JC (1999) Structure, function and regulation of pyruvate carboxylase. *Biochem J* **340 (Pt 1):** 1-16.

Johnson JL, Ordal EJ (1968) Deoxyribonucleic acid homology in bacterial taxonomy: effect of incubation temperature on reaction specificity. *J Bacteriol* **95:** 893-900.

Jones DH, Franklin FC, Thomas CM (1994) Molecular analysis of the operon which encodes the RNA polymerase sigma factor sigma 54 of *Escherichia coli*. *Microbiology* **140 (Pt 5):** 1035-1043.

Jurado P, Ritz D, Beckwith J, de Lorenzo V, Fernández LA (2002) Production of functional single-chain Fv antibodies in the cytoplasm of *Escherichia coli*. *J Mol Biol* **320**: 1-10

Kabsch W (1993) Automatic processing of rotation diffraction data from crystals of initially unknown symmetry and cell constants. *Journal of Applied Crystallography* **26:** 795-800.

Kotte O, Zaugg JB, Heinemann M (2010) Bacterial adaptation through distributed sensing of metabolic fluxes. *Mol Syst Biol* **6:** 355.

Krell T, Busch A, Guazzaroni M, Lacal J, Gallegos M, Terán W (2007) The use of Microcalorimetry to Study Regulatory Mechanism in *Pseudomonas*. In *Pseudomonas A Model System in biology*, Ramos JL, Filloux A (eds), pp 255-277. Netherlands: Springer.

Kundig W, Ghosh S, Roseman S (1964) Phosphate Bound to Histidine in a Protein as an Intermediate in a Novel Phospho-Transferase System. *Proc Natl Acad Sci U S A* **52:** 1067-1074.

Laue TM, Shah B, Ridgeway TM, Pelletier S (1992) Computer-aided interpretation of sedimentation data for proteins. In *Analytical Ultracentrifugation in Biochemistry and Polymer Science*, Harding SE, Horton JC, Rowe AJ (eds), pp 90-125. Cambridge, England: Royal Society of chemistry.

Lebowitz J, Lewis MS, Schuck P (2002) Modern analytical ultracentrifugation in protein science: a tutorial review. *Protein Sci* **11:** 2067-2079.

Lee CR, Cho SH, Yoon MJ, Peterkofsky A, Seok YJ (2007) *Escherichia coli* enzyme IIA^{Ntr} regulates the K^+ transporter TrkA. *Proc Natl Acad Sci U S A* **104:** 4124-4129.

Lee CR, Koo BM, Cho SH, Kim YJ, Yoon MJ, Peterkofsky A, Seok YJ (2005) Requirement of the dephospho-form of enzyme IIA^{Ntr} for derepression of *Escherichia coli* K-12 *ilvBN* expression. *Mol Microbiol* **58:** 334-344.

Lessie TG, Phibbs PV, Jr. (1984) Alternative pathways of carbohydrate utilization in pseudomonads. *Annu Rev Microbiol* **38:** 359-388.

Lewis M, Chang G, Horton NC, Kercher MA, Pace HC, Schumacher MA, Brennan RG, Lu P (1996) Crystal structure of the lactose operon repressor and its complexes with DNA and inducer. *Science* **271:** 1247-1254.

Lobry de Bruyn CA, van Ekenstein WA. (1895) Action of alkalis on the sugars. Reciprocal transformation of glucose, fructose and mannose. *Rec. Trav. Chim.* **14**: 201-206.

Loh KC, Cao B (2008) Paradigm in biodegradation using *Pseudomonas putida*-A review of proteomics studies. *Enzyme and Microbial Technology* **43:** 1-12.

Lundin A, Thore A (1975) Comparison of methods for extraction of bacterial adenine nucleotides determined by firefly assay. *Appl Microbiol* **30:** 713-721.

Luttmann D, Heermann R, Zimmer B, Hillmann A, Rampp IS, Jung K, Gorke B (2009) Stimulation of the potassium sensor KdpD kinase activity by interaction with the phosphotransferase protein IIA^{Ntr} in *Escherichia coli*. *Mol Microbiol* **72:** 978-994.

Manoil C, Beckwith J (1985) TnphoA: a transposon probe for protein export signals. *Proc Natl Acad Sci U S A* **82:** 8129-8133.

Martins dos Santos VA, Timmis KN, Tummler B, Weinel C (2004) Genomic features od *Pseudomonas putida* strain KT2440. In *Pseudomonas: Genomics, Life atyle and Molecular Architecture*, Ramos JL (ed), Vol. 1, pp 77-83. New York: Kluwer Academic/Plenum publishers.

McCoy AJ, Grosse-Kunstleve RW, Adams PD, Winn MD, Storoni LC, Read RJ (2007) Phaser crystallographic software. *J Appl Crystallogr* **40:** 658-674.

Meyer JM (2000) Pyoverdines: pigments, siderophores and potential taxonomic markers of fluorescent *Pseudomonas* species. *Arch Microbiol* **174:** 135-142.

Miller JH (1972) *Experiments in molecular genetics*. N.Y.: Cold Spring Harbor.

Moore ER, Tindall BJ, Martins dos Santos VA, Pieper DH, Ramos JL, Palleroni NJ (2006) Nonmedical: *Pseudomonas*. In *The prokaryotes*, Dworkin M, Falkow S, Rosenberg E, Schleifer KH, Stackebrandt E (eds), Third edition edn, p 655. New York: Springer.

Munch R, Hiller K, Barg H, Heldt D, Linz S, Wingender E, Jahn D (2003) PRODORIC: prokaryotic database of gene regulation. *Nucleic Acids Res* **31:** 266-269.

Munch R, Hiller K, Grote A, Scheer M, Klein J, Schobert M, Jahn D (2005) Virtual Footprint and PRODORIC: an integrative framework for regulon prediction in prokaryotes. *Bioinformatics* **21:** 4187-4189.

Murray MG, Thompson WF (1980) Rapid isolation of high molecular weight plant DNA. *Nucleic Acids Res* **8:** 4321-4325.

Navas MA, Cerdan S, Gancedo JM (1993) Futile cycles in *Saccharomyces cerevisiae* strains expressing the gluconeogenic enzymes during growth on glucose. *Proc Natl Acad Sci U S A* **90:** 1290-1294.

Negre D, Bonod-Bidaud C, Geourjon C, Deleage G, Cozzone AJ, Cortay JC (1996) Definition of a consensus DNA-binding site for the *Escherichia coli* pleiotropic regulatory protein, FruR. *Mol Microbiol* **21:** 257-266.

Negre D, Oudot C, Prost JF, Murakami K, Ishihama A, Cozzone AJ, Cortay JC (1998) FruR-mediated transcriptional activation at the *ppsA* promoter of *Escherichia coli*. *J Mol Biol* **276:** 355-365.

Nelson KE, Weinel C, Paulsen IT, Dodson RJ, Hilbert H, Martins dos Santos VA, Fouts DE, Gill SR, Pop M, Holmes M, Brinkac L, Beanan M, DeBoy RT, Daugherty S, Kolonay J, Madupu R, Nelson W, White O, Peterson J, Khouri H, Hance I, Chris Lee P, Holtzapple E, Scanlan D, Tran K, Moazzez A, Utterback T, Rizzo M, Lee K, Kosack D, Moestl D, Wedler H, Lauber J, Stjepandic D, Hoheisel J, Straetz M, Heim S, Kiewitz C, Eisen JA, Timmis KN, Dusterhoft A, Tummler B, Fraser CM (2002) Complete genome sequence and comparative analysis of the metabolically versatile *Pseudomonas putida* KT2440. *Environ Microbiol* **4:** 799-808.

Neves AR, Ramos A, Nunes MC, Kleerebezem M, Hugenholtz J, de Vos WM, Almeida J, Santos H (1999) In vivo nuclear magnetic resonance studies of glycolytic kinetics in *Lactococcus lactis*. *Biotechnol Bioeng* **64:** 200-212.

Ninfa AJ (2007) Regulation of carbon and nitrogen metabolism: adding regulation of ion channels and another second messenger to the mix. *Proc Natl Acad Sci U S A* **104:** 4243-4244.

Nogales J, Palsson BO, Thiele I (2008) A genome-scale metabolic reconstruction of *Pseudomonas putida* KT2440: iJN746 as a cell factory. *BMC Syst Biol* **2:** 79.

Ohno Y, Ward KJ (1961) Acid epimerization of D-Glucose. *J. Org. Chem.* **26**: 3928-3931.

Ow DS, Lee RM, Nissom PM, Philp R, Oh SK, Yap MG (2007) Inactivating FruR global regulator in plasmid-bearing *Escherichia coli* alters metabolic gene expression and improves growth rate. *J Biotechnol* **131:** 261-269.

Palleroni NJ (2003) Prokaryote taxonomy of the 20th century and the impact of studies on the genus *Pseudomona*s: a personal view. *Microbiology* **149:** 1-7.

Palleroni NJ, Ballard RW, Ralston E, Doudoroff M (1972) Deoxyribonucleic acid homologies among some *Pseudomonas* species. *J Bacteriol* **110:** 1-11.

Palleroni NJ, Kunisawa R, Contopoulou R, Doudoroff M (1973) Nucleic acid homologies in the genus *Pseudomonas*. *Int J Syst bacteriol* **23:** 333-339.

Palleroni NJ, Moore E (2004) Taxonomy of Pseudomonads: Experimental approaches. In *Pseudomonas: Genomics, Life atyle and Molecular Architecture*, Ramos JL (ed), Vol. 1, pp 3-15. New York: Kluwer Academic/Plenum publishers.

Panjikar S, Parthasarathy V, Lamzin VS, Weiss MS, Tucker PA (2005) Auto-Rickshaw: an automated crystal structure determination platform as an efficient tool for the validation of an X-ray diffraction experiment. *Acta Crystallogr D Biol Crystallogr* **61:** 449-457.

Parikh A, Miranda ER, Katoh-Kurasawa M, Fuller D, Rot G, Zagar L, Curk T, Sucgang R, Chen R, Zupan B, Loomis WF, Kuspa A, Shaulsky G Conserved

developmental transcriptomes in evolutionarily divergent species. *Genome Biol* **11:** R35.

Paulsen IT, Press CM, Ravel J, Kobayashi DY, Myers GS, Mavrodi DV, DeBoy RT, Seshadri R, Ren Q, Madupu R, Dodson RJ, Durkin AS, Brinkac LM, Daugherty SC, Sullivan SA, Rosovitz MJ, Gwinn ML, Zhou L, Schneider DJ, Cartinhour SW, Nelson WC, Weidman J, Watkins K, Tran K, Khouri H, Pierson EA, Pierson LS, 3rd, Thomashow LS, Loper JE (2005) Complete genome sequence of the plant commensal *Pseudomonas fluorescens* Pf-5. *Nat Biotechnol* **23:** 873-878.

Peekhaus N, Conway T (1998) What's for dinner?: Entner-Doudoroff metabolism in *Escherichia coli*. *J Bacteriol* **180:** 3495-3502.

Penin F, Geourjon C, Montserret R, Bockmann A, Lesage A, Yang YS, Bonod-Bidaud C, Cortay JC, Negre D, Cozzone AJ, Deleage G (1997) Three-dimensional structure of the DNA-binding domain of the fructose repressor from *Escherichia coli* by 1H and 15N NMR. *J Mol Biol* **270:** 496-510.

Perrenoud A, Sauer U (2005) Impact of global transcriptional regulation by ArcA, ArcB, Cra, Crp, Cya, Fnr, and Mlc on glucose catabolism in *Escherichia coli*. *J Bacteriol* **187:** 3171-3179.

Pfluger K, de Lorenzo V (2007a) Growth-dependent phosphorylation of the PtsN (EII^{Ntr}) protein of *Pseudomonas putida*. *J Biol Chem* **282:** 18206-18211.

Pfluger K, de Lorenzo V (2008) Evidence of in vivo cross talk between the nitrogen-related and fructose-related branches of the carbohydrate phosphotransferase system of *Pseudomonas putida*. *J Bacteriol* **190:** 3374-3380.

Pfluger K, di Bartolo I, Velazquez F, de Lorenzo V (2007b) Non-disruptive release of *Pseudomonas putida* proteins by in situ electric breakdown of intact cells. *J Microbiol Methods* **71:** 179-185.

Pfluger-Grau K, Chavarria M, de Lorenzo V (2011) The interplay of the EIIA(Ntr) component of the nitrogen-related phosphotransferase system (PTSNtr) of *Pseudomonas putida* with pyruvate dehydrogenase. *Biochim Biophys Acta*. In press.

Pfluger-Grau K, Gorke B (2010) Regulatory roles of the bacterial nitrogen-related phosphtransferase system. *Trends Microbiol* **18:** 205-214.

Plumbridge J (2002) Regulation of gene expression in the PTS in *Escherichia coli*: the role and interactions of Mlc. *Curr Opin Microbiol* **5:** 187-193.

Portais JC, Delort AM (2002) Carbohydrate cycling in micro-organisms: what can (13)C-NMR tell us? *FEMS Microbiol Rev* **26:** 375-402.

Postma PW, Lengeler JW, Jacobson GR (1993) Phosphoenolpyruvate:carbohydrate phosphotransferase systems of bacteria. *Microbiol Rev* **57:** 543-594.

Powell BS, Court DL, Inada T, Nakamura Y, Michotey V, Cui X, Reizer A, Saier MH, Jr., Reizer J (1995) Novel proteins of the phosphotransferase system encoded within the *rpoN* operon of *Escherichia coli*. Enzyme IIA^{Ntr} affects growth on organic nitrogen and the conditional lethality of an erats mutant. *J Biol Chem* **270:** 4822-4839.

Prost JF, Negre D, Oudot C, Murakami K, Ishihama A, Cozzone AJ, Cortay JC (1999) Cra-dependent transcriptional activation of the *icd* gene of *Escherichia coli*. *J Bacteriol* **181:** 893-898.

Puchalka J, Oberhardt MA, Godinho M, Bielecka A, Regenhardt D, Timmis KN, Papin JA, Martins dos Santos VA (2008) Genome-scale reconstruction and analysis of the *Pseudomonas putida* KT2440 metabolic network facilitates applications in biotechnology. *PLoS Comput Biol* **4:** e1000210.

Rabus R, Reizer J, Paulsen I, Saier MH, Jr. (1999) Enzyme I(Ntr) from *Escherichia coli*. A novel enzyme of the phosphoenolpyruvate-dependent phosphotransferase system exhibiting strict specificity for its phosphoryl acceptor, NPr. *J Biol Chem* **274:** 26185-26191.

Ramseier TM, Bledig S, Michotey V, Feghali R, Saier MH, Jr. (1995) The global regulatory protein FruR modulates the direction of carbon flow in *Escherichia coli*. *Mol Microbiol* **16:** 1157-1169.

Ramseier TM, Chien SY, Saier MH, Jr. (1996) Cooperative interaction between Cra and Fnr in the regulation of the *cydAB* operon of *Escherichia coli. Curr Microbiol* **33:** 270-274.

Ramseier TM, Negre D, Cortay JC, Scarabel M, Cozzone AJ, Saier MH, Jr. (1993) In vitro binding of the pleiotropic transcriptional regulatory protein, FruR, to the *fru*, *pps, ace, pts and icd* operons of *Escherichia coli* and *Salmonella typhimurium*. *J Mol Biol* **234:** 28-44.

Reizer J, Sutrina SL, Wu LF, Deutscher J, Reddy P, Saier MH, Jr. (1992) Functional interactions between proteins of the phosphoenolpyruvate:sugar phosphotransferase systems of *Bacillus subtilis* and *Escherichia coli*. *J Biol Chem* **267:** 9158-9169.

Rollin C, Morgant V, Guyonvarch A, Guerquin-Kern JL (1995) 13C-NMR studies of *Corynebacterium melassecola* metabolic pathways. *Eur J Biochem* **227:** 488-493.

Romano AH, Conway T (1996) Evolution of carbohydrate metabolic pathways. *Res Microbiol* **147:** 448-455.

Ronimus RS, Morgan HW (2001) The biochemical properties and phylogenies of phosphofructokinases from extremophiles. *Extremophiles* **5:** 357-373.

Saier MH, Jr., Ramseier TM (1996) The catabolite repressor/activator (Cra) protein of enteric bacteria. *J Bacteriol* **178:** 3411-3417.

Saier MH, Jr., Reizer J (1994) The bacterial phosphotransferase system: new frontiers 30 years later. *Mol Microbiol* **13:** 755-764.

Sambrook J, T. Maniatis, and T. Fritsch (1989) *Molecular cloning: a laboratory manual*. N.Y.

Sarkar D, Siddiquee KA, Arauzo-Bravo MJ, Oba T, Shimizu K (2008) Effect of *cra* gene knockout together with *edd* and *iclR* genes knockout on the metabolism in *Escherichia coli*. *Arch Microbiol* **190:** 559-571.

Sauer U, Eikmanns BJ (2005) The PEP-pyruvate-oxaloacetate node as the switch point for carbon flux distribution in bacteria. *FEMS Microbiol Rev* **29:** 765-794.

Sauer U, Lasko DR, Fiaux J, Hochuli M, Glaser R, Szyperski T, Wuthrich K, Bailey JE (1999) Metabolic flux ratio analysis of genetic and environmental modulations of *Escherichia coli* central carbon metabolism. *J Bacteriol* **181:** 6679-6688.

Sawyer MH, Baumann P, Baumann L, Berman SM, Canovas JL, Berman RH (1977) Pathways of D-fructose catabolism in species of *Pseudomonas*. *Arch Microbiol* **112:** 49-55.

Scarabel M, Penin F, Bonod-Bidaud C, Negre D, Cozzone AJ, Cortay JC (1995) Overproduction, purification and structural characterization of the functional N-terminal DNA-binding domain of the fru repressor from *Escherichia coli* K-12. *Gene* **153:** 9-15.

Schleissner C, Reglero A, Luengo JM (1997) Catabolism of D-glucose by P*seudomonas putida* U occurs via extracellular transformation into D-gluconic acid and induction of a specific gluconate transport system. *Microbiology* **143 (Pt 5):** 1595-1603.

Schuck P (2000) Size-distribution analysis of macromolecules by sedimentation velocity ultracentrifugation and lamm equation modeling. *Biophys J* **78:** 1606-1619.

Schuck P (2004) A model for sedimentation in inhomogeneous media. I. Dynamic density gradients from sedimenting co-solutes. *Biophys Chem* **108:** 187-200.

Schumacher MA, Choi KY, Lu F, Zalkin H, Brennan RG (1995) Mechanism of corepressor-mediated specific DNA binding by the purine repressor. *Cell* **83:** 147-155.

Schumacher MA, Choi KY, Zalkin H, Brennan RG (1994) Crystal structure of LacI member, PurR, bound to DNA: minor groove binding by alpha helices. *Science* **266:** 763-770.

Segura D, Espin G (1998) Mutational inactivation of a gene homologous to *Escherichia coli ptsP* affects poly-beta-hydroxybutyrate accumulation and nitrogen fixation in *Azotobacter vinelandii*. *J Bacteriol* **180:** 4790-4798.

Sheldrick GM (2002) Macromolecular phasing with SHELXE. *Zeitschrift für Kristallographie* **217:** 644-650.

Shimada T, Fujita N, Maeda M, Ishihama A (2005) Systematic search for the Cra-binding promoters using genomic SELEX system. *Genes Cells* **10:** 907-918.

Shimada T, Yamamoto K, Ishihama (2011) A Novel members of the Cra regulon involved in carbon metabolism in *Escherichia coli*. *J Bacteriol* **193:** 649-659.

Shulman RG, Brown TR, Ugurbil K, Ogawa S, Cohen SM, den Hollander JA (1979) Cellular applications of 31P and 13C nuclear magnetic resonance. *Science* **205:** 160-166.

Simossis VA, Heringa J (2005) PRALINE: a multiple sequence alignment toolbox that integrates homology-extended and secondary structure information. *Nucleic Acids Res* **33:** W289-294.

Smyth GK (2004) Linear models and empirical bayes methods for assessing differential expression in microarray experiments. *Stat Appl Genet Mol Biol* **3:** Article3.

Smyth GK, Speed T (2003) Normalization of cDNA microarray data. *Methods* **31:** 265-273.

Stanier RY, Palleroni NJ, Doudoroff M (1966) The aerobic pseudomonads: a taxonomic study. *J Gen Microbiol* **43:** 159-271.

Steinbuchel A (1986) Expression of the *Escherichia coli pfkA* gene in *Alcaligenes eutrophus* and in other gram-negative bacteria. *J Bacteriol* **166:** 319-327.

Stjepandic D, Weinel C, Hilbert H, Koo HL, Diehl F, Nelson KE, Tummler B, Hoheisel JD (2002) The genome structure of *Pseudomonas putida*: high-resolution mapping and microarray analysis. *Environ Microbiol* **4:** 819-823.

Stover CK, Pham XQ, Erwin AL, Mizoguchi SD, Warrener P, Hickey MJ, Brinkman FS, Hufnagle WO, Kowalik DJ, Lagrou M, Garber RL, Goltry L, Tolentino E, Westbrock-Wadman S, Yuan Y, Brody LL, Coulter SN, Folger KR, Kas A, Larbig K, Lim R, Smith K, Spencer D, Wong GK, Wu Z, Paulsen IT, Reizer J, Saier MH, Hancock RE, Lory S, Olson MV (2000) Complete genome sequence of *Pseudomonas aeruginosa* PAO1, an opportunistic pathogen. *Nature* **406:** 959-964.

Terwilliger TC (2000) Maximum likelihood density modification. *Acta Cryst* **D56:** 965-972.

Timmis KN (2002) *Pseudomonas putida*: a cosmopolitan opportunist par excellence. *Environ Microbiol* **4:** 779-781.

Unden G, Achebach S, Holighaus G, Tran HG, Wackwitz B, Zeuner Y (2002) Control of FNR function of *Escherichia coli* by O_2 and reducing conditions. *J Mol Microbiol Biotechnol* **4:** 263-268.

Unden G, Schirawski J (1997) The oxygen-responsive transcriptional regulator FNR of *Escherichia coli*: the search for signals and reactions. *Mol Microbiol* **25:** 205-210.

Van Dijken JP, Quayle JR (1977) Fructose metabolism in four *Pseudomonas* species. *Arch Microbiol* **114:** 281-286.

Van Duyne GD, Standaert RF, Karplus PA, Schreiber SL, Clardy J (1993) Atomic structures of the human immunophilin FKBP-12 complexes with FK506 and rapamycin. *J Mol Biol* **229:** 105-124.

Velazquez F, di Bartolo I, de Lorenzo V (2004) Genetic evidence that catabolites of the Entner-Doudoroff pathway signal C source repression of the sigma54 *Pu* promoter of *Pseudomonas putida*. *J Bacteriol* **186:** 8267-8275.

Velazquez F, Pfluger K, Cases I, De Eugenio LI, de Lorenzo V (2007) The phosphotransferase system formed by PtsP, PtsO, and PtsN proteins controls production of polyhydroxyalkanoates in *Pseudomonas putida*. *J Bacteriol* **189:** 4529-4533.

Vicente M (1975) The uptake of fructose by *Pseudomonas putida*. *Arch Microbiol* **102:** 163-166.

Vicente M, Canovas JL (1973a) Glucolysis in *Pseudomonas putida*: physiological role of alternative routes from the analysis of defective mutants. *J Bacteriol* **116:** 908-914.

Vicente M, Canovas JL (1973b) Regulation of the glucolytic enzymes in *Pseudomonas putida*. *Arch Mikrobiol* **93:** 53-64.

Vicente M, Pedro MA, Torrontegui G, Canovas JL (1975) The uptake of glucose and gluconate by *Pseudomonas putida*. *Mol Cell Biochem* **7:** 59-64.

Vodovar N, Vallenet D, Cruveiller S, Rouy Z, Barbe V, Acosta C, Cattolico L, Jubin C, Lajus A, Segurens B, Vacherie B, Wincker P, Weissenbach J, Lemaitre B, Medigue C, Boccard F (2006) Complete genome sequence of the entomopathogenic and metabolically versatile soil bacterium *Pseudomonas entomophila*. *Nat Biotechnol* **24:** 673-679.

Wallace AC, Laskowski RA, Thornton JM (1995) LIGPLOT: a program to generate schematic diagrams of protein-ligand interactions. *Protein Eng* **8:** 127-134.

Warren GB, Tipton KF (1974) Pig liver pyruvate carboxylase. The reaction pathway for the decarboxylation of oxaloacetate. *Biochem J* **139:** 321-329.

Wernimont A, Edwards A (2009) In situ proteolysis to generate crystals for structure determination: an update. *PLoS One* **4:** e5094.

Williams PA, Murray K (1974) Metabolism of benzoate and the methylbenzoates by *Pseudomonas putida* (arvilla) mt-2: evidence for the existence of a TOL plasmid. *J Bacteriol* **120:** 416-423.

Wilson CJ, Das P, Clementi C, Matthews KS, Wittung-Stafshede P (2005) The experimental folding landscape of monomeric lactose repressor, a large two-domain protein, involves two kinetic intermediates. *Proc Natl Acad Sci U S A* **102:** 14563-14568.

Wirth R, Friesenegger A, Fiedler S (1989) Transformation of various species of gram-negative bacteria belonging to 11 different genera by electroporation. *Mol Gen Genet* **216:** 175-177.

Wittekind M, Reizer J, Deutscher J, Saier MH, Klevit RE (1989) Common strutural changes accompany the functional inactivation of HPr by seryl phosphorylation of by serine to aspartate substitution. *Biochemistry* **28**: 9908-9912.

Wittkopp PJ Variable transcription factor binding: a mechanism of evolutionary change. *PLoS Biol* **8:** e1000342.

Wong SM and Mekalanos JJ (2000) Genetic footprinting with mariner-based transposition in *Pseudomonas aeruginosa*. *Proc Natl Acad Sci U S A* **97**:10191-10196.

Wu X, Monchy S, Taghavi S, Zhu W, Ramos J, van der Lelie D (2011) Comparative genomics and functional analysis of niche-specific adaptation in *Pseudomonas putida*. *FEMS Microbiol Rev* **35:** 299-323.

Yuste L, Hervas AB, Canosa I, Tobes R, Jimenez JI, Nogales J, Perez-Perez MM, Santero E, Diaz E, Ramos JL, de Lorenzo V, Rojo F (2006) Growth phase-dependent expression of the *Pseudomonas putida* KT2440 transcriptional machinery analysed with a genome-wide DNA microarray. *Environ Microbiol* **8:** 165-177.

Zamboni N, Fischer E, Sauer U (2005) FiatFlux--a software for metabolic flux analysis from 13C-glucose experiments. *BMC Bioinformatics* **6:** 209.

Zhou D, Yang R (2006) Global analysis of gene transcription regulation in prokaryotes. *Cell Mol Life Sci* **63:** 2260-2290.

Zimmer B, Hillmann A, Gorke B (2008) Requirements for the phosphorylation of the *Escherichia coli* $EIIA^{Ntr}$ protein *in vivo*. *FEMS Microbiol Lett* **286:** 96-102.

VIII. ANNEXES

Table 7. Identified Cra boxes in *P. putida*.

Gene Name/Acc	Sequence	ATG-Distance	Location
FruB (GE00180219)	TGAAACGTTTAA	116	intergenic
Gap-1 (GE00180435)	TGAAACGGTTTT	52	intergenic
Edd (GE00180436)	TGAAACGGTTTT	202	intergenic
HisA (GE00179724)	TGAAGCGTTTTC	204	coding region
PP0300 (GE00179732	TGAATGGCTTCA	163	coding region
AccB (GE00179987)	TGAAACGTTTCT	54	intergenic
PP0711 (GE00180137)	TGAAGCGATTCT	167	coding region
FruR (GE00180218)	TGAAACGTTTAA	158	intergenic
PP0891 (GE00180317)	TGAAGCGGTTAT	329	coding region
PP1181 (GE00180606)	TGAACCGTTTTT	150	intergenic
RuvA (GE00180641)	TGAAGCGCTTAC	102	coding region
Mqo-2 (GE00180676)	TGAATCGTTTTT	203	intergenic
OprB-2 (GE00180868)	TGAAGCGTTTCA	90	intergenic
SugE (GE00181123)	TGAATCGTTTTC	181	intergenic
PP1868 (GE00181288)	TGAATCGATAAT	297	intergenic
PP2061 (GE00181476)	TGAATCGTTTGC	227	coding region
PP2267 (GE00181681)	TGAATCGCTTCG	225	intergenic
PP2425 (GE00181838)	TGAATCGTTTCA	151	intergenic
PP2426 (GE00181839)	TGAATCGTTTCA	20	intergenic
PP2533 (GE00181943)	TGAATCGGTTCC	248	coding region
PP2828 (GE00182237)	TGAATGGTTTTT	289	intergenic
PP2868 (GE00182277)	TGAATCGCTTCT	71	coding region
PP3443 (GE00182846)	TGAATCGTTTCA	42	coding region
PP3754 (GE00183149)	TGAATCGCTTTC	175	coding region
PP3768 (GE00183163)	TGAAACGTTTAT	4	intergenic
PP3769 (GE00183164)	TGAAACGTTTAT	129	intergenic
PP3783 (GE00183178)	TGAAGCGCTTAT	111	coding region
FliA (GE00183721)	TGAACCGTTTCC	311	coding region
RadA (GE00184018)	TGAAGCGTTTAA	118	intergenic
MscL (GE00184019)	TGAAGCGTTTAA	48	intergenic
PP4658 (GE00184032)	TGAAACGCTTTT	110	intergenic
IlvB (GE00184054)	TGAAGCGATTTT	326	intergenic

DapB (GE00184098)	TGAAGCGCTTCT	28	coding region
ProA (GE00184181)	TGAATGGCTTAA	254	intergenic
PP4812 (GE00184182)	TGAATGGCTTAA	41	intergenic
PP4948 (GE00184316)	TGAAACGTTTCC	250	intergenic
NtrB (GE00184413)	TGAAACGTTTAA	185	intergenic
GltB (GE00184442)	TGAAGCGTTTCA	228	intergenic
PP5330 (GE00184696)	TGAATCGTTTAC	297	intergenic
PP5331 (GE00184697)	TGAATCGTTTAC	54	intergenic
PP5404 (GE00184769)	TGAATCGATTGA	14	coding region

Summary of the thesis in Spanish by sections

I. RESUMEN

La bacteria del suelo *Pseudomonas putida* es conocida por su versatilidad metabólica y resistencia a diversos tipos de estrés. Esto requiere diversos niveles de control para coordinar la expresión génica y así mantener la fisiología general de la célula en diversas condiciones. Un importante sensor fisiológico es el sistema de transporte fosfoenolpiruvato fosfotransferasa de azúcares (PTS), que lleva a cabo la asimilación de hidratos de carbono hacia el metabolismo central, así como funciones reguladoras (*p.e.* en el fenómeno de represión catabólica). Aparte de los sistemas PTS clásicos, muchos procariotas tienen un tipo de sistema PTS que no está involucrado en el tráfico de hidratos de carbono, el cual participa en la regulación de algunos procesos metabólicos. En *P. putida*, el sistema PTS de azúcar específico para el transporte de fructosa (FruA / EIIBC y FruB / EI-HPR-EIIA) coexiste con el llamado sistema PTS de nitrógeno PTS^{Ntr} (PtsP / EI^{NTR}, PtsO / Npr, y PtsN / $EIIA^{Ntr}$).

En este trabajo se analiza: [i] el flujo del carbono en el metabolismo central de *P. putida*, así como su interacción con el sistema PTS^{Ntr} y [ii] el control ejercido por el regulador transcripcional Cra sobre los sistemas PTS de esta bacteria. En concreto, en el **Capítulo 1** se analizó a través de herramientas de fluxómica y metabolómica la utilización de varias fuentes de carbono (PTS y no PTS). Los resultados mostraron que el Entner-Doudoroff (ED) es la vía más común para la degradación de azúcares en *P. putida*. Además, se demostró que la vía del ED en *P. putida* opera en un inusual modo cíclico. Además, en el **Capítulo 1** a través de análisis de flujos y ensayos enzimáticos se demostró que la proteína $EIIA^{Ntr}$ controla *el desvío del piruvato (pyruvate shunt)* que controla la conexión entre el piruvato y el ciclo de Krebs. El **Capítulo 2** describe a través de estudios *in vitro* la relación entre el sistema PTS^{Fru}, el regulador transcripcional Cra y su efector (fructosa 1-fosfato; F1P). Ensayos de movilidad electroforética (EMSA) y de microcalorimetría de titulación isotérmica (ITC), mostraron que Cra reconoce la secuencia palindrómica TTAAACGTTTCA en la región reguladora del operón *fruBKA*. Además, la estructura cristalina del regulador se obtuvo en ausencia y presencia de la F1P. Por tanto, todos nuestros resultados apuntan a la F1P como el único efector de este regulador transcripcional bacteriano. Por último, en el **Capítulo 3**, se mostró con

experimentos *in vivo* que Cra es un represor del sistema PTS^{Fru} en *P. putida*. Por otra parte, se observó que Cra controla bajo ciertas condiciones metabólicas el estado de fosforilación de PtsN a través de FruB.

En este trabajo hemos contribuido a la comprensión del metabolismo central y los sistemas PTS en la bacteria del suelo *P. putida* los cuales, de acuerdo a nuestros resultados, pueden diferir en importantes aspectos a otras bacterias modelo como *E. coli* o *B. subtilis*.

II. INTRODUCCIÓN

1. Descripción de *Pseudomonas putida*

P. putida pertenece al grupo de *Pseudomonas* fluorescentes bien conocidas por la producción de pigmentos fluorescentes (Meyer, 2000). Las cepas de *P. putida* presentan una amplia gama de actividades metabólicas, lo cual es indicativo de su adaptación a diferentes nichos (Jensen et al, 2004). *P. putida* KT2440 (Nelson *et al*, 2002) es probablemente la cepa saprofítica de laboratorio, que mejor ha conservado su capacidad para sobrevivir y funcionar en el ambiente (Frank *et al*, 2011; Jiménez *et al*, 2002). Esta bacteria es derivada de la bacteria aislada en Japón por Hosahawa en 1963 (Nelson *et al*, 2002), que fue designada originalmente como *Pseudomonas arvilla* mt-2 y que se reclasificó como *P. putida* mt-2 (Williams y Murray, 1974). *P. putida* KT2440 fue el primer sistema huésped seguro para la clonación de genes de bacterias del suelo Gram-negativas (Duque *et al*, 2007; Stjepandic *et al*, 2002). Esta cepa se ha utilizado ampliamente como huésped para la clonación y expresión de genes, y su característica más prominente es su capacidad para degradar compuestos aromáticos como el tolueno o el *m*-xileno por lo que se considera como un organismo modelo para estudios de biodegradación (Jiménez *et al*, 2002; Loh *et al*, 2008). Por tanto, *P. putida* KT2440 es considerada como el caballo de batalla para la investigación en *Pseudomonas* (Martins dos Santos *et al*, 2004; Timmis, 2002; Wu *et al*, 2011).

2. Metabolismo de carbohidratos en *P. putida*

El genoma de *P. putida* KT2440 contiene todos los genes que codifican las enzimas que

forman las tres vías metabólicas de degradación de carbohidratos más importantes en bacterias: la ruta del Entner-Doudoroff (ED), la ruta de Embden-Meyerhof-Parnas (EMP) y la ruta de las pentosas (PP, Fig. 1) con la excepción de la enzima glicolítica 6-fosfofructoquinasa, PFK (Velázquez *et al*, 2004). La ausencia de esta enzima en *P. putida* explica por qué esta bacteria utiliza sólo la ruta de ED para catabolizar la glucosa lo cual ha sido previamente demostrado a través de experimentos de radiactividad con ^{14}C (Vicente y Cánovas, 1973) y análisis de flujos metabólicos (Fuhrer, 2005). Por otra parte, el catabolismo de la fructosa difiere ligeramente del metabolismo de hexosas ya que este azúcar entra directamente a la ruta de EMP a través de las proteínas FruBKA (Velázquez *et al*, 2004; Velázquez *et al*, 2007; Vicente, 1975). En principio, la fructosa puede ser degradada a través del paso ED y/o el paso EMP (Velázquez *et al*, 2004), sin embargo, estudios previos demostraron que la fructosa es catabolizada principalmente a través de la vía ED (Sawyer *et al*, 1977). Por lo tanto, parece que la ruta de ED es la vía más importante para la degradación de azúcares en el metabolismo central de *P. putida*.

3. Regulación de la proteína Cra sobre el metabolismo central

La proteína Cra (también conocida como FruR) es un regulador pleitrópico que desempeña un papel clave en el control del flujo de carbono en *E. coli* y *Salmonella typhimurium* (Saier *et al*, 1996). En primera instancia, este factor transcripcional fue identificado como un represor que inhibe la expresión del operón de la fructosa (PTS^{Fru}) cuando el azúcar no estaba disponible, por lo que fue llamado FruR (Ramseier *et al*, 1993). Más tarde se demostró que la misma proteína reprime genes que codifican a otras enzimas del metabolismo central *(pfkA, pyka, pykF, edd, eda, mtlADR y gapB*; Bledig *et al*, 1996; Ay *et al*, 2007; Saier *et al*, 1996; Sarkar *et al*, 2008) y activa otros (*ppsA, fbp icd, pckA, aceA y aceB*; Cortay *et al*, 1994; Negre *et al*, 1998; Ramseier *et al*, 1996; Saier *et al*, 1996), lo que sugiere un carácter dual de Cra (represor y activador transcripcional). Por lo tanto, Cra aparentemente controla la dirección del flujo de carbono en *E. coli* y por lo tanto afecta la utilización de varias fuentes de carbono.

Ya sea positivo o negativo, los efectos de Cra en la transcripción se pueden contrarrestar *in vitro* por concentraciones micromolares de fructosa-1-fosfato (F1P) o concentraciones milimolares de fructosa-1,6-bisfosfato (FBP; Ramseier *et al*, 1995). De hecho, la naturaleza de los efectores metabólicos de este regulador transcripcional es

intrigante. Esto se debe a que F1P y FBP pueden ser originados por diferentes rutas metabólicas y son producidos a diferentes niveles dependiendo de la fuente de carbono. Además, las densidades electrónicas de estas dos sustancias químicas son distintas, por lo que es improbable que el mismo sitio de unión de la proteína reconozca ambos metabolitos. En la literatura se pueden encontrar puntos de vista contradictorios acerca de la naturaleza de los efectores de Cra. Experimentos de retardo con radioactividad (EMSA) indican claramente que la F1P es un efector de Cra pero no autentican lo mismo de la FBP. Algunos estudios sugieren que la respuesta *in vitro* de Cra hacia la FBP se debe a una posible contaminación de este metabolito con (Ramseier *et al* 993) F1P. Sin embargo, otros autores sostienen que FBP es un auténtico efector de Cra (Bledig *et al*, 1996; Kotte *et al*, 2010). Por tanto, en estos momentos el papel de la FBP como agonista del regulador Cra es incierto (F1P esta fuera de toda duda). Además de la función incierta de la FBP, los estudios de la regulación ejercida por Cra se han realizado sólo en enterobacterias, mientras que en otras especies como *P. putida* sus funciones siguen siendo desconocidas.

4. Sistemas PTS en P. putida

En *P. putida*, un sistema de fosfotransferasas (PTS) para el transporte de fructosa (FruA/EIIBC y FruB/EI-HPr-EIIA) coexiste con un sistema de fosfotransferasas alterno denominado sistema PTS de nitrógeno (PTS^{Ntr}; $PtsP/EI^{Ntr}$, PtsO/NPr, y $PtsN/EIIA^{Ntr}$). En ambos sistemas el fosfato de alta energía se deriva de fosfoenolpiruvato (PEP) y luego es trasferido de EI a través de HPr/NPr a las enzimas EII (fig. 5; Postma *et al*, 1993). En *P. putida*, se demostró que PTS^{Fru} y PTS^{Ntr} no representan dos sistemas completamente separados, ya que se comunican en determinadas condiciones *in vivo* por el intercambio de grupos fosfato (fig. 5; Pfluger *et al*, 2008).

Mutantes de *P. putida* en una o más proteínas PTS^{Ntr} muestran numerosos fenotipos (Cases *et al*, 2001a; Cases *et al*, 1999; Cases *et al*, 2001b; Pfluger *et al*, 2007; Pfluger-Grau *et al*, 2011; Velázquez *et al*, 2007). Por ejemplo, se ha observado que las proteínas PTS^{Ntr} están involucradas en la regulación de la acumulación de polihidroxialcanoatos (PHAs) y de la actividad de la ruta de degradación del tolueno. Además, mutantes en estas proteínas muestran diferentes velocidades de crecimiento cuando se cultivan en distintas mezclas de fuentes de carbono/nitrógeno (Velázquez *et al*, 2007). Más recientemente, se

demostró que la forma no fosforilada de PtsN directamente reprime la actividad de la piruvato deshidrogenasa (PDH), un complejo enzimático responsable de la descarboxilación del piruvato a acetil-CoA. De la misma manera que en otras bacterias, la mayoría de los mecanismos por los cuales las proteínas PTS^{Ntr} controlan algunos procesos permanecen inciertos en *P. putida*.

III. OBJETIVOS

Objetivo general

Investigar la regulación de los sistemas PTS (sistemas PTS^{Fru} y PTS^{Ntr}) de *P. putida*, así como su conexión con el metabolismo central.

A través de los siguientes objetivos específicos:

1. Analizar las principales rutas metabólicas y el flujo del carbono en el metabolismo central de *P. putida*.

2. Estudiar la interacción entre los sistemas de PTS y el metabolismo central de *P. putida.*

3. Estudiar la regulación ejercida por la proteína Cra sobre los sistemas PTS de *P. putida.*

IV. RESULTADOS Y DISCUSIÓN

1. Capítulo I: Metabolismo central y su interacción con los sistemas PTS de *P. putida*

El metabolismo central es el responsable de la generación de energía y los precursores necesarios para la biosíntesis de los componentes esenciales para la vida. Ensayos enzimáticos y de análisis de flujos metabólicos del catabolismo de azúcares en *P. putida* demostraron que la ruta de Entner-Doudoroff (ED) es la vía más frecuente para la degradación de carbohidratos en el metabolismo central de esta bacteria. Además, el genoma de *P. putida* revela la ausencia de la enzima 6-fosfofructoquinasa (PFK) lo que hace que la glucólisis no sea funcional en esta bacteria. En un esfuerzo por activar la

glucólisis y redirigir el flujo del carbono en *P. putida*, se expresó el gen *pfkA* de *E. coli* en la cepa salvaje *P. putida* y en un mutante que no puede utilizar la vía ED (*eda*-). La enzima PfkA fue expresada exitosamente, pero no fue capaz de redirigir el flujo del carbono del paso de ED hacia la glucólisis. Sorprendentemente, la presencia de esta enzima fue perjudicial para el crecimiento bacteriano y la producción de biomasa, tanto en fuentes de carbono glicolíticas como gluconeogénicas. Para examinar este hecho, hemos analizado en profundidad el metabolismo central de *P. putida* a través de la medición de las concentraciones intracelulares de varios compuestos del metabolismo central en diferentes fuentes de carbono (glucosa, fructosa y succinato). En todos los sustratos se encontraron concentraciones micromolares de dihidroxiacetona fosfato (DHAP), fructosa 1,6-bisfosfato (FBP), fructosa 6-fosfato (F6P), glucosa 6-fosfato (G6P) y 6-fosfogluconato (6PG). Teniendo en cuenta los actuales modelos metabólicos y genes que codifican a las enzimas anotadas en el metabolismo central de *P. putida*, el modelo metabólico que mejor explica nuestros resultados es que la ruta de ED funciona en un modo cíclico, de tal forma que las triosas fosfato son recicladas a hexosas (DHAP→FBP→F6P→G6P→6PG) a través de las enzimas gluconeogénicas TpiA, Fda, Fbp, Pgi, Zwf, Pgl, Edd y Eda.

Experimentos de crecimiento con mutantes de genes que codifican a las enzimas que forman la vía cíclica de ED sugieren que la ocurrencia del mismo es vital para la célula. La operación de un ED cíclico en *P. putida* explica el escaso crecimiento de la cepa salvaje cuando la enzima PfkA es expresada ya que esta se opone al flujo innato del carbono. Por tanto, estos resultados podrían explicar la ausencia de cualquier Pfk en *Pseudomonas* y sugieren que la expresión de esta enzima en esta especie genera un ciclo fútil en el metabolismo central que produce un desbalance en el metabolismo central y consume el ATP necesario para otras funciones biológicas y la formación de biomasa.

Con el fin de explorar un posible rol de las proteínas PTS^{Ntr} sobre la regulación del metabolismo central de *P. putida*, se analizaron los flujos metabólicos en cepas isogénicas con mutaciones en cada uno de los genes de los sistemas PTS (PTS^{Fru} y PTS^{Ntr}). Los resultados mostraron que la utilización de carbohidratos por los pasos del ED, EMP y PP no se vio afectada por ninguna de las mutaciones. Sin embargo, el hallazgo más importante en este análisis de flujos fue que la proteína $EIIA^{Ntr}$/PtsN regula *el desvío del piruvato (pyruvate shunt)* que controla la conexión entre el piruvato y el ciclo de Krebs. Esta

influencia de $EIIA^{Ntr}$ en el desvío del piruvato se verificó mediante ensayos de actividad de la enzima málica y la piruvato carboxilasa. Los efectos de PtsN sobre el metabolismo central se atribuyen a la sola presencia/ausencia de esta proteína, independientemente de su estado de fosforilación. Por tanto, nuestros datos sugieren un papel de PtsN en la regulación del metabolismo central para ajustar los flujos y concentraciones intracelulares de algunos metabolitos para satisfacer las demandas anabólicas y energéticas de la célula.

2. Capítulo II. El regulador transcripcional Cra de P. putida y su relación con el sistema PTS^{Fru}: estudios in vitro

El regulador transcripcional Cra, es un sensor global que regula los flujos en el metabolismo central de bacterias Gram-negativas, sin embargo, el efector real (o efectores) de esta proteína que se encarga(n) de dar la señal a la proteína no se han determinado de forma inequívoca. Para abordar esta pregunta, la proteína Cra de *P. putida* se purificó, caracterizó, y su estructura tridimensional fue determinada. Análisis por ultracentrifugación analítica, de filtración en gel y ensayos de movilidad electroforética (EMSA) mostraron que Cra es un dímero que se une al operador identificado en la región promotora del operón *fruBKA*. Además, se observó que la fructosa 1-fosfato (F1P) fue el único metabolito capaz de disociar el complejo Cra/ADN. Los parámetros termodinámicos de la interacción F1P-Cra-ADN calculados por calorimetría de titulación isotérmica revelaron que el factor transcripcional se une fuertemente a la secuencia de ADN 5'-TTAAACGTTTCA-3' (K_D = 26.3 ± 3.1 nM) y que la F1P se une a la proteína con una estequiometría aparente de 1.06 ± 0.06 moléculas por monómero de Cra con una K_D de 209 ± 20 nM. Otros efectores como la fructosa 1,6-bisfosfato (FBP; que hasta ahora se ha considerado como un posible efector de Cra) no mostraron ninguna afinidad por el regulador. Por otra parte, la estructura de Cra y su co-cristal con F1P sugieren que cualquier otra molécula pequeña distinta a F1P difícilmente puede ajustarse a la geometría del sitio de unión del efector. Por tanto, nuestros resultados apuntan a la F1P como el único efector del regulador bacteriano Cra.

3. Capítulo III. Regulación de la proteína Cra sobre los sistemas PTS de P. putida: estudios in vivo

La proteína Cra es un regulador transcripcional dual que controla el metabolismo central en enterobacterias, sin embargo, sus funciones en otras familias de bacterias con un nicho ecológico distinto, no han sido exploradas todavía. Continuando con nuestros estudios sobre el funcionamiento y regulación de los sistemas PTS de *P. putida*, en este capítulo, se estudió a través de experimentos *in vivo* el efecto de la mutación de Cra sobre los sistemas PTS (PTS^{Fru} y PTS^{Ntr}). En primer lugar, de determinó la actividad del promotor del operón de la fructosa y las concentraciones intracelulares de F1P y FBP en *P. putida* en diferentes fuentes de carbono. Los resultados revelaron que PTS^{Fru} se expresa solamente en fructosa y mantiene bajos niveles en glucosa y succinato (fructosa >> glucosa > succinato). Por otro lado, el análisis de este promotor en el mutante Cra, reveló que la ausencia de este regulador produce la desrepresión del sistema PTS^{Fru} en todas las fuentes de carbono probadas.

Finalmente, se observó que Cra controla bajo ciertas condiciones metabólicas el estado de fosforilación de PtsN a través del *cross-talk* con la proteína FruB. Por tanto, nuestros resultados sugieren que Cra es un modulador del estado de fosforilación de PtsN y por tanto del sistema PTS^{Ntr}.

V. CONCLUSIONES

El trabajo descrito a lo largo de esta Tesis ha dado lugar a las siguientes conclusiones:

1. *El metabolismo central en P. putida se lleva a cabo a través de una versión cíclica de la ruta Entner-Doudoroff*. Las diferencias entre el metabolismo central de *P. putida* y otras especies tales como *E. coli*, indican una clara especialización de la maquinaria metabólica como resultado del hábitat y las necesidades nutricionales de cada especie.

2. *El Sistema PTS^{Ntr} desempeña funciones regulatorias sobre el metabolismo central de P. putida.* Esta regulación es llevada a cabo por la proteína $EIIA^{Ntr}$ (PtsN), donde hemos demostrado que esta proteína controla la conexión entre el piruvato y el ciclo de Krebs reprimiendo la actividad del desvío del piruvato (*pyruvate shunt*).

3. *La F1P es el único efector del regulador transcripcional bacteriano Cra.* En este trabajo, hemos estudiado la proteína Cra de *P. putida*, sin embargo, consideramos que todas nuestras observaciones sobre su efector pueden ser generalizadas a otras especies como *E. coli* y *S. typhimurium*, debido a la alta similitud en la secuencia y estructura tridimensional del sitio de unión en las proteínas Cra de estas especies. Por lo tanto, nuestros resultados indican que F1P es el único efector del regulador bacteriano Cra.

4. *Cra es un represor transcripcional del sistema PTS^{Fru} de P. putida*. Experimentos *in vitro* e *in vivo* demostraron que Cra es un represor muy fuerte del operón de la fructosa, donde el proceso de expresión está controlado enteramente por las concentraciones intracelulares de F1P.

5. *Cra es un modulador del sistema PTS^{Ntr} de P. putida*. La regulación ejercida por Cra sobre el operón fructosa modula el estado de fosforilación de la proteína PtsN bajo ciertas condiciones metabólicas.

Curriculum Vitae

MAX CHAVARRÍA VARGAS

Systems Biology Program
National Center of Biotechnology (CNB-CSIC)
Cantoblanco, Darwin Street, 3, Madrid, Spain, 28049
tel. (34) 915854573, fax (34) 915854603
mchavarria@cnb.csic.es, max.chavarria@ucr.ac.cr

Personal

Birth: 06 September 1979; San José, Costa Rica.

Education

-Autonomous University of Madrid, PhD student in Molecular Biology Department, 2007-present

-University of Costa Rica, M.S. Chemistry, 2005

-University of Costa Rica, B.S. Chemistry, 2003

Professional History

-2007-present: *Ph.D student*; Systems Biology Program, National Center of Biotechnology (CNB-CSIC).

-Oct-Dic. 2007: *Student visitor;* Institute of Molecular Systems Biology (IMSB), Eidgenössische Technische Hochschule Zürich (ETH Zürich), Switzerland. Lab. Prof. Dr. Uwe Sauer.

-2000-2007: *Teaching Assistant;* Chemistry School, University of Costa Rica (UCR).

-2006: *Research Assistant;* Phytochemistry Laboratory, Research Center on Natural Products (CIPRONA), University of Costa Rica.

-2000-2002: *Research Assistant;* Environmental Pollution Research Center (CICA), University of Costa Rica.

Grants

-2007-present, Ph.D degree scholarship UCR-CSIC.

-2003-2005, M.S degree scholarship University of Costa Rica.

-1999-2003, B.S. degree scholarship University of Costa Rica.

Publications

-Soledad Mora, Victor Castro, Luis Poveda, **Max Chavarría** & Renato Murillo. Two new 3,4-seco-*ent*-kaurenes and other constituents from the Costa Rican endemic species *Croton megistocarpus*. *Helv. Chim. Acta.* (2011) doi: 10.1002/hlca.20110012.

-**Max Chavarría**, César Santiago, Raúl Platero, Tino Krell, José M. Casasnovas & Víctor de Lorenzo. Fructose 1-Phosphate is the preferred effector of the metabolic regulator Cra of *Pseudomonas putida*. *J. Biol. Chem.* (2011) 286, 9351-9359.

-Katharina Pflüger-Grau, **Max Chavarría** & Víctor de Lorenzo. The interplay of the $EIIA^{Ntr}$ component of the N-related phosphotransferase system (PTS^{Ntr}) of *Pseudomonas putida* with pyruvate dehydrogenase. *Biochim Biophis Acta.* (2011), doi: 10.1016/j.bbagen.2011.01.002.

- Erick Castellón, **Max Chavarría**, Victor de Lorenzo, Marcos Zayat & David Levy. An Electro-optical device from a biofilm structure created by bacterial activity. *Adv. Mater. (2010) 22, 43, 4846-4850.*

- Juan Araya & **Max Chavarría.** *Ejercicios de espectroscopia química.* Editorial Universidad de Costa Rica. 2008.

- **Max Chavarría**, Victor Castro, Luis Poveda & Renato Murillo. Four new compounds from the non-polar extract of the plant Amyris brenesii (Rutaceae) from Costa Rica. *Rev. Biol. Trop.* (2008) 56, 3, 1043-1052.

- Guiselle Lutz, **Max Chavarría**, María Laura Arias & Julio Mata-Segreda. Microbial degradation of palm biodiesel. *Rev. Biol. Trop.* (2006) 54, 1, 59-63.

Patents

-Spanish patent. Register number ES1641.698. Title: Combinación de una bio-película bacteriana y cristal líquido para la preparación de un dispositivo electro-óptico. Inventors: Erick Castellón, **Max Chavarría**, Víctor de Lorenzo, Marcos Zayat & David Levy.

Public Presentations

-January, 2011. WE-Heraeus-Seminar on Biothermodynamics of Metabolic and Ecological Networks. "Carbon central metabolism in *Pseudomonas putida*: Evidence for a cyclic operation of the Entner-Doudoroff pathway". (**Poster**) Bad Honnef. Germany.

-September 2010. European Molecular Biology Organization (EMBO) meeting. "Regulatory duties of the catabolite repressor/activator (Cra) protein of *Pseudomonas putida*". (**Poster**) Barcelona, Spain.

-June 28-July 2 2009. FEMS. 3rd Congress of European Microbiologists. "The regulatory duties of the phosphotransferase system (PTS^{Ntr}) revealed by the metabolic flux analysis of *Pseudomonas putida*". (**Poster**) Gothenberg, Sweden.

-December, 2008. 4th Meeting of the Spanish Systems Biology Network (REBS): From genomes to *in silico* and back. "The regulatory duties of the phosphotransferase system (PTS^{Ntr}): A metabolic flux analysis of *Pseudomonas putida*". (**Talk**) Valencia, Spain.

-June, 2008. Trends in Metabolomics - Analytics and Applications. DECHEMA-Haus. "Effect of PtsN (IIA^{Ntr}) protein on the central carbon metabolism of *Pseudomonas putida*: a metabolic-flux approach". (**Poster**) Frankfurt am Main, Germany.

-September 2006. XV Congress of Italo-Latin American Society of Ethno-medicine (SILAE). "A new phytochemistry study of *Amyris brenesii*". (**Poster**) Perugia, Italia.

-September 2006. XV Congress of Italo-Latin American Society of Ethno-medicine (SILAE). "Lignans of *Phenax soneratii*". (**Poster**) Perugia, Italia.

Short courses and seminars

-2007. Minisymposium; Joining Forces. Single Cell Analytics. Eidgenössische Technische Hochschule Zürich. ETH Zürich, Switzerland.

-2006. Workshop: Alternative sources of energy from plants. UCR-DAAD, San José, Costa Rica.

-2004. XVI Congress of the Iberoamerican Society of Electrochemistry. San José, Costa Rica.

-2004. Seminar: Enzymatic Biotechnology. Principles and selected topics. Research Center on Natural Products (CIPRONA), UCR. San José, Costa Rica.

-2004. Course: GC-MS Methods, Techniques and Validation". Agilent Technologies. San José, Costa Rica.

-2002. Course: Electrochemistry and corrosion. UCR. San José, Costa Rica.

-2002. Course: Organic Structure Analysis. UCR. San José, Costa Rica.

-2002. Course: Basic metrology and quality control. Mexican National Metrology Center (CENAM) and UCR. San José, Costa Rica.

-2000. Course: Interpretation of analytical results in wastewater. Environmental Pollution Research Center (CICA), University of Costa Rica.

THE JOURNAL OF BIOLOGICAL CHEMISTRY VOL. 286, NO. 11, pp. 9351–9359, March 18, 2011

Fructose 1-Phosphate Is the Preferred Effector of the Metabolic Regulator Cra of *Pseudomonas putida*[*] [S]

Received for publication, September 22, 2010, and in revised form, December 18, 2010 Published, JBC Papers in Press, January 14, 2011, DOI 10.1074/jbc.M110.187583

Max Chavarría[‡1], César Santiago[§1], Raúl Platero[‡], Tino Krell[¶], José M. Casasnovas[§], and Víctor de Lorenzo[‡2]

From the [‡]Systems Biology Program and [§]X-ray Crystallography Unit, Centro Nacional de Biotecnología-Consejo Superior de Investigaciones Científicas, 28049 Cantoblanco-Madrid, Spain, and the [¶]Department of Environmental Protection, Estación Experimental del Zaidín, Consejo Superior de Investigaciones Científicas, C/Profesor Albareda 1, Granada, E-18008, Spain

The catabolite repressor/activator (Cra) protein is a global sensor and regulator of carbon fluxes through the central metabolic pathways of Gram-negative bacteria. To examine the nature of the effector (or effectors) that signal such fluxes to the protein of *Pseudomonas putida*, the Cra factor of this soil microorganism has been purified and characterized and its three-dimensional structure determined. Analytical ultracentrifugation, gel filtration, and mobility shift assays showed that the effector-free Cra is a dimer that binds an operator DNA sequence in the promoter region of the *fruBKA* cluster. Furthermore, fructose 1-phosphate (F1P) was found to most efficiently dissociate the Cra-DNA complex. Thermodynamic parameters of the F1P-Cra-DNA interaction calculated by isothermal titration calorimetry revealed that the factor associates tightly to the DNA sequence 5′-TTAAACGTTTCA-3′ (K_D = 26.3 ± 3.1 nM) and that F1P binds the protein with an apparent stoichiometry of 1.06 ± 0.06 molecules per Cra monomer and a K_D of 209 ± 20 nM. Other possible effectors, like fructose 1,6-bisphosphate, did not display a significant affinity for the regulator under the assay conditions. Moreover, the structure of Cra and its co-crystal with F1P at a 2-Å resolution revealed that F1P fits optimally the geometry of the effector pocket. Our results thus single out F1P as the preferred metabolic effector of the Cra protein of *P. putida*.

The central metabolism of bacteria is controlled through the interplay of global and specific regulators, the outcome of which depends on the nature of the carbon and energy sources and the particular culture conditions (1). The catabolite repressor/activator (Cra) protein (also known as FruR) is a pleiotropic regulatory protein that plays a key role in the control of carbon flow in *Escherichia coli* and *Salmonella typhimurium* (2). This factor was first identified as a repressor that inhibited expression of the fructose operon of these two bacteria when the sugar was not available, thereby the earlier name FruR (3). Later work, however, revealed that the same protein represses genes for many other enzymes of the central metabolism (*pfkA*, *pykA*, *pykF*, *acnB*, *edd*, *eda*, *mtlADR*, and *gapB*; Refs. 2 and 4–6) and activates others (*ppsA*, *fbp*, *pckA*, *acnA*, *icd*, *aceA*, and *aceB*; Refs. 2 and 7–10), suggesting a dual character of Cra as both a transcriptional repressor and an activator.

From a structural point of view, the Cra protein has been classified as a member of the GalR-LacI superfamily of DNA-binding transcriptional regulators (11, 12). In *E. coli*, the Cra monomer is organized in two functional domains. The N-terminal helix-turn-helix module accounts for the binding of the protein to the cognate DNA operator sequence, whereas the C-terminal portion mediates the interactions between subunits and triggers changes in the protein upon effector binding (12).

Earlier studies of the Cra proteins of *E. coli* and *S. typhimurium* suggested that the regulator is a tetramer that recognizes an imperfect palindromic DNA sequence to which it binds asymmetrically (2). It is generally believed that promoters containing a Cra operator upstream of the RNA polymerase binding site might become activated by the factor, thereby stimulating transcription of downstream genes. In contrast, Cra binding sites overlapping those bound by RNA polymerase originate a typical negative regulation scenario (2). Whether positive or negative, the effects of Cra on transcription can be counteracted *in vitro* by micromolar concentrations of fructose 1-phosphate (F1P)[3] or millimolar concentrations of fructose-1,6-bisphosphate (FBP, Refs. 2, 3, 5, 13). In fact, the nature of the metabolic effector(s) alleged to make Cra release target DNA sites is intriguing. This is because F1P and FBP are originated by different metabolic routes and produced at levels that depend on the consumed carbon source. Furthermore, electronic densities of these two chemicals are not alike, making it puzzling that the same effector recognition pocket can bind both of them. Conflicting publications on this matter bear witness of

[*] This work was supported by grants of the CONSOLIDER program of the Spanish Ministry of Science and Innovation, by the BACSINE and MICROME Contracts of the European Union, and by funds of the Autonomous Community of Madrid. This work was also supported by a doctoral scholarship of the Universidad de Costa Rica and the CSIC (to M. C.). C. S. was supported by the Centro Nacional de Biotecnología, Consejo Superior de Investigaciones Científicas.

[S] The on-line version of this article (available at http://www.jbc.org) contains supplemental Figs. S1–S4 and Table S1.

The atomic coordinates and structure factors (codes 3O74, 3O75, and 2IKS) have been deposited in the Protein Data Bank, Research Collaboratory for Structural Bioinformatics, Rutgers University, New Brunswick, NJ (http://www.rcsb.org/).

[1] Both authors contributed equally to this work.

[2] To whom correspondence should be addressed: Centro Nacional de Biotecnología-CSIC, Campus de Cantoblanco, Madrid 28049, Spain. Tel.: 34-91-585-4536; Fax: 34-91-585-45-06; E-mail: vdlorenzo@cnb.csic.es.

[3] The abbreviations used are: F1P, fructose 1-phosphate; FBP, fructose 1,6-phosphate; PTS^{Fru}, phosphoenol pyruvate phosphotransferase carbohydrate system of *P. putida*; ITC, isothermal microcalorimetry; F6P, fructose 6-phosphate; G6P, glucose 6-phosphate; MES, 4-morpholineethanesulfonic acid; ΔH, reaction enthalpy; ΔG, change in free energy; ΔS, change in entropy; T, absolute temperature; K_A, binding constant.

such a problem in the relevant literature. Gel retardation experiments with a labeled DNA fragment bearing a Cra operator (3, 5) could authenticate F1P as one *bona fide* effector, but not FBP. Some studies suggest that the *in vitro* response of Cra to FBP is due to a possible contamination of FBP with F1P (3). Yet, other authors have produced evidence that FBP is an authentic effector of Cra (5, 14). The consensus at this point is that F1P is the major agonist of the enterobacterial regulator, but FBP can do the same at much higher concentrations. But what is the situation in other types of bacteria?

This work addresses the nature of the metabolic signal(s) that control(s) binding of Cra to its genomic binding sites in the soil microorganism *Pseudomonas putida*. This bit of information is important for setting reliable connections between the central fluxes for catabolism/anabolism of carbohydrates (which are often reported by FBP levels, Ref. 3) and the metabolic and non-metabolic transcriptome (14) in this bacterium. The Cra regulator of *P. putida* is an ortholog of the virtually identical gene/protein found in *E. coli*. But in contrast to the protein of *E. coli*, crystals of the purified $Cra_{P.\ putida}$ diffracted at a very high resolution (see below), thereby revealing an unprecedented structural detail of the effector-protein interaction that could not be attained with the enterobacterial variant (11). As shown below, analysis of such a structure along with other biochemical and biophysical tests indicates that F1P is the preferred metabolic effector of $Cra_{P.\ putida}$. As a sidelight, we could produce evidence that this Cra variant represses expression of the fructose-related phosphoenol pyruvate phosphotransferase carbohydrate system of *P. putida* in a fashion (predictably) dependent on F1P binding.

EXPERIMENTAL PROCEDURES

Cloning, Expression, and Protein Purification—The DNA sequence encoding the Cra protein of *P. putida* KT2440 (PP0792) was amplified from the chromosome of this bacterium with primers Cra-F (5′-GGGAATTCCATATGAAACTCAGCGATATCGCCCGT-3′) and Cra-R (5′-CCGGCTCGAGTCAGGCCACTGAGAT-3′). The resulting PCR product was digested with NdeI/XhoI and cloned into the bacterial expression vector pET28a (Novagen), which adds six histidines to the N terminus of the encoded protein. Note that we included a stop codon (TCA) in the Cra-R primer immediately after the XhoI sequence to avoid addition of more His residues in the C terminus by the vector. The resulting plasmid (pET28aCra) was transformed into the specialized host strain *E. coli* BL21(DE3). For expression of the His_6-tagged protein, the transformed strain was grown at 37 °C in LB to $A_{600} = 0.5$, and 0.5 mM of isopropyl-β-D-thiogalactoside was added, after which the cultures were grown for an additional 3 h. Cells were then harvested by centrifugation and the pellets frozen at −80 °C until further use. For purification, cells were thawed, resuspended in 50 mM sodium phosphate buffer (pH 7.0) and 200 mM NaCl (1 ml of culture, $A_{600} = 0.5$ in 50 μl), and mechanically lysed using a French press (Thermo Electron Corp.). Cell debris was removed by centrifugation (20,000 × *g* for 30 min at 4 °C) and the native His_6-Cra protein isolated to apparent homogeneity from the supernatant of the cell lysate using TALON metal affinity resin (Clontech) according to the manufacturer's instructions (see supplemental Fig. S1 for details). The purified protein was kept in the elution buffer at 4 °C until its utilization as indicated in each case. On the other hand, selenium-methionine (Se/Met)-derivatized *P. putida* Cra was purified as before from cells grown in M9 minimal medium (15) in the presence of 0.2% glucose, selenium-methionine, and other amendments known to inhibit methionine biosynthesis (for protocol details see Ref. 16). All buffers for (Se/Met)-Cra purification were supplemented with 5 mM dithiothreitol, but the isolation procedures were otherwise identical to those employed for the non-derivatized protein.

Identification and Synthesis of the Cra Operator—The reference *E. coli* consensus sequence for Cra binding sites was retrieved from the PRODORIC database (17). The resulting DNA motif (Fig. 1*A*) was then searched in the genome of *P. putida* KT2440 (18) by means of the Virtual Footprint software (version 3.0, Ref. 19), which revealed the presence of at least 89 possible Cra binding sites. One of these sites (5′TTAAACGTTTCA3′) happened to occur within the intergenic and divergent promoter region of the *fruR/fruBKA* gene cluster (*P. putida* chromosomal coordinates 908211–915030, Fig. 1*B*) which, because of its proximity to the *cra* (*fruR*) gene of this bacterium was likely to be functional. This plausible operator was synthesized as part of a 22-bp double-stranded DNA fragment (see below) and employed in the mobility shift and isothermal microcalorimetry (ITC) assays described under "Results."

NonRadioactive EMSA—The 22-bp DNA fragment used for EMSA with the Cra protein was prepared by heating an equimolar (50 nmol) mixture of complementary oligonucleotides containing the presumed Cra binding site of the *fruR/fruBKA* promoter region (forward, 5′-TCAGATTAAACGTTTCAGCTGC-3′; and reverse, 5′-GCAGCTGAAACGTTTAATCTGA-3′) in 1 ml of TE buffer (10 mM Tris/HCl, pH 8.0; 1 mM EDTA) at 95 °C for 10 min and then keeping the annealed product chilled on ice until further use. The Cra-DNA binding reaction was assembled in a final volume of 20 μl containing 2 μl of TGED binding buffer 10× (final concentrations, 10 mM Tris-HCl (pH 8.0), 5% v/v glycerol, 0.1 mM EDTA, 1 mM dithiothreitol, 20 μg/ml poly (deoxyinosinic-deoxycytidylic), 200 μg/ml BSA, 0.75 μM Cra site-containing DNA fragment) and increasing amounts of the pure Cra. Mixtures were incubated for 15 min at 30 °C and electrophoresed in a nondenaturing 10% (w/v) polyacrylamide (bisacrylamide gel in Tris-glycine buffer 1× (pH 8.9)). Finally, the gels were stained with ethidium bromide and visualized using a Gel Doc XR (Bio-Rad). In the experiments for identification of potential effectors, Cra was incubated with the DNA fragment in the presence of 1 mM fructose (Fluka, 99% purity), 1 mM F1P (Sigma, 100% purity), FBP (Sigma, 98% purity), fructose 6-phosphate (F6P, Sigma, 98% purity), glucose 6-phosphate (G6P, Sigma, 100% purity), and then the samples were run in a gel and analyzed as described before.

ITC—ITC experiments were performed on a VP microcalorimeter (MicroCal, Northampton, MA) at 25 °C. Prior to experiments, Cra was thoroughly dialyzed in 25 mM Tris-HCl, 50 mM NaCl, and 1 mM DTT (pH 8.0). After dialysis, the protein solution was filtered through a 0.45-μm filter, and its concentration

was determined by UV absorption spectroscopy using an extinction coefficient of 1.217×10^5 cm M^{-1} at 280 nm (20). Effectors were prepared by diluting pure powdered products in filtered dialysis buffer so that the ligand and protein solvent were the same. Each titration involved a single 1.6-μl injection and a series of 4.8-μl injections of a 250 μM preparation of each of the effectors into a 7.5 μM protein solution deposited in the 1.4-ml chamber of the apparatus. For DNA binding studies, the 22-bp DNA fragment used in EMSA experiments (see above) was dialyzed so that the DNA and protein solvent were the same. In this case, the assays consisted of the injection of 4.8-μl aliquots of 60 μM DNA into a protein solution of 10 μM in the same 1.4-ml chamber. The mean enthalpies measured from injection of the ligands into the buffer were subtracted from raw titration data prior to data fitting using the One Binding Site model of the MicroCal version of the ORIGIN software. From the curves thus fitted, the parameters ΔH (reaction enthalpy), K_A (binding constant, $K_A = 1/K_D$), and n (reaction stoichiometry) were determined. From the values of K_A and ΔH, the change in free energy (ΔG) and in entropy (ΔS) were calculated with the equation: $\Delta G = -RT \ln K_A = \Delta H - T\Delta S$, where R is the universal molar gas constant and T is the absolute temperature.

Analysis of the Cra Oligomerization State—Analytical ultracentrifugation experiments were performed in a Beckman Optima XL-A analytical ultracentrifuge with a UV-visible absorbance detection system. Sedimentation velocity measurements were carried out on an An50Ti eight-hole rotor in phosphate buffer with 150 mM imidazole and 200 mM NaCl (pH 7.0) (elution buffer in protein purification) at 45,000 rpm, with 400 μl of protein solution (0.5, 1, and 1.3 mg/ml) in each cell, using double-sector Epon-charcoal centerpieces. Differential sedimentation coefficient distributions c(s) were calculated by least squares boundary modeling of sedimentation velocity data using the SEDFIT program (21, 22). From this analysis, the experimental sedimentation coefficients (s) were corrected for solvent composition and temperature to obtain the corresponding standard s values ($s_{20,w}$, standard solvent conditions, pure water at 20 °C) using the SEDNTERP program (23). Partial specific volume of 0.7312 ml g^{-1} at 20 °C was calculated from the amino acid composition (24). Sedimentation equilibrium experiments were performed at 20 °C by centrifugation of 80-μl samples of Cra at 11,000, 13,000, and 19,000 rpm in the Optima XL-A ultracentrifuge. Conservation of mass in the cell was verified in all the experiments. After the equilibrium scans, a high-speed centrifugation run (45,000 rpm) was done to estimate the corresponding baseline offsets. Weight-average buoyant molecular weights were determined by fitting a single-species model to the experimental data using the Hetero-Analysis program (25). The absolute molecular weight of the Cra protein was determined using the partial specific volume (0.7312 ml g^{-1}) and the solvent density (1.0207 mg/ml). In addition, the oligomerization form of *P. putida* Cra was confirmed by size exclusion chromatography. To this end, a protein solution of 1.0 mg/ml was run through a Superdex 200 column (Amersham Biosciences) in 25 mM Tris-HCl and 50 mM NaCl (pH 8.0). The molecular weight markers were run under the same conditions. Proteins in the eluted fractions were monitored by SDS-PAGE.

Protein Crystallization—The affinity-purified His-tagged Cra protein (see above) was concentrated to 15 mg/ml for its crystallization. During concentration, the sample buffer was diluted ~50 times against 25 mM Tris (pH 8.0), 50 mM NaCl, and 1 mM DTT. This procedure allowed a high concentration of the protein and avoided amorphous precipitation while simultaneously clearing the samples of the potentially disturbing imidazole left after eluting the protein from the metallo-affinity column. Crystals of the native Cra protein were then generated from a 15-mg/ml protein sample by the sitting-drop vapor-diffusion method. Drops were prepared by mixing 150 nl of protein with 150 nl of crystallization solution and equilibrated against 100 μl of the crystallization solution in Greiner plates. Crystals appeared after 2 days in drops prepared with a solution containing 15% (w/v) of polyethylene glycol 8000, 0.2 M sodium acetate, and 0.1 M MES buffer (pH 6.5). Selenium-methionine (Se/Met)-derivatized Cra protein was crystallized using identical conditions. The resulting crystals were dialyzed against the same solution supplemented with 20% glycerol before cryofreezing in liquid nitrogen (see below). For the ligand binding experiments, native Cra protein crystals were soaked for 4–7 h in the cryofreezing solution containing 1 mM of each tested candidate effectors (F1P, FBP, F6P, G6P, and fructose).

Data Collection and Structure Resolution—Datasets from the native, effector-less Cra protein, its (Se/Met)-derivatized variant, and the ligand-containing complexes F1P and FBP were collected at the European Synchrotron Radiation Facility (Grenoble, France) at beamlines ID14–1, ID23–1, and ID14–2 (crystals soaked with F6P, G6P, and fructose did not show any diffraction). The crystals, which belonged to the space group $P2_1$, contained two Cra molecules in the asymmetric unit and a solvent content around 43%. Diffraction data were processed with X-ray detector software (XDS) (26) and scaled with SCALA (27). The structure of the protein without effector was solved first by the Single-wavelength anomalous dispersion (SAD) method using the Autorickshaw server (28) and diffraction data extending up to a 2.5-Å resolution. Structure resolution and phasing in the server was carried out by the SHELX programs (29). The initial model built by RESOLVE (30) gave R-factor/R-free values of 22 and 28%, respectively. The model was manually adjusted using Coot (31) and refined using PHENIX 1.6-289 (32) with data up to a 2.0-Å resolution to a final R-factor and R-free of 18.4 and 21.8, respectively (supplemental Table S1). Crystal structures of the Cra protein in complex with F1P and FBP were determined by the molecular replacement method using the effector-less structure and the PHASER program (33), followed by refinement with PHENIX 1.6-289 (32, supplementary Table S1). The structure of the Cra protein prepared by soaking the crystal with FBP gave an electron density map in the effector binding site that was indistinguishable from the Cra-F1P complex and therefore has not been included separately in supplemental Table S1 (not shown). All residues are in the most favored region (91.7%) or the additional allowed regions (7.9%) of the Ramachandran plot, except the effector-binding Asp-148 that lies in a disallowed region in all structures. Coordinates of the Cra structure and its complex with

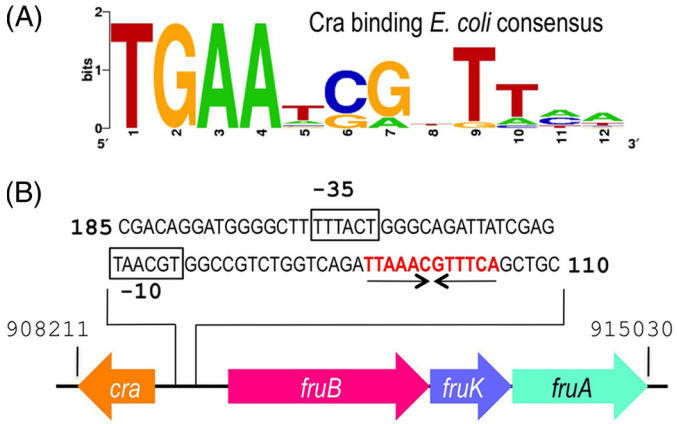

FIGURE 1. ***E. coli* Cra binding consensus sequence and regulatory region of the fructose operon of *P. putida*.** *A*, the *E. coli* consensus sequence for the Cra binding site was retrieved from the PRODORIC database (17). This sequence forms an incomplete palindrome in which the left half-site is considerably better conserved than the right half-site. *B*, the regulatory region of the *fruBKA* operon in *P. putida* was analyzed and one single operator identified as shown. The sequence TTAAACGTTTCA (in *red*) corresponds to the palindromic Cra-binding motif, whereas the *black boxes* show the putative −35/-10 promoter region upstream of the *fruBKA* operon.

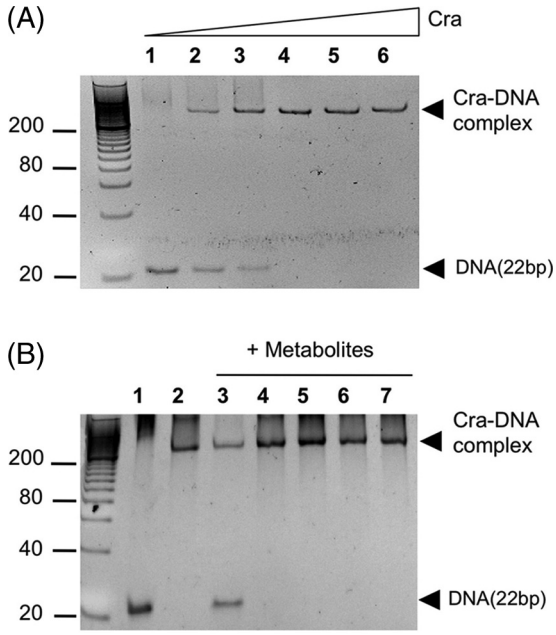

FIGURE 2. **Nonradioactive EMSA of Cra and its binding site in the intergenic *fruR/fruBKA* region of *P. putida*.** *A*, EMSA experiment with increasing concentrations of pure Cra protein. Molar ratios of DNA:Cra were 1:0 (*lane 1*), 1:0.5 (*lane 2*), 1:1 (*lane 3*), 1:2 (*lane 4*), 1:4 (*lane 5*), and 1:8 (*lane 6*). *B*, Cra effector identification. DNA (0.75 μM) was incubated with pure protein (1.5 μM) in the presence of 1 mM of different metabolites: F1P (*lane 3*), FBP (*lane 4*), F6P (*lane 5*), G6P (*lane 6*), and fructose (*lane 7*). *Lanes 1* and *2* correspond to DNA in the absence and presence of Cra, respectively, without any added metabolite. Note that only F1P prevents the binding of the protein to DNA.

F1P have been deposited in the Protein Data Bank with the following codes: PP-Cra, 3O74 and PP-Cra/F1P, 3O75.

RESULTS AND DISCUSSION

Identification and Gross Characterization of the Cra Protein of P. putida—The genome of the soil bacterium *P. putida* bears an ORF for a protein (PP0792) of 331 amino acid residues (coordinates 909206–908211) and 38.4-kDa molecular mass that shares 74% similarity and 48% identity with the *E. coli* Cra protein (supplemental Fig. S2). This identity goes up to 70% in the predicted DNA binding domain of the proteins, suggesting that the target genomic sequences ought to be similar (if not identical) as well. All these criteria qualifies PP0792 as a *bona fide* ortholog of the reference enterobacterial counterpart. Yet, unlike *E. coli* and *S. typhimurium*, the $cra_{P.\ putida}$ variant maps adjacent and divergently oriented to the *fruBKA* operon (Fig. 1*B* and supplemental Fig. S3). This gene cluster encodes proteins for phosphorylation and transport of fructose (34) through the phosphoenol pyruvate phosphotransferase carbohydrate system of *P. putida* (Ref. 34; PTS^{Fru}). Because of this proximity, PP0792 was formerly annotated as FruR, not as Cra (18). To ensure the functional assignment, the $cra_{P.\ putida}$ sequence was amplified, a metallo-affinity His_6-tag was added, and the protein was purified to apparent homogeneity as explained under "Experimental Procedures" (see supplemental Fig. S1). On the other hand, analysis of the intergenic region (Fig. 1*B*) revealed the presence of a motif (5′-TTAAACGTTTCA-3′) with a high score to the consensus binding site for the Cra regulator of *E. coli* and *Salmonella* (Fig. 1*A*, Refs. 3, 35, 36). To examine whether such a sequence was in fact the operator of $Cra_{P.\ putida}$, a 22-bp double-stranded DNA fragment containing the candidate target was synthesized and employed in the mobility shift assay shown in Fig. 2. The results indicated the formation of one specific complex between the DNA and the $Cra_{P.\ putida}$, the abundance of which increased with Cra concentration (Fig. 2*A*). The molar ratio where the DNA band disappeared entirely from the gel grossly corresponded to a molar DNA:Cra ratio of 1:2. These results verified the interaction of the protein with its predicted binding site within the *fruR/fruBKA* promoter region and laid the basis for determination of key parameters as explained below.

The Cra Regulator of P. putida Is a Dimeric Protein—The oligomerization state of purified $Cra_{P.\ putida}$ was determined by means of analytical ultracentrifugation experiments. The sedimentation profile (Fig. 3*A*) showed the occurrence of one main species to 3.9S with $s_{20,w}$ of 4.8 ± 0.1 (f/f_0 = 1.35), which accounted for 88–94% of the observed molecules and which was compatible with a dimeric form of the protein. The sedimentation equilibrium results (data not shown) predicted a mass value of 72.4 ± 6.0 kDa, which was slightly lower than the theoretical mass for the dimeric form of the protein. But taken together, the velocity and equilibrium sedimentation results indicated that Cra existed mainly as a dimer in solution at the concentrations used. The protein oligomerization state was confirmed by size exclusion chromatography (Fig. 3*B*), in which one main peak of ~60–80 kDa (*i.e.* a dimer) was followed by much less abundant species, tailing between the 21–50 kDa markers (*i.e.* a monomer). These results thus consistently documented that the Cra protein of *P. putida* occurs predominantly in a dimeric form, a feature that differs from the same regulator of *E. coli*, known to be a tetramer (37–39). However, this divergence is understandable because the leucine mini-zipper that causes tetramerization of proteins of the LacI family through their carboxyl-terminal regions is conserved in *E. coli* Cra (8) but not in the *P. putida* counterpart (Fig. 3*C*). On the other hand, the Cra binding site in the *fruBKA* promoter region

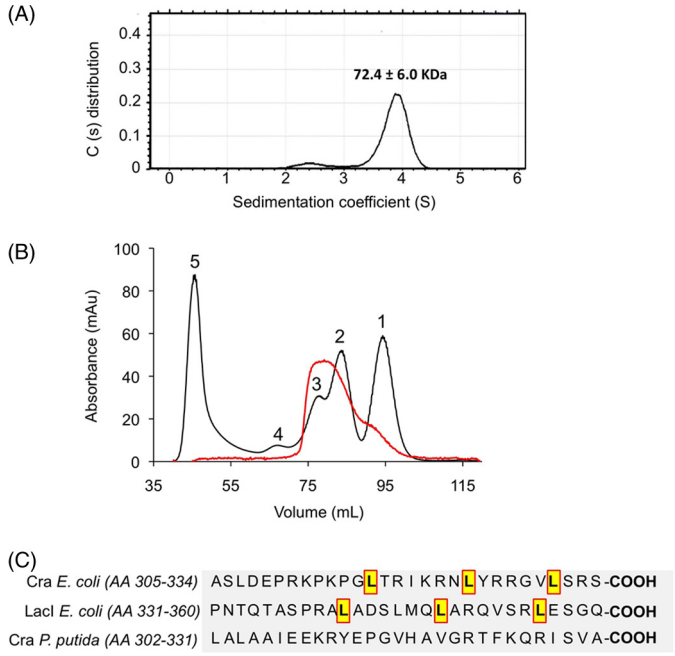

FIGURE 3. **Oligomerization of the Cra protein of *P. putida*.** *A*, distribution of sedimentation coefficient population (*c(s)*) against sedimentation coefficient (*s*), obtained by sedimentation velocity experiments. The assays were performed with 0.5, 1, and 1.3 mg/ml of pure Cra protein. The sedimentation profile was dominated by a species of 3.9S, accounting for 88–94% of the observed molecules, followed by a small peak at 2.4S (2.3–8.9%). The predominant species with sedimentation coefficient of 3.9S was corrected to $s_{20,w}$ using the viscosity value of the solution (measured in a viscometer Anton Paar AMVn). The corrected sedimentation coefficient was 4.8S, which is compatible with a globular dimer of the protein. Equilibrium sedimentation experiments predicted that the dominant peak has a molecular mass of 72.4 ± 6.0 kDa. *B*, gel filtration. The oligomerization form of *P. putida* Cra was confirmed by size exclusion chromatography as shown. The main peak of 60–80 kDa is consistent with a dimer, whereas the minor tail of 21–50 kDa surely corresponds to residual monomeric species. The chromatogram shows the superposition of two different runs: Cra alone (*red line*) and standards used as molecular mass marker (*black line*). The proteins in the elution fractions were monitored by SDS-PAGE. Molecular weight markers were run under the same conditions. Chymotrypsin (21 kDa) (*1*), albumin (50 kDa) (*2*), BSA (70 kDa) (*3*), Ab (170 kDa) (*4*), and Dextran (*5*). *C*, alignment of the C-terminal amino acid sequence of regulators Cra (*E. coli*), LacI (*E. coli*), and Cra (*P. putida*). Note that the *E. coli* tetrameric regulators Cra and LacI contain a leucine mini-zipper, which seems to be required to tetramerization. This mini-zipper is absent in the *P. putida* Cra protein.

of *E. coli* contains two nearby operators, O_1 (TGAAAC|GTTTCA) and O_2 (TGAATC|GTTTCA), which could accommodate the cognate repressor tetramer (3). In contrast, the same region of the *P. putida* genome has only one Cra site (Fig. 1*B*). A plausible consequence of this is that the affinity of the Cra dimer for the single site in the *fruBKA* promoter region of *P. putida* ought to be high to compensate the more extended range of interactions of the tetramer/two-operator scenario of the same regulatory device in *E. coli*. This possibility was addressed next.

Cra Strongly Binds Its Single Operator in the fruR/fruBKA Region of P. putida—The interaction parameters of the $Cra_{P.\ putida}$ protein with the operator DNA found within the *fruBKA* promoter segment (Fig. 1*B*) were examined by means of ITC. The corresponding results are shown in Fig. 4*A*. Note that in the *upper panel* peaks go upwards, which indicates that the binding of Cra to DNA is an endothermic process (ΔH = 7.66 ± 0.09 kcal/mol). Because enthalpy changes are unfavorable, binding ought to be entirely entropy-driven ($T\Delta S$ = 17.68 ± 0.15 kcal/mol, ΔG = −10.02 ± 0.10 kcal/mol). This situation is not infrequent, as the binding of proteins to DNA is often endothermic but also fostered by the positive entropic effect of the displacement of DNA-bound water molecules (40). Subsequent calculations allowed us to determine a protein-DNA dissociation constant (K_D) of 26.3 ± 3.1 nM that reflects a very strong interaction and that likely enables $Cra_{P.\ putida}$ to exert a considerable repression on expression of the *fruBKA* genes.

Surveying Metabolic Intermediates as $Cra_{P.\ putida}$ Effector Candidates—To shed light on the nature of Cra effector(s), DNA samples were incubated with pure Cra protein in the presence of different metabolites and submitted to EMSA experiments as before, except for the addition of candidate molecules to the binding mixtures prior to loading the gel. The chemical species that were listed as possible Cra inducers able to release its strong binding to DNA included fructose, F1P, FBP, F6P, and G6P. The EMSA experiments shown in Fig. 2*B* (*lanes 3–7*) indicated that at 1.0 mM of the effector in the binding mixture, only F1P was able to prevent binding of the repressor to the *fruBKA* regulatory region (Fig. 1*B*), confirming this metabolite as a Cra binder.

The experiment shown in Fig. 1*B*, however, did not altogether rule out that the other small molecules could interact with the target protein at much higher concentrations not suitable for the conditions of the EMSA test. Furthermore, the gel of Fig. 2*B* revealed the persistence of a fraction of the Cra-DNA complex that did form even in the presence of F1P (Fig. 2*B*, *lane 3*). To elucidate these ambiguities, we again resorted to the ITC technology described before. First, we ran isothermal titration experiments with purified Cra and the various candidate effectors as the interaction partners. The results shown in Fig. 4*B* indicated that binding of F1P to Cra was both enthalpy-driven (ΔH = −5.94 ± 0.39 kcal/mol) and entropy-driven ($T\Delta S$ = 3.16 ± 0.4 kcal/mol), producing a total free energy change (ΔG) of −9.10 ± 0.06 kcal/mol. Favorable (negative) enthalpy changes can be attributed to bond formation between F1P and amino acids in the cognate binding site, whereas favorable (positive) entropy changes are generally caused by the ligand-induced release into the medium of otherwise bound water, thereby increasing the disorder (entropy) of the system. Further calculations revealed not only an apparent stoichiometry of 1.06 ± 0.06 molecules of F1P per Cra monomer, but also demonstrated a high protein-effector affinity (K_D = 209 ± 20 nM). It is noteworthy that this affinity value is significantly higher than the corresponding figures for other transcriptional regulators of the GalR-LacI family. For instance, the K_D of isopropyl-β-D-thiogalactoside binding to LacI is 2.8 μM (41), that of 2-ketogluconate to PtxS, 15 μM (42), and so on. In contrast, ITC experiments indicated that Cra had little (if any) affinity for the other metabolites examined. Specifically, the test run with FBP as a Cra effector-to-be (*assay I* in Fig. 4*B*) did not produce any indication of interaction, at least at the concentrations employed in the assay. The same was true for other candidate effectors (*e.g.* G6P, glucose, and fructose; supplemental Fig. S4), indicating that the repressor is highly selective for F1P. Finally, to clarify whether some residual Cra-DNA complex could still

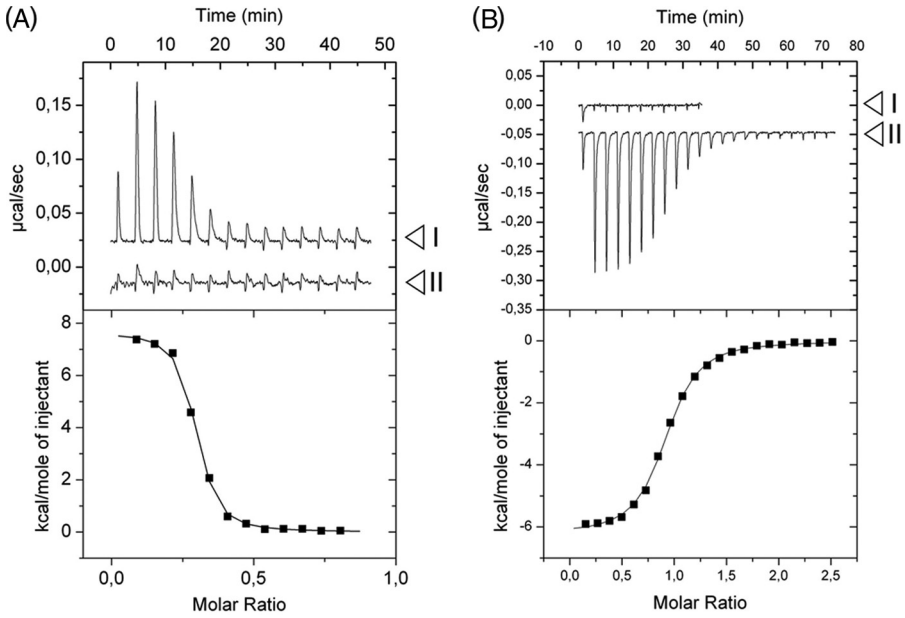

FIGURE 4. **ITC assays with Cra, effectors, and DNA.** The *upper panels* plot raw data from representative ITC experiments, whereas the *lower panels* show the fitted curves of the same results but integrated and corrected for dilution. *A*, titration of Cra protein with DNA in the absence (*I*) and presence (*II*) of F1P. Positive peaks represent an endothermal event. Note that no interaction between Cra and the DNA is detected in the presence of F1P. The thermodynamic values calculated for protein-DNA interaction were $K_D = 26.3 \pm 3.1$ nM, $\Delta H = 7.66 \pm 0.09$ kcal/mol, $T\Delta S = 17.68 \pm 0.15$ kcal/mol, and $\Delta G = -10.02 \pm 0.10$ kcal/mol. *B*, titration of Cra protein with (*I*) FBP and (*II*) F1P. The experiment covered concentrations of the effectors in the chamber ranging from 300 nM to 20 μM. Note that only the titration with F1P produces a heat change in the experiment at the tested concentrations. Negative peaks are indicative of an exothermic event. The thermodynamic values calculated by curve fitting were $K_D = 209 \pm 20$ nM, $\Delta H = -5.94 \pm 0.39$ kcal/mol, $T\Delta S = 3.16 \pm 0.40$ kcal/mol, and $\Delta G = -9.10 \pm 0.06$ kcal/mol. The sigmoidal shape of the binding curve allows determination of the protein-effector stoichiometry, which corresponds to the molar ratio (*x* axis in lower panel) at the point of inflection of the curve. In this case, such a molar ratio was 1:1, indicating that one molecule (calculated, 1.06 ± 0.06 molecules) of F1P interacts with one molecule of Cra monomer.

be formed in the presence of F1P, a mixture of Cra and F1P was incubated with the same target DNA employed above for the repressor-operator binding experiments. The resulting ITC curves (Fig. 4*A*, *assay II*) confirmed that the Cra-F1P complex was altogether unable to bind DNA. This set of data clearly points at F1P as the preferred metabolic effector of Cra, whereas it raised doubts regarding whether the role FBP as an inducer of this repressor reported in the literature for the enterobacterial protein (5, 14) held true for the counterpart of *P. putida*.

Cra Crystallization and Structure Resolution—Although the results above confirmed the nature of F1P as a Cra effector, they did not discount that the effector-binding site of the repressor could accommodate other, thus far unidentified, metabolites. To shed light on this possibility, we set out to determine the actual three-dimensional structure of such a pocket in both the effector-less and the effector-bound Cra structure by x-ray crystallography. The protein was crystallized as described under "Experimental Procedures." SDS-PAGE of extensively washed crystals showed a single, sharp band of ~30 kDa for the crystallized sample, smaller than the theoretical size of 38 kDa. This suggested a precise excision of an ~8-kDa fragment from the protein body during the crystallization process (see below). MALDI-time-of-flight analysis of the truncated protein produced a predominant peak of 30.4 kDa, confirming the previous observation. Proteolytic removal of nonstructured or unstable polypeptides often help the crystallization of the rest of the protein core (43). This appeared to be our case because the occurrence of such a cleavage during the concentration and crystallization of Cra was ultimately beneficial. Crystals were obtained that belonged to the $P2_1$ space group, contained two Cra molecules in the asymmetric unit, and did diffract to a resolution of 2 Å (see supplemental Table S1).

The structure of the Cra protein was determined for both the effector-free and the F1P-bound forms, in which last-case crystals were soaked in a solution containing a 1.0 mM concentration of the metabolite (see "Experimental Procedures"). The corresponding three-dimensional architectures are shown in Fig. 5*A*. Note that the dimers of the effector-less Cra and its F1P-bound counterpart were very similar, with a root mean square deviation of 0.48 Å for 270 residues. Note also that, as expected, the crystal structure lacks the leading N-terminal 59 amino acid residues. As mentioned above, this deletion is irrelevant (if not beneficial) for our purpose because the missing segment includes the DNA-binding domain and a short linker (supplemental Fig. S2) but leaves intact the effector-binding site of the protein.

As shown in Fig. 5*A*, both Cra monomers are related by a pseudo 2-fold axis and share an interface surface of 1700 Å^2 per monomer. The N-terminal regulatory subdomain (N-RSD) comprising residues from Thr-63 to Ser-161 and from His-293 to Val-320, specifically α helices I and II and β strand B (Fig. 5*A*), contributes most of the interactions to form the dimer. Residues from this region are implicated in 12 salt bridges and 80% of the hydrogen bonds between domains. In contrast, the C-terminal regulatory subdomain (C-RSD, residues Asp-163 to Ala-290 and Tre-323 to Lys-325) contributes only with six hydrogen bonds to the interaction through helices VII and IX (Fig. 5*A*). Structural comparisons using the DALI server (44)

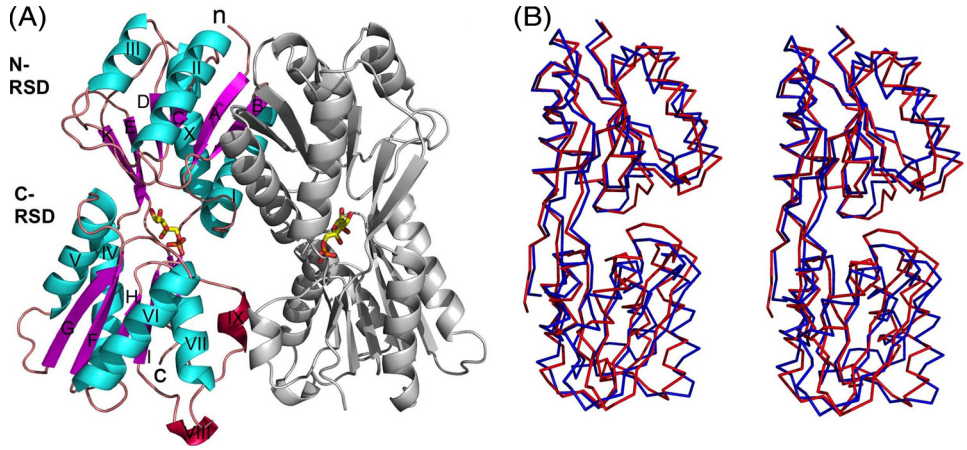

FIGURE 5. **Crystal structure of Cra in complex with F1P.** *A*, ribbon representation of the crystal structure of the regulatory subdomain of Cra in complex with its ligand F1P. β-strands are colored in *magenta*, helixes in *cyan*, 3_{10} helixes in *red*, and loops in *orange*. F1P is shown with sticks, with carbons indicated in *yellow*, phosphorus in *orange*, and oxygens in *red*. The N and C termini are marked with lowercase letters and the secondary structure elements with uppercase letters. The N-regulatory subdomain consists of strand A (amino acids 63–68), helix I (74–89), strand B (93–98), helix II (103–115), strand C (120–123), helix III (133–139), strand D (144–147), strand E (157–164), helix X (293–310), and strand K (316–320). The C-regulatory subdomain is composed of helix IV (163–175), strand F (181–187), helix V (192–204), strand G (211–217), helix VI (222–236), strand H (242–245), helix VII (239–248), helix VIII (263–265), strand I (269–273), helix IX (277–280), strand J (286–290), and strand L (323–325). *B*, lateral stereo view (Cα representation) of the superimposed regulatory domains of Cra from *P. putida* (*red*) and *E. coli* (*blue*, PDB code 2IKS).

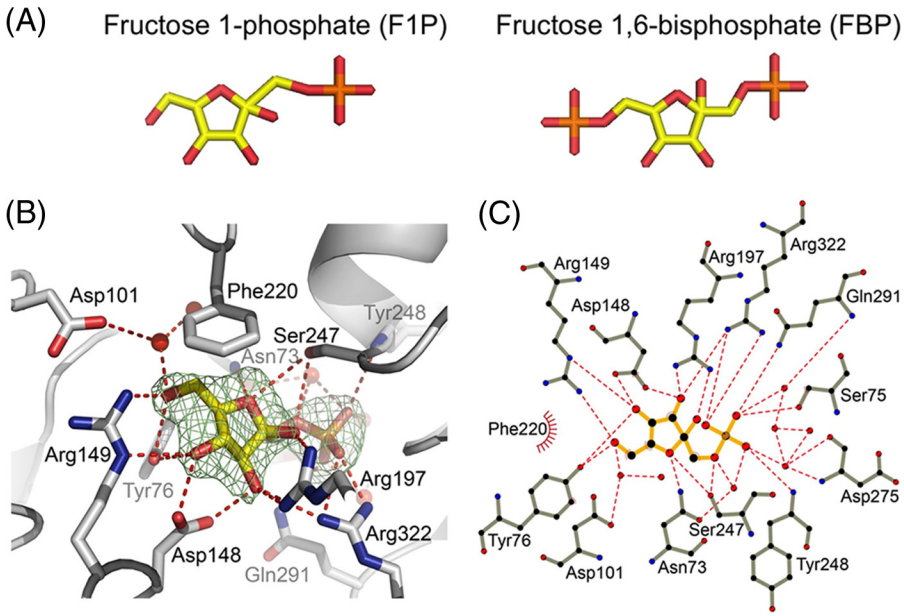

FIGURE 6. **Detail of the interaction between Cra and F1P.** *A*, stick representation of F1P and FBP with the same color code as in Fig. 5*A*. *B*, F1P-Cra interactions in the protein binding pocket. The electron density map (Fo-Fc) determined in the absence of the F1P molecule is represented as a *green mesh* at a 3.5-σ contour level. C atoms are represented in *gray*, oxygens in *red*, and nitrogens in *blue*. Hydrogen bonds are indicated as *dashed red lines* and water molecules are shown as *red spheres*. *C*, Ligplot scheme of F1P interaction with Cra (54); the color code is as in *B*. C atoms are marked in *black*, and hydrophobic interactions are indicated by *red arcs* with spokes radiating toward the interacting atom.

gave a top solution with a Z score of 33 and a sequence identity of 44% with the fructose repressor (Cra/FruR) of *E. coli* deposited in the RCSB data base (PDB code 2IKS) but not yet published. Structural comparison is shown in Fig. 5*B*. The folds observed in both proteins were close to the domain organization of other members of the family such as LacI (45) and PurR (46). These were defined by a central parallel β-sheet formed by six β strands (A–E and K) surrounded by four α helices (I–III and X) for the N-RSD, and a parallel β sheet composed of four β strands (G–I), an antiparallel β sheet with two β strands (J and L) with four α helices (IV–VII), and two 3_{10} helices (VIII and IX) for the C-RSD.

Geometry of the Cra Inducer-binding Pocket—The F1P molecule could be coherently fitted in the electronic density maps obtained after refinement of the structures determined for the crystal soaked in F1P (Fig. 6). Yet, an attempt was made to generate an additional complex between FBP (instead of F1P) and Cra by soaking effector-less protein crystals in a 1 mM solution of this metabolite as above. The structures obtained from crystals exposed to F1P and FBP were virtually identical, with a root mean square deviation for their superposition in the range of 0.45 Å. But once the structure of the putative FBP-Cra complex was inspected, it was found that the molecule occupying the effector site was no other than F1P. These results suggested

that it was the residual F1P present in the nominally 98% pure FBP preparation (see "Experimental Procedures") the protein recognized as sole interaction partner. That such selective binding to F1P happened even in the presence of a large excess of FBP confirms the very high affinity for the first, consistently detected with the other procedures described above.

The cavity where F1P molecules bind Cra is formed by portions of the N-RSD and C-RSD subdomains (Fig. 5*A*), at the intermodule cleft. Incubation of Cra native crystals with 1 mM F1P for 1 h was enough to obtain an equimolecular 1:1 association of the ligand to each domain present in the asymmetric unit of the crystals. The F1P molecule fitted to perfection the electron density map of the cognate protein cavity determined in the absence of the effector (Fig. 6*B*). The F1P molecule has a solvent-accessible area of 372 Å^2, which is completely buried by contacts with the interacting protein residues and solvent molecules. Interactions occur with polar and aromatic residues in that cavity through direct hydrogen bonds with residues Tyr-76, Ser-75, Asn-73, and Asp-148 of the N-RSD, as well as Arg-149, Arg-197, Ser-247, and Tyr-248 of the C-RSD (Fig. 6, *B* and *C*). Moreover, two residues (Gln-291 and Gln-322) of the hinge regions connecting both domains contribute with two extra direct hydrogen bonds to the interactions. In addition, water-mediated hydrogen bonds connect F1P with Asn-73 and Asp-101 of the N-RSD and Asp-275 and Gln-291 of the C-RSD. Hydrophobic interactions also play a role in the strong affinity and specificity of Cra for F1P. These involve the furanose ring of the effector, which sits between the side chains of Tyr-76 (part of Ser-75 and Asp-148) and Phe-220. These amino acids provide not less than five interactions that trap the sugar ring between two hydrophobic surfaces. The dense constellation of interactions between F1P and Cra shown in Fig. 6 creates a high degree of specificity that accounts for the extraordinary preference of the *P. putida* regulator for this (and not for other) possible effectors.

CONCLUSION

The biochemical and structural results presented above constitute strong evidence that F1P is the most favored effector of the Cra protein of *P. putida*. The extensive contacts of F1P with Cra lead to a high affinity binding interaction ($K_D \sim 200$ nM). In contrast, we found no proof of binding to either FBP or other metabolites at the concentrations employed in the assays, a body of (negative) data, which somehow diverges from the results reported for the enterobacterial protein (5, 14). Furthermore, the extensive similarity between the proteins of *P. putida* and *E. coli* suggest that they could also share the same structural transmission pathway to regulate its function, which is likely to be identical to that of known members of the family (46, 47).

That F1P is the preferred effector of Cra$_{P.\ putida}$ opens interesting questions because current metabolic models for this microorganism entertain F1P appearance only as a result of fructose phosphorylation by the PTS^{Fru} system (48–50). Furthermore, in contrast to *E. coli*, *P. putida* lacks a real glycolytic route, which makes virtually impossible any significant accumulation of FBP when cells grow in glucose (51). Although the regulatory scope of Cra in *P. putida* remains to be explored, it could well happen that (similarly to *E. coli*) the factor controls a large number of genes (4, 52), in which case there must be alternative ways of producing F1P as a descriptor of metabolic activity (14) in this bacterium. One way or the other, it is likely that the first regulatory duty of Cra was that of a repressor of fructose metabolism which was later co-opted as a global regulator (2).

A sidelight of the results presented in this work is the evidence that Cra regulates the PTS^{Fru} system in *P. putida* by binding strongly as a dimer to a single palindromic sequence within the *cra/fruB* intergenic region (which is different to those of *E. coli* and *S. typhimurium*), and that only F1P can lift such down-regulation. Because there is cross-talk between PTS^{Fru} and the nitrogen-related branch of the PTS system in this bacterium (53), it is possible that Cra closes the loop that connects N consumption and metabolic C fluxes. These hypotheses are being actively examined in our laboratory.

Acknowledgments—We thank the European Synchrotron Radiation Facility (ESRF) for provision of synchrotron radiation facilities through the Block Allocation Group (BAG)-Madrid project.

REFERENCES

1. Downs, D. M. (2006) *Annu. Rev. Microbiol.* **60,** 533–559
2. Saier, M. H., Jr., and Ramseier, T. M. (1996) *J. Bacteriol.* **178,** 3411–3417
3. Ramseier, T. M., Nègre, D., Cortay, J. C., Scarabel, M., Cozzone, A. J., and Saier, M. H., Jr. (1993) *J. Mol. Biol.* **234,** 28–44
4. Ow, D. S., Lee, R. M., Nissom, P. M., Philp, R., Oh, S. K., and Yap, M. G. (2007) *J. Biotechnol.* **131,** 261–269
5. Bledig, S. A., Ramseier, T. M., and Saier, M. H., Jr. (1996) *J. Bacteriol.* **178,** 280–283
6. Sarkar, D., Siddiquee, K. A., Araúzo-Bravo, M. J., Oba, T., and Shimizu, K. (2008) *Arch. Microbiol.* **190,** 559–571
7. Nègre, D., Oudot, C., Prost, J. F., Murakami, K., Ishihama, A., Cozzone, A. J., and Cortay, J. C. (1998) *J. Mol. Biol.* **276,** 355–365
8. Cortay, J. C., Nègre, D., Scarabel, M., Ramseier, T. M., Vartak, N. B., Reizer, J., Saier, M. H., Jr., and Cozzone, A. J. (1994) *J. Biol. Chem.* **269,** 14885–14891
9. Prost, J. F., Nègre, D., Oudot, C., Murakami, K., Ishihama, A., Cozzone, A. J., and Cortay, J. C. (1999) *J. Bacteriol.* **181,** 893–898
10. Ramseier, T. M., Chien, S. Y., and Saier, M. H., Jr. (1996) *Curr. Microbiol.* **33,** 270–274
11. Penin, F., Geourjon, C., Montserret, R., Böckmann, A., Lesage, A., Yang, Y. S., Bonod-Bidaud, C., Cortay, J. C., Nègre, D., Cozzone, A. J., and Deléage, G. (1997) *J. Mol. Biol.* **270,** 496–510
12. Scarabel, M., Penin, F., Bonod-Bidaud, C., Nègre, D., Cozzone, A. J., and Cortay, J. C. (1995) *Gene* **153,** 9–15
13. Ramseier, T. M., Bledig, S., Michotey, V., Feghali, R., and Saier, M. H., Jr. (1995) *Mol. Microbiol.* **16,** 1157–1169
14. Kotte, O., Zaugg, J. B., and Heinemann, M. (2010) *Mol. Syst. Biol.* **6,** 355
15. Miller, J. H. (1972) *Experiments in Molecular Genetics*, pp. 431–432, Cold Spring Harbor, New York
16. Van Duyne, G. D., Standaert, R. F., Karplus, P. A., Schreiber, S. L., and Clardy, J. (1993) *J. Mol. Biol.* **229,** 105–124
17. Münch, R., Hiller, K., Barg, H., Heldt, D., Linz, S., Wingender, E., and Jahn, D. (2003) *Nucleic Acids Res.* **31,** 266–269
18. Nelson, K. E., Weinel, C., Paulsen, I. T., Dodson, R. J., Hilbert, H., Martins dos Santos, V. A., Fouts, D. E., Gill, S. R., Pop, M., Holmes, M., Brinkac, L., Beanan, M., DeBoy, R. T., Daugherty, S., Kolonay, J., Madupu, R., Nelson, W., White, O., Peterson, J., Khouri, H., Hance, I., Chris Lee, P., Holtzapple, E., Scanlan, D., Tran, K., Moazzez, A., Utterback, T., Rizzo, M., Lee, K., Kosack, D., Moestl, D., Wedler, H., Lauber, J., Stjepandic, D., Hoheisel, J., Straetz, M., Heim, S., Kiewitz, C., Eisen, J. A., Timmis, K. N., Düsterhöft, A., Tümmler, B., and Fraser, C. M. (2002) *Environ. Microbiol.* **4,** 799–808

19. Münch, R., Hiller, K., Grote, A., Scheer, M., Klein, J., Schobert, M., and Jahn, D. (2005) *Bioinformatics* **21,** 4187–4189
20. Gasteiger, E., Hoogland, C., Gattiker, A., Duvaud, S., Wilkins, M. R., Appel, R. D., and Bairoch, A. (2005) in *The Proteomics Protocols Handbook* (Walker, J. M., ed) pp. 571–607, Humana Press
21. Schuck, P. (2000) *Biophys. J.* **78,** 1606–1619
22. Schuck, P. (2004) *Biophys. Chem.* **108,** 187–200
23. Lebowitz, J., Lewis, M. S., and Schuck, P. (2002) *Protein. Sci.* **11,** 2067–2079
24. Laue, T. M., Shah, B., Ridgeway, T. M., and Pelletier, S. (1992) in *Analytical Ultracentrifugation in Biochemistry and Polymer Science* (Harding, S. E., Horton, J. C., and Rowe, A. J., eds) pp. 90–125, Royal Society of Chemistry, Cambridge, England
25. Cole, J. L. (2004) *Methods Enzymol.* **384,** 212–232
26. Kabsch, W. (1993) *J. Appl. Crystallogr.* **26,** 795–800
27. (1994) *Acta Crystallogr D Biol Crystallogr* **50,** 760–763
28. Panjikar, S., Parthasarathy, V., Lamzin, V. S., Weiss, M. S., and Tucker, P. A. (2005) *Acta Crystallogr. D. Biol. Crystallogr.* **61,** 449–457
29. Sheldrick, G. M. (2002) *Z. Kristallogr.* **217,** 644–650
30. Terwilliger, T. C. (2000) *Acta Crystallogr.* **56,** 965–972
31. Emsley, P., Lohkamp, B., Scott, W. G., and Cowtan, K. (2010) *Acta Crystallogr. D Biol. Crystallogr.* **66,** 486–501
32. Adams, P. D., Afonine, P. V., Bunkóczi, G., Chen, V. B., Davis, I. W., Echols, N., Headd, J. J., Hung, L. W., Kapral, G. J., Grosse-Kunstleve, R. W., McCoy, A. J., Moriarty, N. W., Oeffner, R., Read, R. J., Richardson, D. C., Richardson, J. S., Terwilliger, T. C., and Zwart, P. H. (2010) *Acta Crystallogr. D Biol. Crystallogr.* **66,** 213–221
33. McCoy, A. J., Grosse-Kunstleve, R. W., Adams, P. D., Winn, M. D., Storoni, L. C., and Read, R. J. (2007) *J. Appl. Crystallogr.* **40,** 658–674
34. Velázquez, F., Pflüger, K., Cases, I., De Eugenio, L. I., and de Lorenzo, V. (2007) *J. Bacteriol.* **189,** 4529–4533
35. Nègre, D., Bonod-Bidaud, C., Geourjon, C., Deléage, G., Cozzone, A. J., and Cortay, J. C. (1996) *Mol. Microbiol.* **21,** 257–266
36. Shimada, T., Fujita, N., Maeda, M., and Ishihama, A. (2005) *Genes Cells* **10,** 907–918
37. Chakerian, A. E., Tesmer, V. M., Manly, S. P., Brackett, J. K., Lynch, M. J., Hoh, J. T., and Matthews, K. S. (1991) *J. Biol. Chem.* **266,** 1371–1374
38. Chen, J., and Matthews, K. S. (1992) *J. Biol. Chem.* **267,** 13843–13850
39. Alberti, S., Oehler, S., von Wilcken-Bergmann, B., and Müller-Hill, B. (1993) *EMBO J.* **12,** 3227–3236
40. Krell, T., Busch, A., Guazzaroni, M., Lacal, J., Gallegos, M., and Terán, W. (2007) in *Pseudomonas: A Model System in Biology* (Ramos, J. L., and Filloux, A., eds) pp. 255–277, Springer, Utrecht, The Netherlands
41. Wilson, C. J., Das, P., Clementi, C., Matthews, K. S., and Wittung-Stafshede, P. (2005) *Proc. Natl. Acad. Sci. U.S.A.* **102,** 14563–14568
42. Daddaoua, A., Krell, T., Alfonso, C., Morel, B., and Ramos, J. L. (2010) *J. Bacteriol.* **192,** 4357–4366
43. Wernimont, A., and Edwards, A. (2009) *PLoS ONE* **4,** e5094
44. Holm, L., and Rosenström, P. (2010) *Nucleic Acids Res.* **38,** W545–549
45. Lewis, M., Chang, G., Horton, N. C., Kercher, M. A., Pace, H. C., Schumacher, M. A., Brennan, R. G., and Lu, P. (1996) *Science* **271,** 1247–1254
46. Schumacher, M. A., Choi, K. Y., Zalkin, H., and Brennan, R. G. (1994) *Science* **266,** 763–770
47. Schumacher, M. A., Choi, K. Y., Lu, F., Zalkin, H., and Brennan, R. G. (1995) *Cell* **83,** 147–155
48. Sawyer, M. H., Baumann, P., Baumann, L., Berman, S. M., Cánovas, J. L., and Berman, R. H. (1977) *Arch. Microbiol.* **112,** 49–55
49. Puchalka, J., Oberhardt, M. A., Godinho, M., Bielecka, A., Regenhardt, D., Timmis, K. N., Papin, J. A., and Martins dos Santos, V. A. (2008) *PLoS Comput. Biol.* **4,** e1000210
50. Nogales, J., Palsson, B. Ø., and Thiele, I. (2008) *BMC Syst. Biol.* **2,** 79
51. Velázquez, F., di Bartolo, I., and de Lorenzo, V. (2004) *J. Bacteriol.* **186,** 8267–8275
52. Shimada. T., Yamamoto, K., Ishihama, A. (2010) *J. Bacteriol.* **193,** 649–659
53. Pflüger, K., and de Lorenzo, V. (2008) *J. Bacteriol* **190,** 3374–3380
54. Wallace, A. C., Laskowski, R. A., and Thornton, J. M. (1995) *Protein Eng.* **8,** 127–134